THE UNIVERSITY OF CHICAGO

IDENTIFYING AND ENGINEERING IMMUNOMODULATORS TO CONTROL VACCINE ADJUVANTICITY

A DISSERTATION SUBMITTED TO

THE FACULTY OF THE PRITZKER SCHOOL OF MOLECULAR ENGINEERING

IN CANDIDACY FOR THE DEGREE OF

DOCTOR OF PHILOSOPHY

BY

MATTHEW GLENN ROSENBERGER

CHICAGO, ILLINOIS

MARCH 2024

Portions of Chapter 1 have been adapted from: Rosenberger, M. G., Kim, J. Y., Rutledge, N. S., Esser-Kahn, A. P. Next-Generation Adjuvants: Applying Engineering Methods to Create and Evaluate Novel Immunological Responses. *Pharmaceutics* **15**, 1687 (2023).

Portions of Chapter 3 have been adapted from: Rosenberger, M. G., Kim, J. Y., *et. al* Discovery of New States of Immunomodulation for Vaccine Adjuvants via High Throughput Screening: Expanding Innate Responses to PRRs. *ACS Cent. Sci.* **9**, 427–439 (2023).

To Albert Bendelac, and all my dedicated instructors before him. Thank you for sharing your knowledge and passion. To teach is to serve.

"Knowledge Weighs Nothing, Carry All You Can" - Hank Green

TABLE OF CONTENTS

LIST OF FIGURES

LIST OF TABLES

ACKNOWLEDGMENTS

My graduate school experience has been, *by far*, the hardest experience of my life. I would not be where I am today, in more ways than one, without the support of my family, friends, colleagues, and mentors.

I first want to thank Prof. Aaron Esser-Kahn for supporting and encouraging me throughout my time in your lab. Your personal correspondence and openness during my graduate school recruitment were strong factors in my decision to attend UChicago. Thank you for believing in me during the rough transition from undergraduate researcher to scientific independence. You did a phenomenal job of making a large lab seem small with your efforts to schedule meetings. Your openness to feedback and criticism provides a welcome working environment that is adaptable to an ever changing field. I would also like to thank my committee members, Prof. Jeffrey Hubbell and Prof. Nicolas Chevrier, both of which I have been fortunate to meet with, and learn from, throughout my studies.

None of the science included here would have been possible without my mentors in the lab. While I was an undergrad at UT Austin, Wissam taught me fundamental immunoassays and encouraged my interest in pursuing graduate school. I am thankful for the skills I honed while working with you on many summer nights. At UChicago, Brittany fostered my growth into an independent scientist and was an invaluable resource for me and the rest of my labmates, both junior and senior. So much so that she earned the moniker and coveted personalized emoji "lab mom". I finished with almost exactly half of your total Slack messages and I am very proud of that. Both my mentors had a truly outstanding impact on my science, and I have sought to return the favor.

To my labmates, thank you for your companionship during the long days on campus. To my elder UCI transplants - Jainu, Nihesh, Jorge, and Britteny - thank you for welcoming me into the group. To Jeremiah, Oliver, and Samir, thank you for being great project partners and friends. To Bryant, Udoka, and Maria, I wish you all the best in your next-step efforts

in this work. To Brad, thank you for being a great deskmate and resource when I needed a break from failures to talk about sports, chess, life. Please remember I taught you everything you (once) knew about the gym. To Adam, thank you for being a scientific sounding board and measuring stick of what a truly dedicated researcher looks like. Maybe one day you'll make it big enough to bring NUMTOT energy back to Youngstown. To JingJing, thank you for all your help in the animal facility - this work became so much easier when I relied more on you. To Qing, thank you for all the logistical wizardry in keeping this lab afloat.

To my UChicago friends outside the lab, thank you for providing an escape from the ups and downs of science. To my roommate, Nick, thank you for providing camaraderie, support, and consistency from the very beginning. Moving in with you (after your convincing) was literally one of the best decisions I have ever made. To Adarsh, thank you for always providing energy, adventure, and humor to every situation. To Ellie, thank you for being a great crossfire partner and taking me to Hamilton. To Maddie, thank you for your friendship during COVID and beyond, and your willingness to play more board games than you ever thought possible. To Kat, thank you for being an incredible peer in developing the undergrad course and letting me use your lab space. To Rachel, my life became so much more fun and rewarding when you entered it. Thank you for being an incredible partner and for listening to me talk about trains. I very much look forward to our future together.

To those from my life in Texas, thank you for shaping me. To some of my oldest friends, Sara and Jenna, I cherish our time spent together each holiday. To Jonathan, Miguel, Afshan, and Daegi - I loved catching up with each of you here in Chicago throughout my residency. I hope to return the favor and keep in touch in the years to come. Finally, to my family, thank you for raising me to be the person I am today. I am very appreciative of the COVID Thanksgiving where y'all drove all the way to Springfield to see me. To my parents, thank you for your love and selflessness. You have provided me with an abundance of opportunity that I am endlessly grateful for. To my sister, thank you for being a watchful and attentive

older sibling. You paved a rebellious road that made getting away with things much easier.

This is not an exhaustive list of those who have had a positive impact on me throughout my PhD. I am a believer that a rich life is best had through meaningful relationships. To all those past, present, and future, thank you.

ABSTRACT

Vaccines are one of the greatest public health tools and have saved more lives than any other medical intervention in human history. Yet, vaccine efficacy and safety can still be improved. Effective vaccination responses require sufficient activation of innate immunity, which, in turn, initiates adaptive immunity. Innate immune activation in current vaccines often requires adjuvants - helper molecules that generate a more robust response. Immunostimulatory adjuvants bind pattern recognition receptors (PRRs) on antigen presenting cells (APCs), eliciting cytokine and surface marker upregulation.

While many novel adjuvants have been discovered, many of these agonists have never been implemented in approved vaccines. Adjuvants face the challenge of balancing adjuvanticity and reactogenicity. Excess reactogenicity can result in adverse events during clinical trials, causing vaccines to fail FDA safety standards. Current adjuvants amplify all downstream components roughly equally after ligand binding. A more potent agonist will improve the immune response, but at the cost of increased side effects and inflammation. We seek to solve this problem by using "immunomodulators" - molecules that selectively inhibit portions of the downstream signaling cascade. This gives a finer control of vaccine adjuvanticity and can potentially reduce reactogenicity while increasing vaccine efficacy.

In Chapter 1, the components of the immune response are reviewed in the context of successful vaccination. In Chapter 2, a "first-generation" immunomodulator, honokiol, is applied to a CpG adjuvanted subunit vaccine against SARS-CoV-2. In Chapter 3, "second-generation" immunomodulators are identified through high-throughput screening of large libraries of commercially available, diverse small molecules. Data from various immunoassays was compiled to create a quantitative scoring system that highlighted top candidates to study in animal models. In Chapter 4, top candidates are combined with commercial vaccines. In influenza vaccines, immunomodulators increased vaccine efficacy, tolerability, and durability.

CHAPTER 1

INTRODUCTION

1.1 The Immune Response

The immune system is a highly specialized collection of tissues, cells, and molecules with one primary purpose: to keep the organism protected from pathogens and disease. The immune response is responsible for distinguishing between self and non-self in the case of external threats like pathogens, and between self and dangerous self in the case of internal threats like cancer[1; 2]. Broadly, the immune system can be split into two main categories, the innate and adaptive immunity. The innate immune system reacts quickly and non-specifically to perceived danger through a group of first responding cells including neutrophils, macrophages, and dendritic cells, among others. These cells engulf pathogens, recognizing foreign threats through pathogen associated molecular patterns (PAMPs) - molecules that are absent from, or in an aberrant location in, the human body[3]. Innate cells will recruit adaptive immune cells by releasing chemical signals, termed cytokines, and presenting portions of the pathogen, termed antigens, on display proteins on the cell membrane[4; 5]. The adaptive immune system reacts slowly, primarily through T and B lymphocytes. Adaptive immunity is specific, due to the unique antigen receptors found on both these cell types. As posed by Burnet's clonal selection theory, individual lymphocytes can only bind to distinct antigens resulting in proliferation and expansion upon activation[6]. Cytotoxic T cells can distinguish between healthy and infected cells, destroying the latter. B cells produce antibodies that primarily bind and neutralize pathogens. Helper T cells activate both B cells and cytotoxic T cells. A portion of activated lymphocytes can differentiate into memory cells, protecting the body with a quicker response against reinfection. This overly simplistic description of the immune response, from pathogen recognition to clearance, will be elaborated on in the rest of this section.

1.1.1 Innate Immunity

Innate immunity is the first line of defense, reacting to encountered pathogens within minutes of introduction into the body. At its most basic level, innate immunity includes physical and chemical barriers to prevent infection without even the use of cells. Quite simply, the skin and mucosa physically shield the body from microbes. From a chemical standpoint, antimicrobial peptides such as defensins, cathelicidins, and histatins are small, cationic, amphipathic molecules that broadly destroy bacteria, yeasts, fungi, and enveloped viruses by disrupting pathogen membranes[7]. More complexly, the complement system contains a collection of soluble proteins which serve many functions in clearance. Complement proteins can opsonize pathogens with soluble factors and can lyse pathogens by forming a membrane attack complex[8]. While beneficial, these portions of innate immunity are not often exploited by vaccines.

Instead, innate immune cells have functions critical for the effectiveness of vaccines. Innate immune cells, like all leukocytes, derive from hematopoietic stem cells in the bone marrow. Most innate immune cells are derived from a common myeloid progenitor and require timely gene regulation, controlled by epigenetics and transcription factors, to differentiate into a unique cell type[9]. Innate cells include the blood-resident granulocytes - neutrophils, eosinophils, and basophils. Neutrophils are present in large numbers and primarily engulf pathogens via phagocytosis[10]. Eosinophils are critical for defense against parasites[11]. Basophils are still largely not understood, but are implicated in allergy and hypersensitivity[12]. To initiate the adaptive response, innate cells must present portions of phagocytosed pathogens on their cell surfaces, a process known as antigen presentation. While granulocytes can perform this task under unique circumstances, it is primarily left towards "professional" antigen presenting cells[13].

Professional antigen presenting cells include B cells, macrophages, and dendritic cells. B cells are adaptive immune cells that present antigen primarily for their own activation.

B cells will be discussed further in the next subsection. Macrophages are derived from either a progenitor or blood-circulating monocytes and represent the primary phagocytes in tissues. They have roles in both inflammation and tissue repair but are not the explicit target for vaccination strategies[14]. Dendritic cells are the main bridge between innate and adaptive immunity. Dendritic cells are the most common cell type to express pattern recognition receptors (PRRs). PRRs bind PAMPs, resulting in an innate immune signaling cascade that results in increased transcription factor activity and cellular activation[15; 16]. Activated dendritic cells can, in turn, activate naïve T cells through the classical three signal paradigm: (1) recognition of peptide bound in major histocompatibility complex (MHC), (2) co-stimulation through CD40 and CD80/86, and (3) detection of appropriate cytokine secretion. Given this cross-talk with adaptive immunity, dendritic cells are the most important innate immune cells in the vaccine response.

1.1.1.1 Pattern Recognition Receptors and Signaling Pathways

Pattern recognition receptors (PRRs) bind a variety of molecules pathogens - pathogen associated molecular patterns (PAMPs). PAMPs include molecules that are exclusive to pathogens, such as lipopolysaccharide (LPS), a major component of bacterial membranes. PAMPs also include molecules that exist in the human body, but are in an aberrant location, such as DNA in the cytosol[17]. PRRs are divided into five major subclasses: toll-like receptors (TLRs), nucleotide oligomerization domain (NOD)-like receptors (NLRs), retinoic acid-inducible gene-I (RIG-I)-like receptors (RLRs), C-type lectin receptors (CLRs), and absent in melanoma-2 (AIM2)-like receptors (ALRs)[18]. TLRs are the most understood and most targeted PRR for vaccine design. The Hoffman lab first discovered the link between the *Drosopholia* receptor protein *Toll* and a host-defense mechanism in 1996[19]. Shortly thereafter, homologs of this protein were found in humans, hence the name Toll-like receptor[20]. In the decades that followed, researchers have uncovered ten TLRs and their ligands as seen

Receptor	**DAMP Ligand**	**PAMP Ligand**	**Ref**
TLR1/2 TLR2/6	β-defensin-3	Lipomannans, Lipoproteins, Lipoteichoic acids	[21; 22]
TLR3	mRNA	Double-stranded viral RNA	[23; 24]
TLR4	HSP60/70, Fibronectin	Lipopolysaccharide, Lipoteichoic acids	[25; 26]
TLR5	None	Bacterial flagellin	[27]
TLR7 TLR8	Endogenous RNA	Single-stranded viral RNA	[28; 29]
TLR9	Endogenous DNA	Unmethylated CpG DNA motifs	[30; 31]
TLR10	Unknown	Unknown	

Table 1.1: Toll-like Receptors and Sample Ligands

in Table 1.1. TLRs can either be expressed on the cell surface, as in the case of TLRs 1/2, 2/6, 4, and 5, or in the endosome, as in the case of TLRs 3, 7, 8, and 9. The discovery of these receptor-ligand interactions provide attractive strategies for potentiating the immune system.

Humans PRRs contain a ligand-binding domain, an intermediate domain, and an effector domain. Upon binding PAMPs, PRRs either dimerize or undergo a conformational change that results in the initiation of a signaling cascade via the effector domain. The signaling cascade can result in the activation of a variety of different innate immune pathways including the nuclear factor κ-light-chain enhancer of activated B cells (NF-κB) pathway, the interferon regulator factor (IRF) pathway, and the activator protein 1 (AP-1) pathway. Activation of these pathways up-regulates transcription factors that drive expression of cytokines and antigen presentation machinery.

To demonstrate this complex signal transduction, one can observe the mechanisms of the NF-κB pathway. Almost all TLRs result in activation of this pathway after recep-

tor dimerization. The cytoplasmic/intraluminal effector domains, called Toll-IL-1-receptor (TIR) domains, are brought together following this dimerization. This allows other adaptor proteins to associate with the TLRs via their own TIR domains. The primary mammalian adaptor protein is MyD88, which interacts with all TLRs except TLR3. The remaining three other adaptors, MAL, TIRF, and TRAM, also play roles in the downstream signaling of TLR2, 3, and 4[32]. The combination of the adaptor proteins involved heavily influences the eventual response[33]. Opposite of the adaptor proteins' TIR domains is a death domain which recruits the serine-threonine protein kinases IRAK4 and IRAK1 through their own death domains. The result is a scaffolding complex which serves as a site to recruit other intermediate signaling molecules[34]. From here, other intermediate kinases and ubiquitin ligases continue the signal propagation, highlighting both the complexity of these pathways and the opportunity to modulate the signal. For brevity, the pathways converge on a distinct molecule, the inhibitor of κB (IκB), a cytosolic protein that constitutively binds the protein subunits of the NFκB transcription factor. On resting state IκB remains bound to the subunits of NF-κB), preventing them from acting as transcription factors. When the pathway is activated, a kinase phosphorylates IκB, degrading the molecule. Now the various subunits of NF-κB can complex to form differing dimers. The main heterodimer responsible for canonical signaling is the p50/p65 heterodimer. This heterodimer primarily controls the expression of genes related to the inflammatory response[35]. In contrast, the noncanonical signaling pathway contains p52/RelB subunits and has a wider range of functions, from B cell survival to antiviral responses[36]. Aside from these main pathways, many other different homodimers and heterodimers can form to create unique responses[37]. The complexity and regulation of these systems lends many opportunities for engineering manipulations.

1.1.1.2 MHCs and Costimulatory Receptors

Innate cell activation and licensing results in the expression of surface proteins as required to prime T cells. The two main surface proteins, MHC and the costimulatory molecules CD80/86 provide signals 1 and 2, respectively, to T cells. MHCI molecules are loaded with antigens from the cytosol after they are degraded by proteasomes and processed by machinery in the endoplasmic reticulum. MHCII molecules are loaded with antigen that is phagocytosed from the extracellular space. These proteins are processed by proteases known as cathepsins. In some cases, cross-presentation can occur in which extracellular antigens escape the endosome and become loaded on MHCI molecules. This is especially important in initiating the CD8 response. MHC molecules are limited in which peptides they can load from both a structural and genetic standpoint. MHCI and II have closed and open grooves, allowing peptides of 8-11 and 13-25 amino acids in length, respectively. Genetically, individuals have differing MHCs due to polymorphism and polygenism. These differences control the types of peptides that can be presented, and the T cells that can recognize the molecules, known as MHC restriction. In an activated state, the machinery involved in the loading and presentation of MHC is heightened, resulting in an increase in the level of expression.

Additionally, the costimulatory molecules CD80 and CD86 are also expressed at higher levels after activation. These surface proteins engage the CD28 receptor on T cells, providing a crucial second signal of activation. These molecules seem to have redundant functionalities and it is debated the differences in their roles in the immune response. Some studies suggested that signaling through these molecules impacts T cell polarization, with CD80 skewing towards a T_H1 response and CD86 skewing towards a T_H2 response[38]. Other potential roles include balancing T cell activation and regulation through the inhibitory CTLA-4 receptor on T cells. CTLA-4 is the counterpart to CD28, serving as a "checkpoint" inhibitor that negatively regulates T cell activity to stop immune responses after the threat is cleared

and to prevent autoimmunity. CTLA-4 has higher affinity than CD28, but is expressed at lower levels. CD80 has two binding sites and has a much lower affinity than CD86, which only has one binding site[39]. Based on these kinetics, it is suggested that CD80 primarily engages CTLA-4 and CD86 primarily engages CD28[40].

1.1.1.3 Cytokines

PRR recognition also results in the production of secreted proteins, known as cytokines, that can signal to other immune cells. Cytokine signaling is very complex, with more than 110 total cytokines - each of which can act on many different types of target cells. Cytokines bind to receptors on the target cell and eliciting a certain response, most often amplifying an effector mechanism. A subgroup of cytokines, termed chemokines, specialize as chemoattractants which recruit cells and cause them to travel towards the origin of secretion. There are about 50 different chemokines, accounting for roughly half of the total cytokines. The rest of the cytokines primarily regulate inflammation, cell growth/development, and adaptive effector functions. As mentioned, the local concentration of cytokines produced by innate cells is a key determining factor of the adaptive immune response. But cytokines are also secreted by adaptive cells, and the interplay between these two arms of immunity will be discussed in the next subsection.

1.1.2 Adaptive Immunity

In contrast to innate immunity, adaptive immunity is incredibly specific towards individual pathogens. It is more powerful and effective than its innate counterpart, but takes time to initiate a response, initiating on the order of days and lasting on the order of weeks. Adaptive immunity is primarily composed of two cell types: B cells and T cells. B cells are primarily responsible for producing neutralizing antibodies, while T cells are responsible for destroying infected cells.

Both cell types have surface receptors that recognize antigens – components of pathogens that can elicit an immune response. Antigen receptors contain two large protein chains. Each chain is generated through the combination of two to three gene segments in a process called V(D)J recombination – named after the three classes of gene segments: i) variable, ii) diversity, and iii) junction. In addition, the pairing of any of the two individual chains creates additional diversity[41]. This mere selection and pairing of gene segments is known as combinatorial diversity. In human antibodies, this combinatorial diversity alone can give rise to a repertoire of approximately 1.9 x 10^6 different receptors. This, however, is not the only means of diversity. During recombination, the addition or subtraction of nucleotides at the junctions between gene segments can generate mutations from the germline sequence in a process known as junctional diversity. Together, these two methods of diversity yield a staggering repertoire estimated to be at least 10^{11} different receptors[42].

This gives the immune system a vast amount of weapons against many possible pathogens. These antigen receptors vary in specificity between each individual precursor cell. Naïve, unactivated lymphocytes patrol the body until they recognize their cognate antigen. According to the clonal selection theory, given the right innate immune conditions as discussed in the previous section, the naïve cells activate upon antigen binging and proliferate rapidly to address the threat[6]. Effector cells assist in neutralizing pathogens, clearing pathogens, and destroying infected cells. A unique hallmark of the immune system is immunological memory. A small subset of activated cells differentiate into long lived memory cells that persist in the body even after pathogen clearance. Upon re-exposure to their antigen, memory cells respond quickly to proliferate and quell the threat much faster than the initial clearance. This phenomenon is the foundation for the protective effects of vaccination. Both T cells and B cells perform unique functions discussed further in the remainder of this section.

1.1.2.1 T-cells

1.1.2.1.1 Origin and Development T cells are named for the primary lymphoid organ in which they develop, the thymus. They are derived from hematopoietic stem cells in the bone marrow, but the progenitors quickly migrate to the thymus for maturation. Here in the thymus, T cells begin to express their antigen receptor, the TCR, and a variety of other proteins required for development and survival. The antigen for TCRs is a short peptide fragment displayed by antigen presenting cells on the major histocompatibility complex (MHC). It is this combination of peptide and MHC (p:MHC) that is necessary to activate the T cell. The antigen receptor for the T cell, the TCR, recognizes is comprised of two chains, either the major lineage $\alpha\beta$ T cells or the minor lineage, $\gamma\delta$ T cells. $\alpha\beta$ T cells are further classified by the single co-receptor, either CD4 or CD8, that bind to conserved regions of the MHC[43]. These cells undergo a unique process during development in which they cycle from double negative for both these receptors, then double positive, before becoming single positive for one of the receptors[44]. In order to leave the thymus and enter the periphery, T cells must undergo a two pronged selection process. As mentioned, the MHC is key for TCR binding, as many amino acid residues close to the presented peptide also contact residues on the TCR, contributing to binding. Thus, it is essential that developing cells can recognize MHC since genes for MHC vary from individual to individual. In a process known as positive selection, developing T cells need to weakly bind to self-peptide MHC present on stromal cells in the thymus in order to receive key survival signals. Without a weak interaction, T cells will enter a programmed death response, deemed "death by neglect". Too strong of an interaction would be detrimental to the host as these T cells would create a strong autoimmune response and destroy host tissue. Thus, the second selection process, negative selection, will destroy strongly reactive T cells through apoptosis[45].

1.1.2.1.2 Effector Functions There are two broad classes of T cells: CD4 expressing helper T cells and CD8 expressing cytotoxic T cells. CD8 T cells have a simpler function – to eliminate pathogen-infected cells. They do so by recognizing class I MHC complexes (MHCI) loaded with their cognate peptide after they have become activated. First, T cells must become activated through interaction with antigen presenting cells, following the three signal paradigm discussed earlier. The signals are: (1) TCR binding to p:MHC, (2) co-stimulation via CD28 binding with CD80/86, and (3) detection of appropriate cytokine secretion[46; 47]. After this initial priming, activated T cells now patrol for infected cells. MHCI is expressed on all nucleated cells in the body, and proteins in the cytosol are processed and presented as a means of surveillance inside cells. If pathogen components are present, the corresponding CD8 T cells will, upon binding, release perforin and granzyme proteins that create pores in the infected cell's membranes, initiating apoptosis[48; 49].

More unique are CD4 helper T cells which have diverse subtypes and function to assist other cells, hence their nomenclature. CD4 T cells undergo roughly the same process of priming as their CD8 counterparts. Depending on the cytokine environment created by the antigen presenting cell, however, activated CD4 T cells will differentiate into a variety of effector cells. This phenomenon was first discovered with the identification of two types of CD4 T cells, T_H1 and T_H2, defined by the cytokine profiles they expressed[50]. It was proposed that these cells differed in their functions with T_H1 cells primarily helping CD8 T cells and T_H2 cells primarily helping B cells. This theory has evolved over time, with these simplistic prior defined subsets becoming more complex[51]. New cell types were identified including T_H17, T_{FH}, and T_{reg} cells. CD4 T cells are now known to differentiate based on the cytokine environment created by APCs during their initial priming[52]. These cytokines induce different activation patterns of the JAK-STAT pathway, resulting in differing expression of master transcription factors. These transcription factors drive unique gene networks, resulting in the expression of differing secreted cytokines for each T helper subset. An overview

of these conventional T_H subsets can be seen in Table 1.2. These secreted cytokines have a wide range of impacts on both the cells presenting antigen to T cells, and other immune cells away from this reaction. For example, T_{FH} cells secrete IL-4 when recognizing antigen on B cells, resulting in their activation, growth, antibody class switching, and germinal center formation[53]. As a systemic effect, T_H2 cells secrete IL-5 which differentiates hematopoietic stem cells into eosinophils[54]. While this is the most common method of describing T_H subsets, other proposals and models exist and will be further explored in the next section.

Subtype	**Polarizing Cytokines**	**Transcription Factor**	**Secreted Cytokines**
T_H1	IFN-γ, IL-12	T-bet	IFN-γ
T_H2	IL-4	GATA-3	IL-4, IL-5, IL-13
T_H17	TGF-β, IL-6, IL-23	RORγT	IL-17, IL-22
T_{FH}	IL-6	Bcl-6	IL-21
T_{reg}	TGF-β, IL-2	FoxP3	TGF-β, IL-10

Table 1.2: Conventional T_H Subtypes

1.1.2.2 B-cells

1.1.2.2.1 Origin and Development B cells develop in the bone marrow, but were named for the avian organ, the bursa of Fabricius, in which they were discovered[55]. B cell development is dependent on survival signals through the B cell antigen receptor, the BCR. B cells derive from hematopoietic stem cells, and begin to rearrange the genes on the heavy chain of the BCR first, creating a complex known as the pre-BCR[56]. If this is successful, the B cell transitions from a pro-B cell to a pre-B cell, where the light chain begins rearrangement. Successful light chain rearrangement results in immature B cells which are tested for self reactivity before leaving the bone marrow. Strongly self reactive B cells attempt receptor editing, where they alter their BCRs to lose this reactivity in a process known as central tolerance[57]. B cells that are still strongly reactive will undergo

apoptosis, while weakly self reactive B cells will become anergic. Non self reactive B cells will be released into the periphery with a fully formed BCR.

1.1.2.2.2 Effector Functions Once in the periphery, naïve B cells must be activated before they can perform their effector functions. B cells will engulf pathogens via their BCRs. Unlike T cells, the BCR recognizes a three dimensional epitope. Many epitopes are conformational - meaning they are a result of secondary and tertiary protein structure instead of the primary amino acid sequence. Once endocytosed via the BCR, antigens are processed and presented on MHCII molecules. Thus, B cells are actually considered professional antigen presenting cells, like dendritic cells. Most B cells, especially those targeted in vaccines, recognize antigens that are thymus dependent and require T cell help. T_{FH} cells in germinal centers are the primary means for naïve T cell help and maturation. In the germinal center reaction, B cells undergo affinity maturation to more strongly bind antigen through a process known as somatic hypermutation. B cells mutate their BCRs and proliferate these new clones in the dark zone of germinal centers before moving to the light zone[58]. Here, the B cells compete for antigen held by follicular dendritic cells - a misnomer as these cells are of a stromal, not hematopoietic origin. Theoretically, BCRs with higher affinity should be more efficient at antigen uptake, resulting in more T cell help. This T cell help comes in the form of the CD40-CD40L interaction which activates the non-canonical NF-κB pathway.

Once activated, the primary function of B cells is to secrete antibodies, the soluble version of the BCR. B cells can express one of five major isotypes of antibodies (immunoglobulins) IgM, IgA, IgG, IgE, and IgD[59]. IgM can be secreted in a pentameric form, and is typically a lower affinity antibody with a high degree of complement activation. IgA can be secreted as a dimer and is most present in mucosal spaces. IgG is the most abundant isotype in serum/blood, and can be further divided in subclasses, IgG1, IgG2, IgG3, and IgG[60]. IgE is mostly present on mast cells and has a large impact on allergic and anti-parasitic response. IgD is the least understood isotype and is thought to interact with basophils. All B cells

begin by expressing IgM but can change isotypes through a process known as class switching. The genome contains loci for the constant region of each of these isotypes, and enzymes can result in the irreversible excision of exons for each isotype. This process is controlled by the cytokine environment created by helper T cell[61]. In fact, the ratio of subclasses of IgG is often used as a benchmark for the degree of T cell polarization - a high IgG2c/IgG1 ratio is indicative of a T_H1 response.

After activation and participation in the germinal center reaction, most B cells will begin to develop into their terminal state, plasma cells. B cells begin to downregulate surface BCRs, and increase their secretion of antibodies as plasmablasts, an intermediate cell type. Some plasma cells will migrate to the bone marrow where they persist as long lived cells and continue to secrete antibodies. The main role of antibodies is to bind and neutralize pathogens through their variable domain, the antigen binding fragment (Fab). Neutralizing antibodies (NAbs) prevent pathogens from infecting cells, usually binding to protein epitopes that are critical for the pathogen's ability to gain cellular entry. Antibodies can also serve as opsonins, tagging molecules for degradation an phagocytosis. This is mediated by the antibody's fragment crystallizable region (Fc) - a conserved region that is recognized by Fc receptors (FcRs) on other cell types. Finally, antibodies can also activate the complement system through its classical pathway, allowing innate immunity to assist in pathogen clearance.

1.2 Vaccines

Vaccines are considered one of the greatest inventions of modern medicine. In the past century, vaccines have reduced the mortality and morbidity of numerous diseases in developed countries. It is lost on newer generations how devastating these diseases were - it is estimated that vaccines prevent 6 million deaths globally each year[62]. Vaccines serve as sort of "training" of the immune system. They vary in composition and technology, but the general

goal is the same: to elicit immune memory against a specific pathogen. Upon re-exposure to a similar pathogen, the immune system responds rapidly, clearing and destroying the pathogen, ideally before severe infection and pathology can begin. The rest of this section is dedicated to the overview of vaccines: from their history, to their platforms, to the diseases they target.

1.2.1 History of Vaccines

Since ancient Greece, humans have known that encounter with, and survival from, a disease granted the individual increased protection upon re-exposure. In the 1400s, in China and the Middle East, humans used variolation – or the transfer of smallpox pustules from diseased individuals to purposefully created wounds of healthy individuals[63]. In 1796, Edward Jenner noticed that milkmaids seemed to resist infection from smallpox. He postulated this was because of their exposure to cowpox on the animals they worked with. Cowpox, also known as vaccinia, presented as a milder disease in humans. Thus, Jenner inoculated a young boy with cowpox, and, two months later, purposefully exposed the boy to smallpox. While ethically problematic, the cowpox procedure prevented small pox – hence the etymology of vaccines[64]. The result is a strategy still pursued today – mimic infection in a controlled, safe manner to grant protection for against future exposure. Vaccination still took centuries to fully develop into an accepted practice. At the time, Jenner was unaware infectious disease was caused by pathogenic microorganisms. Advancements in microbiology and immunology gave scientists a greater ability to identify the causative agent of diseases. These pathogens could then be isolated and altered for vaccination. The father of modern vaccines, Maurice Hilleman, prolifically developed about 40 whole pathogen vaccines in the mid-to-late 1900s[65]. Some vaccines he developed, notably against measles and mumps, are still used in the childhood vaccination schedule today. This first generation of vaccines provided the first technology platform for vaccination, but others have recently been developed.

Most recently, the SARS-CoV-2 resulted in the commercial realization of mRNA vaccines, a technology that has been in development for decades. The rest of these vaccine technologies, and the diseases they target, will be discussed in the rest of this section.

1.2.2 Types of Vaccines

1.2.2.1 Whole-Pathogen Vaccines

The oldest and most common type of vaccines are whole pathogen vaccines that have been engineered to no longer cause active infection. The vast majority of childhood vaccines are whole pathogen vaccines. These vaccines can be inactivated vaccines which are killed via chemical or heat treatment. Perhaps the most ubiquitous inactivated vaccines are against seasonal influenza. Alternatively, some vaccines are live-attenuated vaccines - meaning the pathogen is still replication competent. These pathogens are typically made attenuated through multiple passages, or generations, through culture from a species different from humans. The pathogen loses its virulence in humans with each passage as it adapts towards the other species. As an example, the childhood MMR vaccine contains live attenuated strains against the causative agents of measles, mumps, and rubella. Whole pathogen vaccines contain endogenous pathogen associated molecular patterns, as they are the vaccines most similar to natural infection. Thus, the pathogen alone is usually sufficient to induce an initial protective immune response. Live attenuated vaccines often provide stronger protection than inactivated vaccines, as inactivated vaccines often require booster injections. Whole pathogen vaccines have some drawbacks, mainly in safety and control of the immune response. Producing the pathogens for these vaccines requires culture of live, infectious agents at large scales. Also, in rare cases, live attenuated vaccines could theoretically mutate back into a virulent strain. This possibility was a contributing factor for the switch from a live attenuated polio vaccine to an inactivated version in the recommended vaccine schedule.

1.2.2.2 Toxoid Vaccines

Some diseases are not caused by the presence of a microbe itself, but rather by toxic substances produced by the microbe. This is most common for bacteria. As an example, the bacterium *Clostridium tetani* produces a neurotoxin responsible for the tetanus disease. Instead of targeting *Clostridium tetani*, tetanus vaccines are toxoid vaccines that target the toxin directly. Similar to whole pathogen vaccines, the toxin is inactivated by chemical or heat treatment. Because they are only proteins in an inactive state, toxoid vaccines are less immunogenic and often require additional immunostimulatory components to provide protection. Both tetanus and diphtheria are examples of toxoid vaccines.

1.2.2.3 Subunit Vaccines

Instead of using a whole pathogen, the next generation of vaccines elicit responses against key components, or a "subunit" of the pathogen. Subunit vaccines often target pathogen components that are responsible for virulence or cellular entry. The first approved subunit vaccines in the US were for Hepatitis B in 1981[66]. This vaccine employs a protein subunit - the Hepatitis B surface antigen (HBsAg). The HBsAg used in the original vaccines was obtained through the blood of infected patients - a methodology that would be impermissible today given the risks considering bloodborne pathogens. Five years later, advances in recombinant protein expression, where manipulated DNA sequences allow transfected cells to produce protein, led to an updated vaccine with the protein created via yeast cells. By selecting the most critical antigens, subunit vaccines result in a more focused immune response which is beneficial for protection. Subunit vaccines are safer than whole pathogen vaccines as they provide a more controlled response as they lack high amounts of endogenous PAMPs. These vaccines are also produced in a safer environment without the risk of contracting infectious disease. This increased safety, however, comes at the cost of reducing the immunogenicity of

the vaccine. Without the proper levels of danger signals, the immune response is markedly lower in subunit vaccines compared to their whole pathogen counterparts. To mitigate this reduction, subunit vaccines often contain helper molecules, known as adjuvants, to boost the innate immune response to the appropriate level. Adjuvants will be discussed in depth in the next section.

1.2.2.3.1 Conjugate Vaccines Subunit vaccines composed of polysaccharide antigens often conjugate these antigens to a carrier proteins, creating a "conjugate vaccine"[67]. Polysaccharide and carbohydrate antigens are not efficiently presented on antigen presenting cells and thus lack a strong T cell response. Antibodies can still be elicited by polysaccharide antigens through the cross-linking of multiple BCRs due to their multivalent structure, though these B cells will not undergo affinity maturation and thus are less likely to create strongly neutralizing antibodies. Thus, conjugating the polysaccharide antigen to a protein carrier can allow for T cell help and a stronger protective response. The first conjugate vaccine for use in humans in the US was approved in 1987 against *Haemophilus influenzae* type b. Other conjugate vaccines have been developed since, mainly targeting the capsules of bacteria. Most of these vaccines employ the toxoid proteins from diphtheria and tetanus, discussed earlier, as their carrier protein.

1.2.2.3.2 Virus-Like Particles Another subset of subunit vaccines, virus-like particles (VLPs) are a novel platform to increase the immunogenicity of unique protein antigens[68]. Some antigens, mainly those that form the capsid of viruses, can self assemble into a particle structure that resembles an "empty shell" of the virus itself. This similarity in structure provides a few key benefits. First, dendritic cells exhibit increased uptake of these particles compared to monomeric protein. Second, VLPs exhibit sizes from 20 to 200 nm, which is ideal for drainage to lymph nodes via the lymphatic system[69]. Finally, the multivalency of the antigen can strongly crosslink BCRs to provide a stronger B cell response, similar

to polysaccharide antigens. Part of the success of the Hepatitis B vaccine mentioned above was due to self-assembly into VLPs. This is challenging because most capsid proteins are not the primary vaccine target for the pathogen. In this case, a chimeric VLP must be generated, with the target antigen interspersed within the structural capsid proteins. Still, this technology platform is being actively explored.

1.2.2.4 Nucleic Acid Vaccines

Instead of provided exogenous antigen as in the case of subunit vaccines, nucleic acid vaccines include DNA and RNA vaccines and rely on endogenous production of the antigen by the host cells. Following the central dogma of biology, this vaccine technology relies on providing genetic information in the form of DNA or RNA. The DNA or RNA is transcribed or translated by host machinery after recognition in the nucleus or cytosol, respectively. Antigen is then released and the immune response is initiated in the same manner as a subunit vaccination. Nucleic acid vaccines face a few challenges. DNA based vectors have safety concerns with integration into host cellular DNA, though this has only been observed at minimal levels. Both vaccine types require proper delivery to the cell. While DNA is more stable, it often requires electroporation to cross the cellular membrane. RNA does not need this treatment, but is fragile and thus is usually formulated into a particle for protection. Both vaccine types can also elicit inflammatory effects via PRRs in innate cells. Thus, nucleoside modifications are often used to minimize this activation. Despite the challenges, nucleic acid vaccines are very attractive as they can be produced and altered quickly and efficiently. This is particularly important in pandemics, as evidenced by the SARS-CoV-2 outbreak which resulted in the first US approval of this vaccine technology with the use of mRNA vaccines from Pfizer-BioNTech and Moderna in 2021.

1.2.2.5 Viral Vector Vaccines

Viral vector vaccines are built on the backbone of a "harmless" virus, also known as the vector. The viral vector genome is edited to induce expression of the antigen of interest, often substituting for the corresponding native protein. Many different vectors have been studied for use in vaccines including vesicular stomatitis viruses (VSV), vaccinia viruses, and adenoviruses. Vectors can either be replication competent, similar to live attenuated vaccines, or engineered to be replication deficient, similar to inactivated vaccines. Viral vector vaccines have the same advantages and drawbacks as other whole pathogen vaccines, with a few differences. As a positive, viral vector vaccines are attractive for use against diseases with severe biosafety hazards. For example, the first viral vector vaccine approved in the US was against Ebola in 2019. This vaccines used a VSV vector with the envelope glycoprotein replaced with that of the glycoprotein from the Kikwit strain of the *Zaire ebolavirus*. Viral vector vaccines allow for the intrinsic immunogenicity of a whole pathogen, but still remain difficult to control even given genetic editing tools. The Oxford-AstraZeneca and Janssen COVID-19 vaccines were engineered with adenovirus backbones, a chimpanzee adenovirus, ChAdOx1, and an adenovirus serotype 26 vector, respectively. Both vaccines were eventually suspended as they exhibited a rare and potentially fatal thrombosis with thrombocytopenia syndrome, a blood clotting disorder which mechanism is still largely unknown. This is likely unique towards the adenovirus backbone, but sill presents an obstacle that could be mitigated with other vaccine platforms.

1.3 Adjuvants

The term adjuvant comes from the Latin “adjuvare”, meaning “to help”, a fitting term as adjuvants help activate innate immunity, increasing the efficacy of a vaccine. Adjuvants work though a complex interplay of innate and adaptive sensors. Broadly, there are two

classes of adjuvants: delivery and immunostimulatory. Delivery adjuvants are those that improve the uptake and availability of vaccine components, but do not necessarily impact innate immune cells. Immunostimulatory adjuvants are most natural or synthetic analogs of PAMPs that directly activate innate immune cells. Adjuvants were first used in human vaccines in 1932, with a singular molecule, alum, remaining the only adjuvant in use for nearly 70 years. This can largely be attributed to the widespread use of whole pathogen vaccines as they contained many endogenous PAMPs resulting in strong immune activation, negating the need for adjuvants. However, with the advent of next generation vaccines, namely subunit vaccines, the need for adjuvants has grown. Yet, there are currently only 7 different adjuvants used in FDA approved vaccines as seen in Table 1.3.

Adjuvant	**Type**	**Description**	**Vaccines**	**Date**	**Ref**
Alum	Delivery	Aluminum Salts $Al(OH)_3$ and $AlPO_3$	Hepatitis A and B, Tdap/DTaP, HIB, HPV, Pneumococcal, Mengicoccal	1932	[70]
AS04	Both	Alum and MPLA (TLR4 Agonist)	HPV	2009	[71]
AS03	Debated	Tocopherol oil-in-water	Pandemic H5N1 Influenza	2013	[72]
MF59	Debated	Squalene oil-in-water	Seasonal Influenza	2016	[73]
$AS01_B$	Stimulatory	QS-21 (saponin), MPLA (TLR4 Agonist)	Zoster (shingles)	2017	[74]
CpG 1018	Stimulatory	TLR9 Agonist	Hepatitis B	2017	[75]
Matrix-M	Stimulatory	QS-21 (saponin)	SARS-CoV-2	2022	[76]

Table 1.3: Adjuvants in FDA Approved Vaccines

As adjuvants greatly influence both the type and quality of immune response, their limited availability and diversity hampers new vaccine development. New adjuvant discovery could help generate protective responses against vaccine-resistant diseases.

1.3.1 Traditional Adjuvant Development

1.3.1.1 Delivery Adjuvants

Adjuvant discovery is historically very empirically driven. The first adjuvant, alum, was discovered fortuitously in the development of a diphtheria vaccine when Alexander Glenny was purifying and concentrating toxoids. He and colleagues noticed that vaccines containing toxoids that were precipitated with aluminum salts led to improved antibody responses[77]. This emulsion with "alum salts" was studied further with the prevailing hypothesis that a "depot effect" caused the increased immune response[78]. The depot effect states the antigens adsorb to alum's charged surface, resulting in a delayed, sustained release from the injection site. The increased availability of the vaccine over time prolongs and strengthens the immune response. At physiological pH, aluminum hydroxide has a positive charge whereas aluminum phosphate has a negative charge[79]. These different charges allow for absorption of protein antigens at wide ranges of isoelectric points. Such a sustained release model is supported by some modern experimentation, such as the sustained release of HIV antigens in an osmotic pump model[80]. However, the depot theory has been challenged by other recent accounts which attribute the adjuvanticity of alum to immunostimulatory effects through the NLRP3 inflammasome[70]. These findings, combined with the immunostimulatory effects of most other adjuvants, suggest a reclassification that no molecule is a pure "delivery" adjuvant.

As further evidence, water-in-oil and oil-in-water adjuvants were initially developed to mimic the depot effects of alum. The water in mineral oil adjuvant, ISA 51, developed by Seppic in the early 2000s, however, was found to be reactogenic[81]. Though this could be due to impurities in the source materials, it is thought that these emulsions can elicit responses akin to damage-associated-molecular patterns (DAMPs)[82]. Perhaps the best example is the squalene oil-in-water emulsion MF59, originally developed in the early 1990s to again sustain and delay antigen release over time. The use of smaller amounts of fully

metabolizable squalene oil reduced the reactogenicity of the adjuvant, but also removed any depot effect inherent to the emulsion[83]. Still, MF59 increased vaccine efficacy through a different mechanism. While still debated, MF59 is also thought to cause tissue damage and the resulting DAMPs cause an cytokine and chemokine environment that recruits innate immune cells and promotes monocyte differentiation into dendritic cells[84]. MF59 is currently in use with Fluad, a commercially available seasonal influenza vaccine. Another very similar adjuvant, AS03, is a squalene oil-in-water emulsion but contains α-tocopherol, a type of Vitamin E. α-tocopherol boosts antibody responses higher than that of MF59 due to increased antigen loading into monocytes, and a slightly altered cytokine environment[85; 86]. AS03 is currently in use in the US stockpile of pandemic influenza vaccines.

1.3.1.2 Immunostimulatory Adjuvants

Direct simulation of the innate immune system is the more commonly adopted strategy of modern adjuvants. As early as 1942, pathogenic components were known to boost the immune response. Jules Freund observed that guinea pigs vaccinated against horse serum exhibited higher sensitization when killed *Mycobacterium tuberculosis* was used in an oil-in-water adjuvant[87]. This would later be known as Complete Freund's Adjuvant (CFA). CFA primarily activates innate immunity through the bacterial cell wall component, lipopolysaccharide (LPS), a potent TLR4 agonist. While LPS is too toxic for use in humans, naturally occurring or synthetic mimetics of PPR agonists are employed in adjuvants today. In fact, a detoxified derivative of LPS, monophosphoryl lipid A (MPLA), was developed as a safer, yet still effective, TLR4 agonist. MPLA is created through a hydrolytic process in which two phosphate groups, polysaccharide side groups, and one or more acyl chains are removed from LPS derived from *Salmonella minnesota*[88]. MPLA is combined with alum in AS04, which became the first new adjuvant in a US approved vaccine in more than 70 years. AS04 was first included in a US vaccine against human papillomavirus (HPV) in 2009.

One of the newly approved adjuvants, QS-21, is a component of a class of molecules, saponins. Saponins were first noted for their adjuvant effect in 1925, while also recognized for its medicinal properties by indigenous peoples[89]. Saponins used in adjuvants are purified from the bark of a Chilean tree, *Quillaja saponaria* using silica and reverse phase chromatography. QS-21, the 21st fraction isolated, was found to be the best combination of minimal toxicity, increased efficacy, and high yield[90]. Clearly, this approach follows the theme of empirical discovery. QS-21 is combined with MPLA in the $AS01_B$ adjuvant, first included in a zoster virus vaccine to prevent shingles in the US in 2017. $AS01_B$ is notoriously very reactogenic, but its efficacy is also highly regarded[91]. Even more recently, QS-21 was developed into the newest adjuvant to be included in an approved vaccine - Matrix-M in the 2022 SARS-CoV-2 vaccine from Novavax. QS-21 is thought to work through activation of the NLRP3 inflammasome, resulting in alterations in antigen presenting cells which drive a T_H1 immune response[92]. QS-21 is a complex and difficult to synthesize molecule, however, with mounting concerns over the sustained availability of the *Quillaja saponaria* tree.

The last adjuvant in an FDA approved vaccine to be discussed is the TLR9 agonist CpG 1018. CpG 1018 is a synthetic oligodeoxynucleotide (ODN) - named such for its regions of unmethylated CpG motifs. These motifs are common in prokaryotic DNA but are rare in eukaryotic DNA. Thus, CpG ODNs are effective PAMPs to trigger innate immunity. These molecules represent a successful attempt at rationally guided adjuvant design after bacterial DNA was noted to activate the immune response in the late 1990s[93; 94]. From this discovery, different exact sequences of CpG ODNs were synthesized and screened for their ability to potentiate TLR9. These efforts resulted in the approval of CpG 1018 in use with the Hepatitis B vaccine from Dynavax in 2017[95]. CpG 1018 has acceptable reactogenicity compared to most other ODNs which can cause adverse events. CpG 1018 is attractive for its ability to generate T_H1 responses, a welcome change from the T_H2 responses generated from the traditional alum adjuvants[96]. CpG 1018 gives a strong success story for next

generation adjuvants as a readily available synthetic analog with a known mechanism and rational design.

1.3.1.3 High Throughput Screening

Adjuvant development has been laborious and slow, but has begun to accelerate over the past decade. Current adjuvant development consists of screening for an activating molecule, formulating lead molecules with an antigen, and testing this combination in an animal model. Advances in high throughput screening (HTS) has allowed researchers to discover and optimize activating molecules at a much quicker rate. To increase throughput, microtiter plates of have been further miniaturized to 384 or even 1536 wells enable more samples to be processed with the same time and reagents. Automated liquid handling and robotic systems have also greatly increased the amount of plates run in a single day. HTS for drug discovery first began to gain popularity in the late 1990s[97]. As biological tools and chemical libraries became more sophisticated, this technique began to yield fruitful results and dispel negative preconceptions[98]. A new class of TLR7/8 agonists, imidizaquinolones were discovered via screening for anti-herpes molecules[99]. The resulting molecules imiquimod (R837) and resiquimod (R848) are potent small molecules that have been explored in cancer clinical trials. To improve biodistribution, 3M developed an imidizaquinolone with a lipid tail, 3M-052, which is currently undergoing clinical trials for an HIV vaccine[100]. HTS is now a uniquitous tool that continues to identify novel PRR agonists that could perhaps be developed into future agonists.

1.3.2 Engineering Next-Generation Adjuvants

1.3.2.1 Target Identification and Signal Engineering

Adjuvants can be improved by selectively modifying signaling pathways to elicit desired immune outcomes. Instead of designing more potent receptor agonists, more diverse results can be had by exploring alternative strategies. Apart from PRRs, other cellular signaling pathways like metabolism and proliferation have been linked to immune outcomes. Innate pathway activation results in fate-specifying cytokines which control helper T-cell polarization. Adjuvants impact this elicited cytokine milieu, and tuning this process gives researchers greater control over adaptive responses. Cytokines are also responsible for vaccine reactogenicity. Reducing cytokines associated with excess inflammation would alleviate adverse side effects, improving the likelihood of clinical translation. Modifying traditionally targeted pathways and exploring new pathways can address all these innate related signaling problems.

1.3.2.1.1 Alternative Pathways for Adjuvanticity Adjuvant targets should continue to expand beyond ligands for traditionally targeted toll-like receptors (TLRs). In the past decade, research efforts have revealed agonists for newly discovered pattern recognition receptors, most notably the STING ligand cGAMP[101; 102]. Additionally, the NLRP3 inflammasome responds to broad disruptions in homeostasis, and serves to recognize a variety of PAMPs and DAMPs[103]. Besides PRRs, other signaling pathways impact innate immune activation and could be exploited for future adjuvant development. Cell death pathways in the form of apoptosis, pyroptosis, and necroptosis may result in increased cross presentation by activated, neighboring cells[104; 105]. Metabolic and epigenetic pathways are altered in trained immunity, a newly emerging concept where innate immune cells exhibit "memory" via heightened activation upon re-exposure to even heterologous pathogens[106]. These

pathways represent a vast pool for novel adjuvants, as many activators of these pathways are currently being discovered.

1.3.2.1.2 Altering T-cell Polarization Adjuvants can control T-cell polarization by inducing specific cytokines, but currently approved adjuvants are limited in this capability. Some adjuvants, like CpG 1018, are potent T_H1 inducers whereas others, like alum, are strong T_H2 inducers[107; 108]. T_H1 responses are typically desired for prophylactic vaccines, but ideally, vaccine and immunotherapies could be uniquely tailored to the application. For example, applications outside of infectious disease could benefit from alternative T_H polarization. T_H17 cells, characterized by the production of IL-17, are implicated in protection against extracellular bacteria, and are critical in host responses to infection by *Klebsiella, Pseudomonas, Salmonella*, and *Bordetella*[109]. T_H17 cells may increase protection against tuberculosis via neutrophil recruitment and inflammation mediation[110]. The extent of T_H17 polarization is important, however, as excess T_H17 responses can also worsen TB pathologies[111]. Thus, fine control over T_H polarization is needed, not simply general shifts from one bias towards another bias. With a limited number of approved adjuvants, this fine control over T_H polarization is challenging. Traditional adjuvant development remains focused on the initiation of signaling events through receptor-ligand interactions with downstream effects like T_H polarization left as an afterthought. Next-generation adjuvant discovery should change this paradigm, focusing on end immunophenotypes like TH polarization.

With expanded understanding of the helper T-cell compartment, the conventional nomenclature for T_H polarization may be limiting[112]. T_H polarization traditionally relies on the profile of secreted cytokines from helper T cells. What started in the late 1980s as a two part T_H1/T_H2 model expanded with the discovery of T_H17 cells in the mid 2000s[50; 113]. Additionally, CD4+ T cells that serve in unique roles, such as regulatory T-cells (T_{regs}) and follicular helper T-cells (T_{FH}), further complicate T_H classification[114; 115]. Finally,

many other T_H subtypes have been proposed in recent years including T_H9, T_H22, and T_HGM[116–118]. The number of potentially expressed cytokines makes the current classification system impractical. Instead, T_H polarization could be classified by the five master transcription factors, T-bet, GATA-3, RORγT, Bcl-6, and FoxP3[119]. Expression of these transcription factors was once thought to be mutually exclusive, but recent studies show that co-expression of transcription factors is possible[120; 121]. T_H polarization could be represented as a location in a multidimensional space with levels of transcription factor as the axis variables. Such a classification could either apply to the total helper T-cell response as an "average" phenotype, or it could also apply to individual helper T-cells. Adjuvants could then be developed to polarize T_H responses across different locations in this multidimensional space, resulting in new vaccine outcomes.

1.3.2.1.3 Reducing Reactogenicity of Adjuvants Reactogenicity is the main challenge against the approval of many new adjuvants[16]. Adjuvants must provide enough stimulation to provide protection, while avoiding excess activation which result in adverse side effects. The inability to control this balance limits the number of clinically approved adjuvants and leads to the withdrawal of certain vaccines. Adjuvant associated local and systemic inflammation leads to side effects like injection site pain, fever, and headache[122]. Inflammation can be tracked through measuring IL-6 and TNF-α between 1 and 24 hours after injection[123]. These cytokines have been extensively studied and their role in inflammation is well explained in these reviews[124–127]. Severe reactogenicity damages not only patient physical health at the individual level, but also public vaccine perception at the population level. Minimizing vaccine reactogenicity while maintaining efficacy is a top priority for next generation adjuvants. It is important to obtain reactogenicity information early in the adjuvant discovery process, to ensure that lead compounds are identified quickly and screened for toxicity or inflammation related side effects.

As an example, reactogenicity limits mRNA vaccine doses as both the mRNA and lipid

nanoparticles induce excess inflammation[128]. Currently, mRNA vaccine reactogenicity is addressed via nucleoside modified mRNA. It remains unknown, though, how lipid nanoparticles activate innate immunity. Many hypotheses have been suggested, from direct sensing of particles to indirect sensing of particle-induced cellular damage[129]. Identifying such innate immune mechanisms is critical to identify effective adjuvants with reduced reactogenicity. With knowledge of the appropriate signaling targets, adjuvants could be screened for reduction of pro-inflammatory cytokines in combination with conventional mRNA vaccine systems.

1.3.2.2 Formulation and Targeted Delivery

Next generation adjuvants are often formulated to enhance delivery and efficacy. Early approved adjuvants did not target cells of interest, mostly using aqueous solutions as simple formulations. But recently approved adjuvants often cannot rely on aqueous solutions alone. Adjuvant systems, like GlaxoSmithKline's AS series, contain many components and are often formulated into nanostructures[130]. Another example is NovaVax's Matrix M, in which immunostimulatory saponins are formulated with phospholipids and cholesterol[131; 132]. As adjuvants become more complex, formulation should be considered earlier in development and discovery. With the use of more and more new molecules, their association with delivery vehicles will become even more critical. Expanding the diversity of adjuvants necessitates trafficking to a variety of subcellular locations to aid receptor binding. Target receptors may be on the outer membrane, endosomes, or cytosol. Formulation warrants its own in-depth review, but discussed here are the most relevant engineering parameters as related to adjuvants.

1.3.2.2.1 Encapsulation and Size Many adjuvants and vaccines can improve cellular delivery through passive targeting via encapsulation in particles[133]. Structures such as

virus like particles and liposomes better mimic pathogen geometries and improve uptake and antigen processing. Simply encapsulating the TLR9 adjuvant, CpG, into a nanoparticulate greatly improves protection against lethal anthrax challenge studies[134]. When using particle-based formulations, size of the particle is an important and simple factor to control. For example, 10-100nm particles are the most efficient in lymphatic drainage, allowing facile diffusion to key secondary lymph organs[69; 135]. Inside of this size range, particles of 50nm are shown to be key in inflammasome activation as they aid in endosomal escape[136]. Alternatively, larger, micron sized particles show reduced cellular uptake, limiting efficacy[137]. If optimizing adjuvanticity, particle size should be selected to aid in the delivery towards the proper location.

1.3.2.2.2 Charge Charge of adjuvants and their formulations is another important property to engineer. Alum, the most widely used adjuvant, relies heavily on surface charge. Particulates, especially polymer-based systems, can also exhibit charge. Combined, the charge of a system alters interaction with innate immune cells[138]. Generally, cationic systems enhance cellular uptake and activation more than anionic systems. Cationic systems also have important benefits after cellular uptake to aid in subcellular targeting. Lipid nanoparticles in the COVID mRNA vaccines contain cationic lipids that, in the proper ratio, aid in endosomal escape and delivery of the mRNA into the cytosol[139; 140]. A cationic system also enhances immune activation of STING agonists, as this innate receptor is also located in the cytosol[141]. At many stages of adjuvant processing, charge has heavy impacts on the end signaling result.

1.3.2.2.3 Targeting Ligands Formulations can also include external targeting ligands to aid delivery to desired cell types. While adjuvant receptors are expressed primarily by immune cell types, bystander cells are sometimes affected by adjuvants. For example, arterial smooth muscle cells express TLR4. Activation of these cells promotes proinflammatory phe-

notypes that are linked to atherosclerotic lesions[142]. Thus, off-target effects on bystander cells should be limited. Not only do targeting ligands decrease side effects, but they also increase efficacy. Recent studies demonstrate the dendritic cells can be targeted via DEC-205 and DC-SIGN[143–145]. When combined with an adjuvant, antigen delivered with DEC-205 ligands result in increased processing and presentation. Endocytosis mediated by DC-SIGN increases cross-presentation, allowing for the activation of CD8+ T cells from extracellular antigen. More niche cell types can also be targeted. As knowledge of fundamental immunology expands, more cell types warrant targeted delivery. Lymphatic endothelial cells, stromal cells that are implicated in long-term antigen storage, could be targeted via the VEGFR3 receptor[146; 147]. First responder cells, dendritic cells that excel at phagocytosis of microstructures, could be targeted via the DAP12 and PRG2 receptors[148; 149]. Altogether, targeting ligands are a critical component of formulations.

1.3.3 Evaluating Next-Generation Adjuvants

With a greater number of approaches to discovery, an improved diagnostic framework is needed to evaluate new adjuvants. Traditional evaluation relies on laborious in vitro assays and synthetic modifications before preclinical studies in mice and non-human primates. This process of adjuvant discovery is notably one of the slowest processes in medicine[70]. Currently, translational results take years to obtain. Showcased here are alternative frameworks to evaluate adjuvants for early correlates of vaccine efficacy. These frameworks can accelerate evaluation and reduce costs of adjuvant discovery. New computational approaches will aid in early-stage screening while rethought animal models will aid in preclinical trials.

1.3.3.1 Computational and Big Data Approaches

Technological and computational advances of the past few decades allow for restructuring of adjuvant discovery. Vaccine and adjuvant design is not limited to the simplistic “guess-and-

check" empirical methods of the past. Instead, newer assays can provide massive amounts of data, assisting researchers on mechanistic understanding and efficacy evaluation. Next generation sequencing and other omics approaches allow for system level data collection. Machine learning and computational power enable in silico binding simulations. High content imaging and processing yield hidden patterns and features. Combined, these computational approaches retool all stages of adjuvant design.

1.3.3.1.1 Systems Vaccinology In the age of "big data", adjuvant discovery benefits from a systems vaccinology approach that integrates large amounts of information. Compared to twenty years ago, immunological assays generate results with vastly improved speed and sensitivity. This allows researchers to collect data from numerous different experiments instead of relying on singular indications like antibody titers. Systems vaccinology looks to consolidate information from high throughput assays on cytokines, proteins, metabolites, gene expression, and other screens to obtain a comprehensive understanding on how an adjuvant affects a vaccine. A multidimensional approach consolidates useful data across in vitro and in vivo experiments to aggregate a snapshot of innate and humoral responses. Recently, researchers have used a systems vaccinology approach to great success. For instance, the transcription factor CREB1 was shown to be a critical for HIV-1 vaccines through a series of UMAP depictions of transcription factor genes[150]. The Sampa lab used UMAP to leverage complex cytokine, and transcriptomic datasets in a refined model of CREB-1 mediated HIV vaccine efficacy. At an organism level, the Chevrier lab tracks antiviral genes and tissue resident memory T cells across most major organs after poxvirus vaccination[151]. Researchers can apply the mechanistic and toxicology insights from organ specific readouts towards new adjuvants. At the population level, Dr. Ofer Levy uses a systems approach through the precision vaccines program. This program profiles vaccine induced responses from different population groups, especially the young and the elderly, working towards effective personalized vaccines[152]. As adjuvant and vaccine discovery continues to evolve, researchers should

use the plethora of immunological data that can be obtained.

1.3.3.1.2 *In Silico* and Machine Learning Computational simulations of biological phenomenon, known as *in silico* experimentation, can improve the speed and accuracy of adjuvant discovery. Machine learning, an artificial intelligence methodology that builds algorithmic models to make probabilistic predictions, is often paired with *in silico* experimentation. Both of these techniques have found utility across chemistry, material science, and immunology[153–155]. For example, *in silico* protein modeling efforts identified small molecule antagonists that served as adjuvants to *Mycobacterium tuberculosis* and *Plasmodium yoelii subunit* vaccines *in vivo*[156]. Antagonizing CCR4 improved the immune response by reducing the inhibitory activity of regulatory T cells. This approach used molecular docking and homology modeling, traditional approaches that are commonplace in the drug discovery field[157]. More recently, researchers are implementing black-box optimization on *in silico* and *in vitro* screens. Black-box optimization is a machine learning technique where in which the models and constraints of a dataset are largely unknown. In drug discovery, the algorithms in this technique might take inputs like small molecule structure and experimental results to output key predictive properties of successful drugs. Three common black-box algorithms include Bayesian optimization, reinforcement learning, and active learning, summarized in a review by Terayama et. al[158]. While finding expanded use in other fields, machine learning has yet to be applied at scale in adjuvant discovery. Machine learning in the adjuvant discovery space could also increase the number of successful compounds that past major transition points in the discovery pipeline. Many in silico screens have failed to replicate computational results upon in vitro validation. Similarly, many compounds have failed to translate from murine models fail to non-human primates[159; 160]. These are large challenges that machine learning may be able to address. Using multidimensional systems vaccine information and meta-analyses, machine learning could identify correlations between hit compounds that would not otherwise be apparent. Additionally, machine learning algo-

rithms could search already established datasets, like those with drugs that did not pass clinical trials, to repurpose them for alternate uses such as adjuvants. As the field of adjuvant discovery continues to develop, greater collaboration with machine learning groups is vital to maximize speed and efficiency of the discovery process.

1.3.3.2 Rethinking Animal Models

Animal models have been the foundation of vaccine immunogenicity studies for centuries, yet there is a concerning lack of translation between preclinical animal work and clinical human results[161]. Mice are the most common animal model due to their cheap cost, easy husbandry, and humanlike immune systems. But while similar, the mouse immune system is not identical to humans. Mice express a variety of different PRRs than humans[162]. Even among commonly held receptors, expression patterns on cell types varies between species. For example, TLR9 is found primarily on macrophages and myeloid dendritic cells in mice, but found primarily on B cells and plasmacytoid dendritic cells in humans[163]. Non-human primates provide an alternative model, but at a steep economic and ethical cost. Instead, humanized systems like transgenic mice, or actual human systems like organoids, provide attractive engineering solutions for clinically relevancy.

1.3.3.2.1 Transgenic Mice Engineers can modify laboratory strain mice into transgenic mice via the addition of recombinant DNA. Transgenic mice enable researchers to study human specific disease and to study mechanistic immunology questions. To study human specific disease, transgenes for human cell surface receptors can be inserted into the mouse genome. For example, mice do not naturally succumb to the pandemic virus SARS-CoV-2. But mice expressing the human transgene angiotensin-converting enzyme 2, the binding target for this virus, experience high levels of viral infection[164]. Thus, transgenic mice supplemented with key human receptors increase the tropism of human-specific pathogens.

To study mechanistic immunology, transgenes can directly modify the mouse innate immune system, recapitulating key human components. In mice, TLR8 responds differently than the human counterpart, though the two receptors are highly conserved[165]. The addition of human TLR8 into transgenic mice provides a better model for studying inflammation[166; 167]. Similarly, mice lack the human TLR10, but transgenic mice expressing the receptor serve as a model to understand negative regulation of TLR signaling[168]. Yet even with these advances, mice obviously cannot fully recapitulate a human model of pathogen infection. While transgenic mice with the human receptor for poliovirus are susceptible to poliomyelitis, most models cannot replicate the proper oral route of viral infection[169]. Poliovirus is also particularly sensitive to murine interferon genes, so an additional modification via interferon receptor knockout is needed to better recapitulate disease[170; 171]. But knocking out a key innate immune sensor creates challenges when studying new adjuvants, many of which rely on stimulation of type-I and type-II interferons for efficacy. This interferon knockout strategy is used in other disease models, too. Many viruses that induced hemorrhagic fever in humans, including Ebola, also do not cause disease in wild type mice, but are virulent in interferon deficient mice[172]. While transgenic mice have uses, and though the use of CRISPR-Cas9 makes their generation much simpler, the approach is not perfect for adjuvant discovery and development.

1.3.3.2.2 Human Primary Cells and Organoids When attempting to replicate human physiology, primary cells and organoids are perhaps the closest available choice. Recent studies have successfully performed high throughput screens on primary human peripheral blood mononuclear cells (PBMCs)[173; 174]. PBMCs are non-trivial to source, but recent miniaturization of assays allows for a larger number of experiments to be performed for the same number of cells[175]. Using primary cells, however, enhances assay variability and is particularly sensitive to effects of donors[173]. Donor effects can be mitigated through increased sample size. Human organoids are human cells that organize three dimensionally and

are a useful tool for mid throughput experimentation[176]. While primary cells can provide some cellular interactions during standard tissue culture, simple cultures do not provide any structural elements. Proper cellular organization is important in lymphoid structures, especially in germinal centers. Germinal centers are microstructures formed during an adaptive immune response, resulting in the creation of high affinity antibodies[177]. As an alternative to in vivo experiments, organoids allow for the study of organized tissues ex vivo. Adjuvants can heavily influence the germinal center reaction, especially in enhancing follicular dendritic cell antigen deposition[178]. The use of organoids in immunoengineering has risen in the past years[179–181]. Yet application of these systems towards adjuvant research has yet to be explored and remains an attractive option.

1.3.4 Immunomodulators Alter Adjuvanticity

As discussed, a large amount of scientific effort has been dedicated towards discovering novel PRR agonists. Yet many of these novel agonists are never implemented in actual vaccines due to high safety expectations. The problem is that these agonists amplify all downstream components roughly equally after ligand binding. A more potent agonist will improve the immune response, but at the cost of increased side effects and inflammation. Future adjuvants could decouple inflammation from adjuvanticity using immunomodulators. These immunomodulators would be a secondary molecule for use in combination with known PRR agonists (Figure 1.1).

The concept of immunomodulation is at the heart of this dissertation. The work presented here is an extension of the first efforts from the Esser-Kahn lab to use immunomodulators in an adjuvanted vaccine setting. The "first generation immunomodulators" were the short peptide SN50 and the small molecule honokiol[182; 183]. SN50 is a cell permeable, synthetic peptide original designed in 1995 by the Hawiger group[184]. SN50 contains the nuclear localization sequence of the p50 subunit of NF-κB, allowing the peptide to serve as

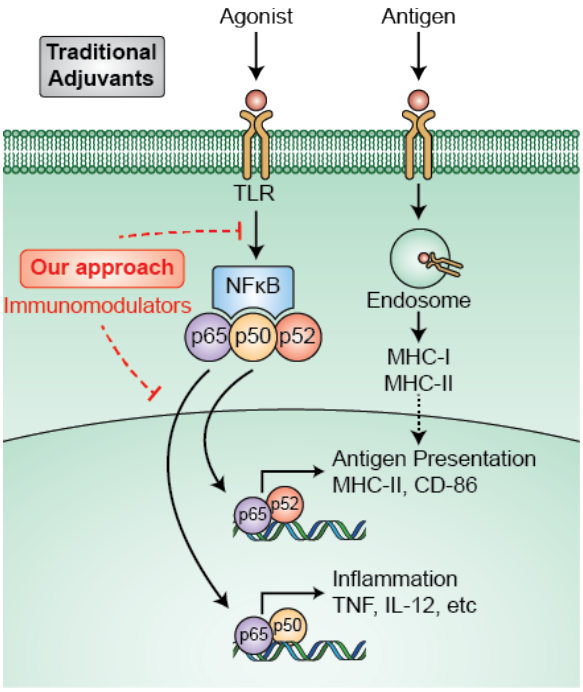

Figure 1.1: Traditional adjuvant discovery for new agonists (black) versus identifying immunomodulators to alter existing adjuvants by inhibiting innate immune signaling (red)

a competitive inhibitor against p50 containing NF-κB dimers. SN50 binds to importin α, a molecule responsible for transporting NF-κB dimers from the cytosol and into the nucleus where they can act as transcription factors[185]. SN50 was originally developed as a tool to probe the effects of NF-κB on inflammation and inflammatory disease, but had not been applied towards adjuvants. When mice were injected with CpG ODN 1826, a potent TLR9 agonist, SN50 reduced systemic inflammatory cytokines measured in the blood 1hr after vaccine administration compared to using the adjuvant without immunomodulator. It is important that the protection elicited by the vaccine is maintained with the addition of the immunomodulator. Somewhat surprisingly, SN50 not just maintained, but increased antigen specific antibodies in both model subunit vaccines and whole inactivated influenza vaccines. Moreover, SN50 increased survival rates in animals receiving vaccine + immunomodulator after a live virus influenza challenge.

The Esser-Kahn group also explored small molecules, again focusing on NF-κB inhibitors.

As a peptide, SN50 presented challenges in scaling its synthesis, particularly in production costs, which could limit its potential use in vaccines that need large quantities of total doses. A peptide therapeutic can also induce immune responses against itself much easier than the small molecule counterpart. We studied a subset of small molecule NF-κB inhibitors including: Cardamonin (40 μM), Caffeic acid phenethyl ester (CAPE) (100 μM), Withaferin A (WA) (400 nM), Resveratrol (10 μM), Salicin (100 nM), 5Z-7-Oxozeaenol (5-z-O) (5 μM), Parthenolide (20 μM), Honokiol (20 μM), Capsaicin (200 μM), PDK1/Akt/Flt dual pathway inhibitor (PDK1) (1 μM), and GYY 4137 (GYY) (200 μM). These small molecules were incubated with a RAW macrophage NF-κB reporter cell line before treatment with LPS. After 24 hours, supernatants were analyzed for inflammatory cytokines. Of these molecules, honokiol showed some of the largest decrease in systemic cytokines. Like SN50, when honokiol was injected with CpG and ovalbumin in a murine vaccination study, systemic inflammatory cytokines were reduced 1 hour after infection while improving antigen-specific antibodies 2 weeks post boost. The success of this molecule drove us to develop honokiol-containing SARS-CoV-2 subunit vaccines as seen in Chapter 2.

CHAPTER 2

IMPROVING A SARS-COV-2 VACCINE VIA A FIRST GENERATION IMMUNOMODULATOR

2.1 Summary

Vaccines have been critical in slowing the adverse effects of the SARS-CoV-2 pandemic, but their efficacy can be improved by enhancing their immunogenicity while minimizing reactogenicity. Previously, we demonstrated a small molecule immunomodulator, honokiol, improved immune responses when combined with subunit vaccines, resulting in increased protection. Here, we studied the application of this immunomodulator towards a CpG adjuvanted subunit SARS-CoV-2 vaccine in both mice and Syrian hamsters. Immunomodulator-containing vaccines increased neutralizing antibody and T-cell responses in mice. In a challenge model in hamsters, these vaccines reduced weight loss, viral load, and tissue damage. These findings demonstrate the possible improvement of current and future vaccines using immunomodulators.

2.2 Introduction

SARS-CoV-2 has resulted in almost one billion confirmed COVID-19 infections since its initial discovery in humans in late 2019[186]. Vaccines have greatly reduced the mortality rates, but infections from variants remain a concern[187; 188]. Further, these infections can result in lingering post-COVID-19 conditions, now termed long COVID[189]. Long COVID is conservatively estimated to occur in 10-12% of vaccinated individuals, rising significantly with the incidence of severe infection and hospitalization[190; 191]. Protection induced by current vaccines would benefit from methods to improve current subunit or mRNA technologies without needing new adjuvants, delivery systems, or formulations. Current vaccines

employ single or integrated adjuvants to improve the immune response[192]. At higher doses, adjuvants create excess inflammation and limit tolerability, resulting in a host of late-stage clinical trial failures and reduced implementation[16]. Thus, balancing activation and tolerability is a critical challenge in vaccine development[193]. We previously reported that peptide or small molecule "immunomodulators" reduce the systemic inflammation caused by potent adjuvants[182; 183]. The immunomodulators don't just maintain, but even improve, the protection of adjuvanted vaccines through increased antibody production and T-cell responses. Moreover, as small molecules, the modulators can be easily added to a host of existing vaccine formulations. We sought to apply these immunomodulators to prophylactic vaccines against SARS-CoV-2. We began by identifying the vaccine platform to study our immunomodulators. The first approved vaccines in the USA were mRNA vaccines: BNT162b2, from Pfizer-BioNTech, and mRNA-1273, from Moderna. These vaccines require efficient delivery of fragile mRNA to the cytosol and are thus formulated with lipid nanoparticles. These formulations present obstacles in testing our immunomodulators. Alternatively, protein subunit vaccines are the most common platform at both the pre-clinical and clinical development stages, comprising 32% and 33% of all vaccines, respectively[194]. Recently, Novavax's subunit vaccine received US approval after demonstrating high levels of antibody and T-cell responses. Subunit vaccines lack the complexity in the formulation and cold chain requirements, lowering production costs compared to their mRNA counterparts[195]. Because of their stability at ambient temperatures, subunit vaccines are critical in providing immunity in low and middle-income countries[195; 196]. The primary protein target for SARS-CoV-2 is the spike (S) protein, as this protein binds to human angiotensin-converting enzyme 2 (ACE2) and allows for viral cell entry. We employed full-length S in our vaccines. The subunit vaccine platform provides a translationally relevant model while validating the use of immunomodulators for potential use in other SARS-CoV-2 vaccine systems. In selecting an adjuvant to combine with the spike protein from SARS-CoV-2, we chose CpG compounds

owing to their ease of access and formulation. We explored both CpG 1826 and CpG 1018 in murine vaccination models before a viral challenge model with CpG 1018 in Syrian hamsters. CpG 1018 is a potent TLR9 agonist developed by Dynavax and is commercially approved in a Hepatitis B subunit protein vaccine, HEPLISAV-B[197]. Dynavax has licensed CpG 1018 as an adjuvant in four Phase III trials: MVC-COV1901 from Medigen, SCB-2019 from Clover Biopharmaceuticals, VLA2001 from Valneva SE, and Corbevax from Biological E[198–201]. We sought to replicate and improve upon the preclinical studies that led to these clinical trials, choosing to model our experiments on strategies employed by MVC-COV1901 in both mice and hamsters[202; 203]. Here, we demonstrate the small molecule NF-κB inhibitor, honokiol, increases the protection of CpG 1018 adjuvanted protein subunit vaccines against SARS-CoV-2.

2.3 Results and Discussion

2.3.1 Immunomdodulators Improve Immune Responses in Mice

We previously reported the small molecule NF-κB inhibitor honokiol reduced systemic inflammatory cytokines while boosting antigen-specific antibodies in a CpG 1826 adjuvanted subunit vaccine containing the model antigen, ovalbumin[183]. We further investigated honokiol's effects on adaptive immune responses following vaccination with CpG 1826 and spike protein from SARS-CoV-2. We followed a typical prime-boost vaccination model in C57BL/6 mice with injections separated by three weeks (Figure 1A). We observed similar antibody and cytokine expression as previous experiments. To monitor antigen specific T-cell responses, mice were sacrificed ten days post-boost with splenocytes processed into a single-cell suspension. These splenocytes were co-cultured with antigen-pulsed, stimulated bone marrow-derived dendritic cells for two days before measuring the supernatant for interferon-γ production, a key marker of vaccine-induced TH1-mediated protection[204; 205]. We observed

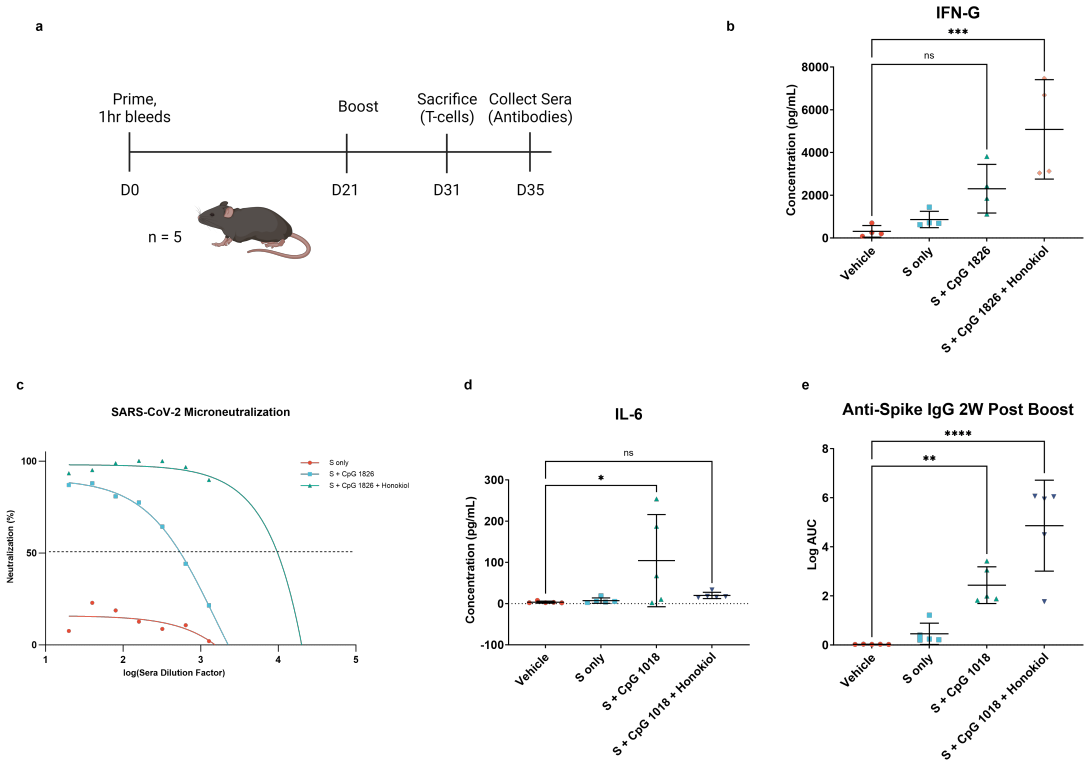

Figure 2.1: A) Study timeline in C57BL/6 mice B) IFN-γ concentration in supernatant after a 48 hr co-culture of 1:1 splenocytes 10 d post boost and LPS-antigen pulsed bone marrow dendritic cells C) Microneutralization assay with SARS-CoV-2 and twofold serially diluted sera samples from vaccinated mice two weeks post boost D) Systemic IL-6 concentration from cheek bleeds 1 hour post injection E) Anti-Spike IgG antibody titers from sera two weeks post boost vaccinations Statistical analyses between were performed by a one-way ANOVA test with Dunnett's multiple comparison post-hoc analysis. (* = $p < 0.05$, ** = $p < 0.01$, *** = $p < 0.001$, **** = $p < 0.0001$)

a significant increase in IFN-γ secretion after restimulation with the addition of honokiol in the subunit vaccine (Figure 1B).

In another cohort of mice, functional antibodies were measured two weeks post-boost with a microneutralization assay. Sera was diluted twofold in an eight-point curve with dilution factors ranging from 20 to 1280. Surprisingly, sera from the honokiol group neutralized live virus even at the strongest dilutions prepared for this or any previous study conducted by this group (Figure 1C). Due to this experimental limitation, we could not calculate and compare IC50 values, but it is qualitatively clear that honokiol generated higher amounts

of neutralizing antibodies, another strong predictor of protection[206]. With this initial experiment validating the approach, we continued the vaccination experiments using CpG 1018 as the adjuvant to (1) be consistent with previous literature and (2) in anticipation of use in Syrian hamsters[202; 203]. In this second study, we observed the same reduction in systemic cytokines one hour after injection while increasing antigen-specific antibodies two weeks post boost (Figures 1D, 1E). With these promising results in mice, we were encouraged to further evaluate the immunomodulator-containing subunit vaccines in a clinically relevant challenge model.

2.3.2 Syrian Hamsters as a SARS-CoV-2 Challenge Model

We chose Syrian hamsters as our animal model to conduct the SARS-CoV-2 challenge. While mice provide a simple model for measuring T cell and antibody responses, mice are not susceptible to infection by the native SARS-CoV-2 strains found in humans. Murine ACE2 differs from human ACE2, reducing viral entry, and thus host infection[207]. Syrian hamsters, on the other hand, have a similar ACE2 homologue to humans, resulting in infection and clinical signs of weight loss and respiratory damage[208; 209]. This small animal model provides results at a more attractive financial and ethical cost than non-human primates for this preliminary stage research. Hamsters were vaccinated at days 0 and 21 with full S, CpG 1018, and two different doses of honokiol: a low dose (LD) at 400μg and a high dose (HD) at 1,200μg. We will herein refer to the vehicle control as the placebo group and the CpG-adjuvanted subunit vaccine group, without immunomodulator, as the "control vaccine" group. Blood was collected at day 31 to measure antibody responses, followed by an intranasal challenge of $5x10^4$ TCID50 of the USA-WA1/2020 strain of SARS-CoV-2 on day 42. After the challenge, weight and temperature was measured at 2, 3, and 6 days post infection (d.p.i). Five animals were sacrificed in each group 3 and 6 d.p.i. for histopathology and viral load analyses in various organs. A study overview can be found in Figure 2.2.

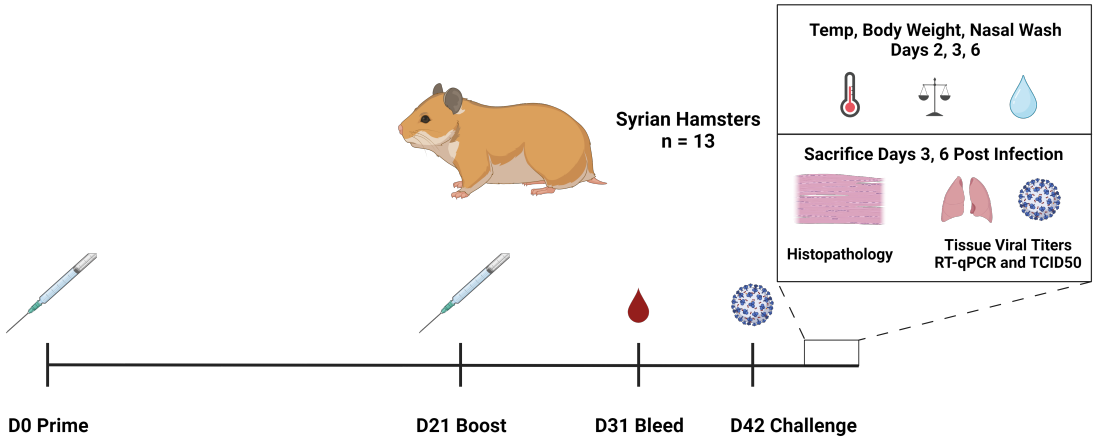

Figure 2.2: Study overview of Syrian hamster challenge. Animals (n = 13) were vaccinated in a prime-boost model separated by three weeks with a saline solution containing vaccines formulated with spike protein (20 μg), CpG 1018 (150 μg), and honokiol (400 μg or 1,200 μg). Three weeks following the boost, hamsters were inoculated with $5x10^4$ TCID50 of SARS-CoV-2. Nasal washes, temperatures, and body weights were measured at days 2, 3, and 6 post infection with animals sacrificed on days 3 and 6 and tissues harvested for viral load and pathology measurements.

2.3.3 Immunomodulator Protects Hamsters from Weight Loss, Reduces Viral Shedding

Following inoculation, hamsters in all groups began to lose weight with varying severity. At 2 d.p.i, both doses of immunomodulator showed significantly less weight loss than the placebo, protein only, and adjuvanted vaccine controls (Figure 2.3).By 3 d.p.i, the control vaccine group had a significant reduction in weight loss, though not as strong as the groups vaccinated with immunomodulator-containing vaccines. The protective effect was strongest at 6 d.p.i. with the immunomodulator groups returning almost to the pre-challenge weight baseline whereas the placebo group exhibited approximately 10% weight loss. Viral shedding was assessed by RT-qPCR and fifty-percent tissue culture infectious dose (TCID50) for nasal washes at 2, 3, and 6 d.p.i. All vaccinated groups had substantially decreased viral shedding as measured by RT-qPCR at all timepoints. At 6 d.p.i., the high dose of immunomodulator

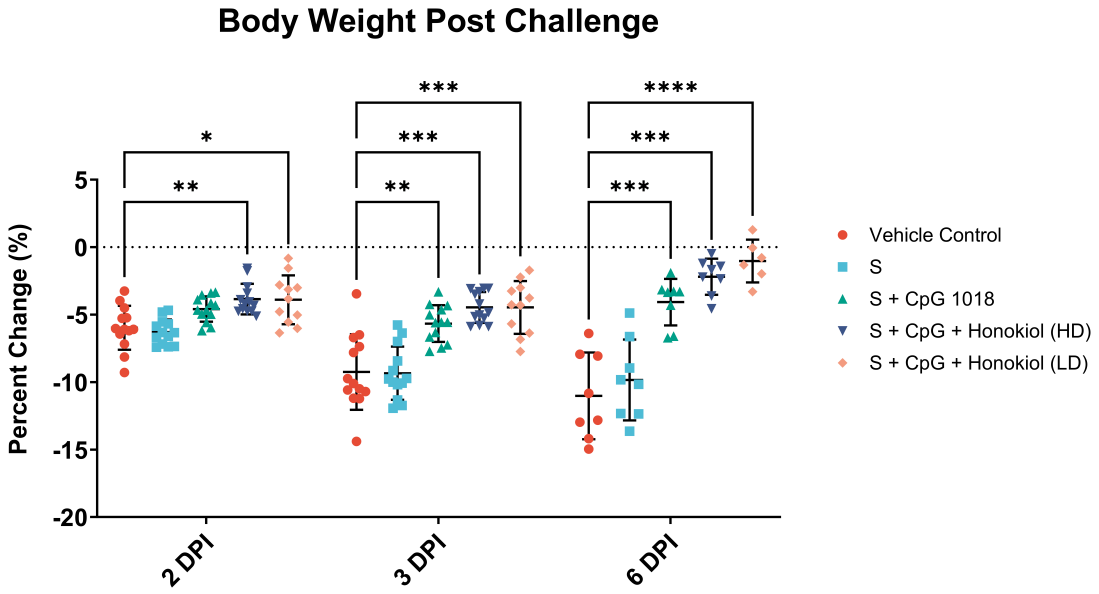

Figure 2.3: Body weight measurements after infection with SARS-CoV-2 virus. All animals (n = 13) were measured at days 2 and 3 post infection. Five animals were sacrificed for tissue harvesting on day 3, resulting in a lower animal count (n = 8) for day 6 post infection. Data represented as mean with standard deviation. Statistical analyses between were performed by a two-way ANOVA test with Dunnett's multiple comparison post-hoc analysis. (* = $p < 0.05$, ** = $p < 0.01$, *** = $p < 0.001$, **** = $p < 0.0001$)

significantly reduced viral shedding compared to the control vaccine (Figure 2.4A). This reduction in viral shedding was confirmed in the cell based TCID50 assay. Adjuvanted vaccine groups had lower TCID50 at 2 and 3 d.p.i, with more significant results upon the addition of the immunomodulator (Figure 2.4B). By 6 d.p.i, no virus was detected as measured by TCID50. Of note, on 2 and 3 d.p.i, the categories containing immunomodulator had >50% of animals with undetectable TCID50 values compared to only 5% for the vaccine containing adjuvant alone. While this does not result in a statistically significant drop, it did demonstrate that many more animals appeared to have undetectable levels of virus starting at 2 d.p.i suggesting increased sterilizing immunity provided by the immunomodulator compounds.

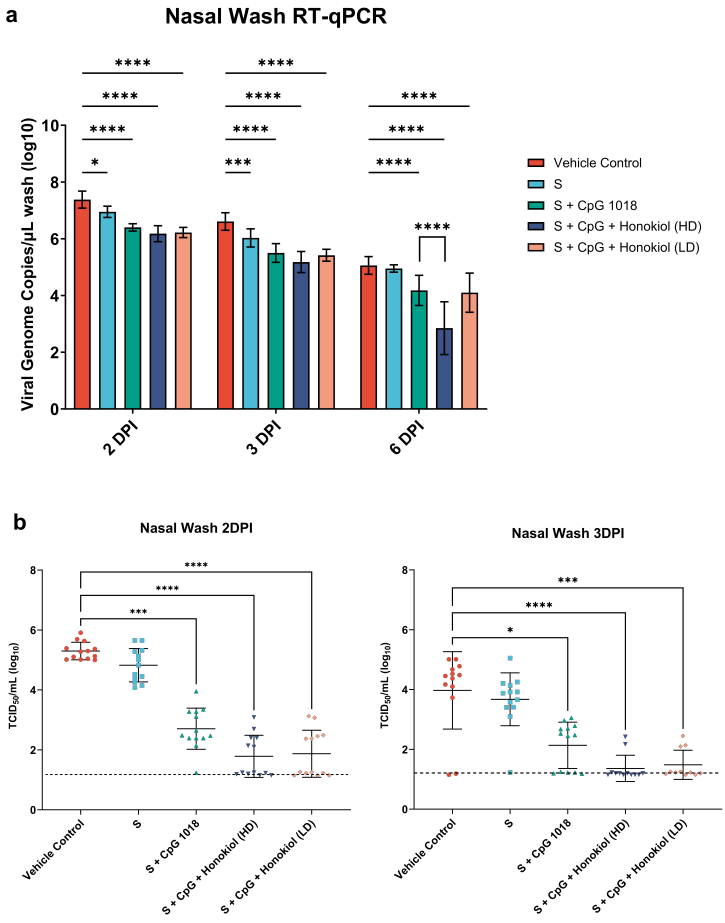

Figure 2.4: A) Viral loads measured via RT-qPCR in nasal washes day 2 (n = 13), day 3 (n = 13) and day 6 (n = 7) post infection. Data represented as mean with standard deviation. B) Viral loads measured via TCID50 nasal washes day 2 (n = 13) and day 3 (n = 13) post infection. Dotted line represents the limit of detection. Statistical analyses were performed in subpanel A by a two-way ANOVA test with Dunnett's multiple comparison post-hoc analysis, and in subpanel B with a Kruskal-Wallis test with Dunn's multiple comparison post-hoc analysis (* = $p < 0.05$, ** = $p < 0.01$, *** = $p < 0.001$, **** = $p < 0.0001$)

2.3.4 Immunomodulator Reduces Viral Loads, Pathology in Respiratory Tract

Next, the effect of vaccination and immunomodulation on the viral loads and pathology in the respiratory tract was analyzed. In the nasal turbinates at 3 d.p.i., only the low dose of immunomodulator significantly reduced viral loads as measured by RT-qPCR. By 6 d.p.i., all

adjuvanted vaccines lowered viral loads in the nasal turbinates (Figure 2.5A). In the lungs at 3

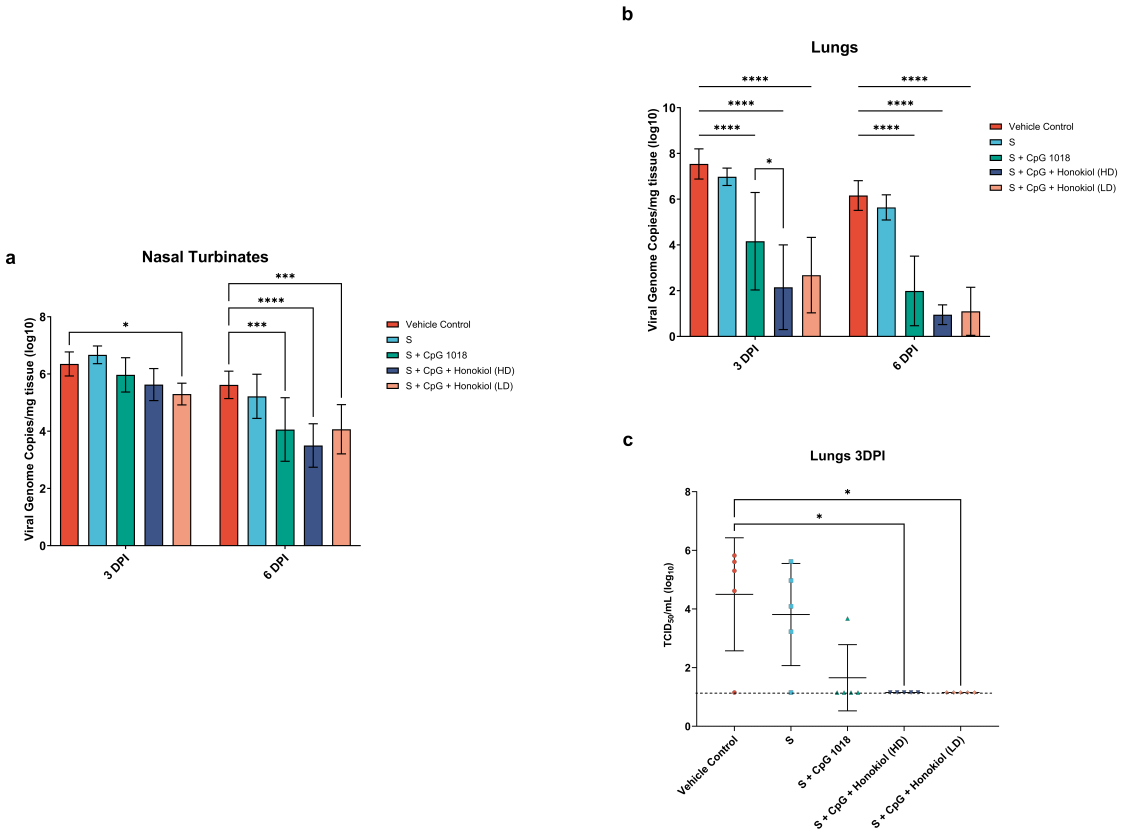

Figure 2.5: Viral loads measured via RT-qPCR in (A) nasal turbinate and (B) lung tissues harvested at days 3 and 6 (n = 5) post infection. (C) Viral loads measured via TCID50 in lung tissues at day 3 post infection (n = 5). Data represented as mean with standard deviation. Statistical analyses in A and B were performed by a two-way ANOVA test with Dunnett's multiple comparison post-hoc analysis. Statistical analysis in C were performed by a Kruskal-Wallis test with Dunn's multiple comparison post-hoc analysis (* = $p < 0.05$, ** = $p < 0.01$, *** = $p < 0.001$, **** = $p < 0.0001$)

d.p.i., all adjuvanted vaccines significantly reduced viral loads compared to the placebo, with a much larger difference than in the nasal turbinates. The high dose of immunomodulator also substantially improved upon the control vaccine, with a 100-fold decrease in measured genome copies per milligram of tissue (Figure 2.5B). By 6 d.p.i., lung viral load was almost nondetectable by RT-qPCR. Lung tissue at 3 d.p.i. were the only samples that provided detectable levels of viral load as measured by TCID50. At 3 d.p.i., both immunomodulator

vaccines significantly lowered viral loads (Figure 2.5C). These viral loads correspond to the pathology seen in the respective organs. In lungs 3 d.p.i., only immunomodulator vaccines showed a significant decrease in the severity scores for alveolar epithelial hyperplasia and bronchointerstitial pneumonia (Figures 2.6A, 2.6B). All adjuvanted vaccines reduced the

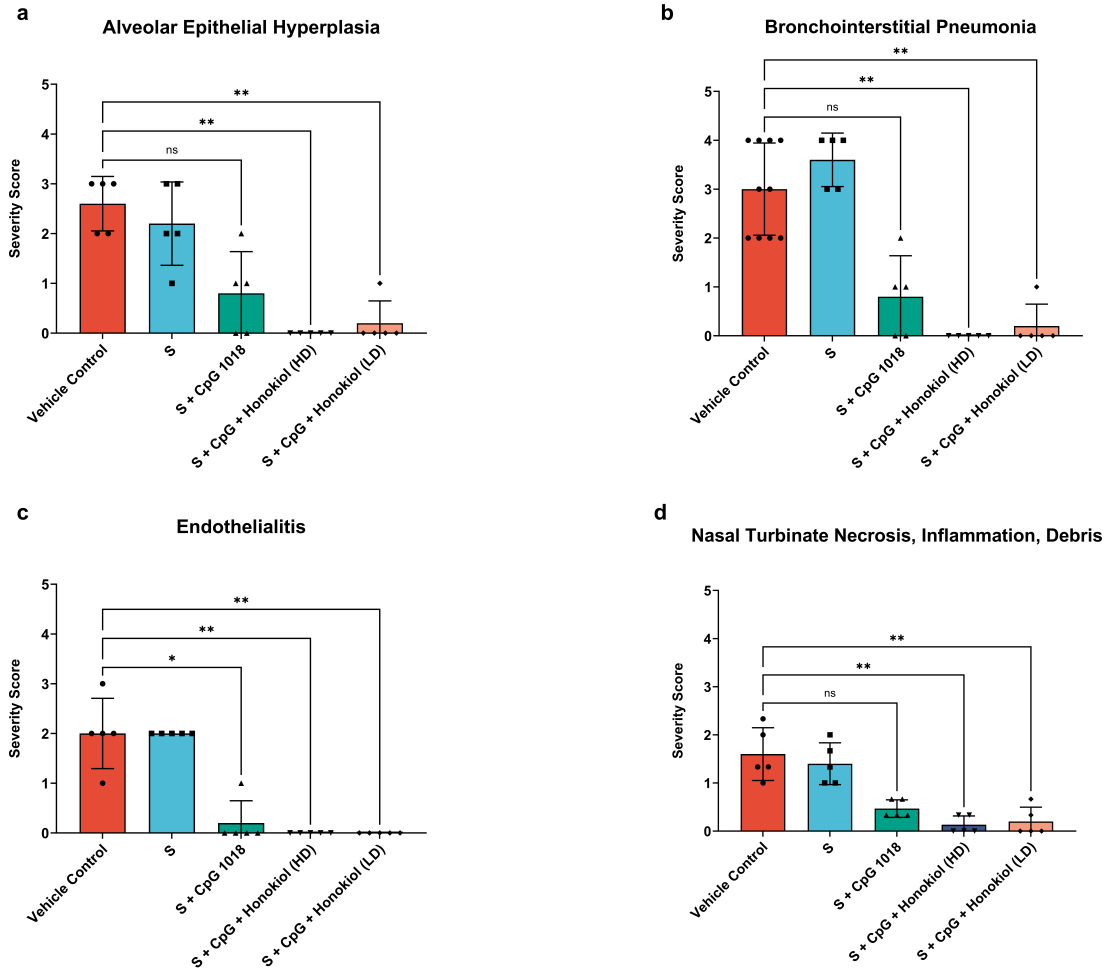

Figure 2.6: (A-C) Histopathology from lung tissues (n = 5) 3 days post infection. Severity scoring is semiquantitative and represents the relative affected area of the examined tissue as outlined in the methods. Data represented as mean with standard deviation. D) Histopathology from nasal turbinates (n = 5) 3 days post infection. Intraluminal cellular debris, epithelial necrosis, and inflammation scores for individual animals were averaged as outlined in the methods. Data represented as mean with standard deviation. Statistical analyses were performed by a Kruskal-Wallis test with Dunn's multiple comparison post-hoc analysis (* = $p < 0.05$, ** = $p < 0.01$, *** = $p < 0.001$, **** = $p < 0.0001$)

severity score for endothelialitis at this timepoint (Figure 2.6C). In the nasal turbinates 3 d.p.i., only immunomodulator vaccines reduced the combined severity score for intraluminal cellular debris, epithelial necrosis, and mixed inflammation (Figure 2.6D). Combined, this data suggests that the immunomodulator improves protection of the vaccine.

2.3.5 Immunomodulator Maintains Antibody Responses

To probe a mechanistic basis for the improved protection, antigen specific antibodies were measured in the sera ten days post booster injections. Binding was measured through a spike

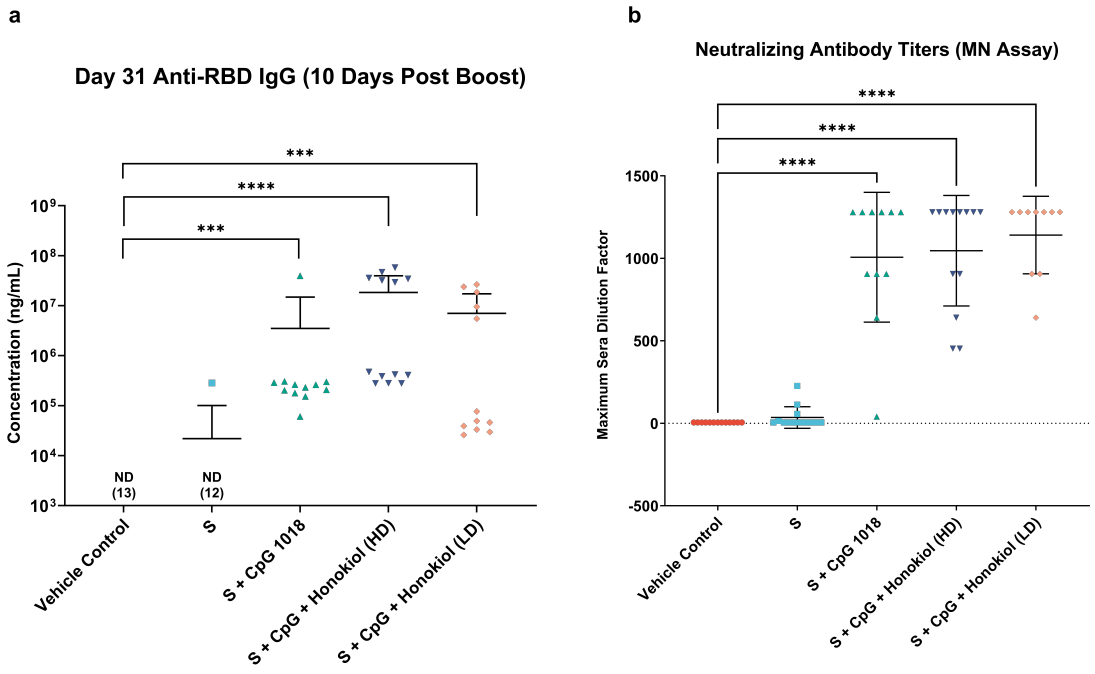

Figure 2.7: Antibody responses from vaccinated hamsters after sera collection ten days post boost shown as (A) antigen specific IgG measured via ELISA or (B) functional antibody titers measured via microneutralization assay. Data represented as mean with standard deviation.
Statistical analyses were performed by a Kruskal-Wallis test with Dunn's multiple comparison post-hoc analysis (* = $p < 0.05$, ** = $p < 0.01$, *** = $p < 0.001$, **** = $p < 0.0001$)

receptor binding domain (RBD) ELISA and functionality was measured via microneutralization (MN) assay. Adjuvanted vaccines increased antibody levels over the controls in both

assays (Figures 2.7A, 2.7B). There were no differences between the control vaccine and the immunomodulator-containing vaccines. This result is in contrast to the effect we observed in mice and indicates that the improved protection may be caused from a more T-cell mediated response.

2.4 Conclusion and Future Directions

This study highlights the benefits of a small molecule immunomodulator, honokiol, in CpG adjuvanted subunit vaccines against SARS-CoV-2. After validating the efficacy of our modulator-containing vaccines in mice, we performed a challenge study in Syrian hamsters. At the organismal level, we see a reduction in weight loss, indicating a milder infection. From nasal washes, we see a decrease in viral shedding – a predictor of both severe infection and viral transmission[210; 211]. In both the upper and lower respiratory tracts, we see a reduction in the viral loads, indicating a milder progression of disease. This is corroborated with decreased pathology in the lung. Alveolar hyperplasia, interstitial pneumonia, and endothelialitis are all indicative of severe infection in humans[212–214]. Notably, we did not observe a strong increase in antibodies in hamsters as we did in mice. We hypothesize the increased protection may be due to an improved T-cell response. We observed an increase in IFN-γ production from T-cells in mice but did not perform a similar analysis in the hamsters. This model is limited as SARS-CoV-2 is not typically lethal to Syrian hamsters. As such, we cannot make claims that immunomodulation could prevent fatalities in severe infections. Nonetheless, our results indicate this immunomodulator improves protection against moderate disease. We believe immunomodulation can be applied to other vaccine platforms, including mRNA or inactivated pathogen vaccines, and further studies to test this hypothesis are currently ongoing.

2.5 Materials and Methods

2.5.1 Mouse Experiments

2.5.1.1 Animals and Vaccinations

All animal procedures were performed under a protocol approved by the University of Chicago Institutional Animal Care and Use Committee (IACUC). 6- to 8-week-old C57/B6 female mice were purchased from the Jackson laboratory. Mice were lightly anesthetized with isoflurane and injected intramuscularly in the left hind leg with 50 μL containing 20 μg of spike protein (R&D Biosystems), 50 μg CpG adjuvant (IDT), and 400 μg honokiol (TCI) in phosphate-buffered saline (PBS, Corning).

2.5.1.2 Cytokine Analysis

Blood was collected from the submandibular vein 1 h post injection. Blood was collected from mice at specified time points in 0.2 mL of heparin-coated collection tubes (VWR Scientific). Plasma was isolated via centrifugation at 2000xg at 4 °C for 15 min. Samples were collected and stored at -80 °C until use. Plasma was analyzed using Bio-Legend's LEGENDPlex™ Mouse Inflammation Cytokine Panel (13-Plex) according to the manufacturer's protocol. Samples were analyzed using a NovoCyte Flow Cytometer. Data were analyzed using LEGENDplex™ Data Analysis Software Suite and GraphPad Prism.

2.5.1.3 Antibody Quantification

Blood was collected at time points indicated in 0.2 mL heparin-coated collection tubes (VWR Scientific). Plasma was isolated via centrifugation at 2000xg at 4C for 15 min. Samples were collected and stored at -80 °C until use. Antibody titers were performed by coating Nunc MaxiSorp ELISA plates (BioLegend) with 100 μL of 2 μg/mL spike protein indicated (R&D

Biosystems) overnight at 4 °C. Plates were washed and blocked with 150 μL 2% (w/v) BSA in PBS + 1% Tween-80 (PBST) for 1 h at RT. Following wash, samples were serially diluted tenfold in blocking buffer for a total volume of 100 μL and incubated for 2 h at RT. Following wash, 100 μL of goat anti-mouse IgG HRP conjugate (Invitrogen) diluted 1:10,000 in 0.4% BSA (in blocking buffer) was incubated for 1hr at RT. Following wash, 100 μL of 1-Step Ultra TMB was incubated for 4.5 min before stopping with 50 μL of 2 M sulfuric acid. ELISA plates were analyzed using a Multiskan FC plate reader (Thermo Fisher) and absorbance was measured at 450 nm with 620 nm correction. Area under the curve measurements were approximated with Riemann sums. Data were analyzed using GraphPad Prism.

2.5.1.4 T-cell Co-Culture for Antigen Recall

Bone marrow was harvested from 6-week-old C57BL/6 mice and differentiated into dendritic cells (BMDCs) using supplemented culture medium: RPMI 1640 (Life Technologies), 10% HIFBS (Sigma-Aldrich), Recombinant Mouse GM-CSF (carrier-free)(20 ng/ml; BioLegend), 2 mM l-glutamine (Life Technologies), 1% antibiotic- antimycotic (Life Technologies), and 50μM β-mercaptoethanol (Sigma-Aldrich). After 6 days of culture, BMDCs were washed and incubated overnight with 100 μg/mL SARS-CoV-2 spike glycoprotein PepMix (JPT) and 100 ng/mL LPS-EK (Invivogen). Ten days after booster vaccination mice were sacrificed and spleens harvested ad placed in RPMI on ice. Spleens were crushed between two frosted glass slides and pushed through a 70-μm filter. Cells were pelleted at 500xg for 5 min and resuspended in 3 mL of ACK lysis buffer (Gibco). 12 mL of PBS was added before pelleting again at 500xg for 5 min. 100k splenocytes and 100k activated BMDCs were seeded 1:1 in 200 μL of RPMI + 10% HIFBS in a 96 well U-bottom plate. After 48 h, supernatant was removed and analyzed using Bio-Legend's LEGENDPlex™ Mouse Inflammation Cytokine Panel (13-Plex) according to the manufacturer's protocol. Samples were analyzed using a NovoCyte Flow Cytometer. Data were analyzed using LEGENDplex™ Data Analysis Software Suite

and GraphPad Prism.

2.5.2 Hamster Experiments

2.5.2.1 Animals and Vaccinations

A total of 100 male Syrian Golden hamsters were purchased from Envigo (Indianapolis, IN). All animals were quarantined for four days prior to the initiation of dosing. Each hamster was uniquely identified numerically by transponder chips (BioMedic data systems, Seaford, DE) and with a corresponding cage card. Procedures for animal care and housing were in accordance with all applicable sections of the Public Health Service Policy on Humane Care and Use of Laboratory Animals (National Institutes of Health's Office of Laboratory Animal Welfare, 2002), and the Guide for the Care and Use of Laboratory Animals (National Research Council, 2011). The test vaccines were delivered via intramuscular injection, 100μL per animal, with 50μL injected into each hind leg.

2.5.2.2 qPCR for Viral Load Measurements

Following collection, nasal wash samples were mixed with DNA/RNA Shield (2 x concentrate, Zymo Research, Irvine, CA) at 1:1 ratio. RNA was extracted with a Quick-RNA Viral Kit (Zymo Research, Irvine, CA) and eluted with 100 μL nuclease free water according to the relevant IITRI SOP. Whole organs were collected at necropsy and weighed and homogenized in DMEM culture medium (organ weight (mg): DMEM volume (μL) = 1:9 for lungs, nasal turbinate and kidneys, organ weight (mg): DMEM volume (μL) = 1:40 for trachea) with Bead Ruptor 12 (Omni International). After homogenization, the homogenate was spun down at 2000 x g for 5 minutes, then 100 μL supernatant from each sample was mixed with DNA/RNA shield (2 x concentrate). RNA was extracted with a Quick-RNA Viral Kit. The eluted RNA samples were stored at <-65 °C freezer until analyzed for viral genome

titers via one-step RT-qPCR analysis. Nasal wash/organ RNA samples were evaluated using a one-step RT qPCR method per the relevant IITRI SOP. Briefly, RNA standard was prepared in advance, aliquoted into multiple tubes, and stored at <-65°C until used. An RNA standard was subjected to serial dilutions with yeast tRNA solution (10 ng/μL in nuclease free water) at RT-qPCR set up stage. Positive control (PC) was prepared with SARS-CoV-2 RNA extracted from culture medium or virus stock using a Quick-RNA viral kit. Extracted PC RNA was then diluted and aliquoted into multiple tubes. PCs were stored at <-65°C until used. Each RT-qPCR plate included ten RNA standards (5 x 10^8, 5 x 10^7, 5 x 10^6, 5 x 10^5, 5 x 10^4, 5 x 10^3, 5 x 10^2, 50, 20, 5 copies per RT-qPCR well) in duplicate, a no template control (NTC) and PC in triplicate wells. Extracted nasal wash or organ RNA samples were analyzed in duplicate wells. One-step RT-qPCR was performed on the CFX384 Touch Real-Time PCR Detection System (Bio-Rad). The threshold baseline of the RT-qPCR assay was manually set at 352.751, which is consistent with previous threshold baseline automatically determined by the Bio-Rad CFX Maestro 1.1 software using the single threshold determination mode on the first qualification plate. Quantitation cycle (Cq) and copy numbers of SARS-CoV-2 in each well were automatically calculated by the Maestro 1.1 software based on the standard curve and the threshold baseline. Data generated by the software was exported to a Microsoft Excel (Microsoft Corporation; Redmond, WA) spreadsheet for data processing. The mean copy number of each sample was then calculated and converted to copy number per μL nasal wash or copy number per mg tissue, log scale of the copy number was also presented.

2.5.2.3 TCID50 for Viral Load Measurements

Nasal wash samples and the left lung lobe were analyzed by the TCID50 assay for viral titers. The left lung was collected into a 7 mL tube prefilled with 2.8 mm beads and weighed to determine the net weight of the lung. The left lung collected was homogenized in DMEM.

Briefly, clarified tissue homogenate supernatants and a portion of nasal wash samples were diluted 1:10 followed by seven 2-fold serial dilutions and added to a 96-well plate pre-seeded with VeroE6 cells. Each sample was plated in triplicate. Plates were allowed to incubate for 72 hr (±4 hr), and cytopathic effect scored (+ or -) for each well for each dilution.

2.5.2.4 Histology

The right lung was inflated with 10% neutral-buffered formalin (NBF) and immersed in 10% NBF. After fixation, tissues were transported to the Charles River Laboratories, Skokie facility where they were trimmed, processed routinely, embedded in paraffin, sectioned at approximately 5 μm, and stained with hematoxylin and eosin. Tissues were evaluated by light microscopy.

2.5.2.5 Severity Scoring

Severity scoring is semiquantitative on a scale of 1-5 and represents the relative affected area of the examined tissue. For lungs, alveolar epithelial hyperplasia was characterized by large cuboidal epithelial cells lining narrowed alveolar spaces with few mitotic figures and/or multinucleated cells. Bronchointerstitial pneumonia represented a pattern of mixed inflammation that initiates at terminal bronchi and extends into adjacent alveolar space and within the alveolar septa. Endothelialitis was characterized by endothelial cell swelling, vacuolation and/or detachment with subendothelial aggregates of inflammation. For nasal turbinates, intraluminal cellular debris was composed of predominantly viable and degenerate neutrophils admixed with fibrin. Epithelial necrosis was characterized by individual shrunken, hypereosinophilic epithelial cells (both nasal epithelium and glandular epithelium in the subepithelial tissue) with pyknotic nuclei. Mixed inflammation is characterized by neutrophils with fewer lymphocytes, plasma cells and macrophages in the subepithelial tissue, occasionally transmigrating the epithelium, and surrounding and occasionally within

glands and lymphatic vessels. Severity scores for the three diagnosis categories (cellular debris, necrosis, and mixed inflammation) were averaged for individual animals.

2.5.2.6 Antibody Quantification

Anti-RBD IgG antibodies were quantified from serum samples collected on Day 31 using a standard sandwich ELISA according to the manufacturer's instructions (Eagle Biosciences). Briefly, individual samples were heat inactivated (56 °C for 30 ±5 min) before diluting 1:1000 in sample diluent. 100 μL of samples or standards were incubated for 1 hour at room temperature, followed by four washes with 300 μL of wash buffer. 100 μL of Goat Anti-Hamster IgG:HRP Conjugate was added to each well and incubated for 1 hour at room temperature, followed by four washes with 300 μL of wash buffer. 100 μL of TMB substrate was added to all wells, followed by incubation at room temperature for 15 minutes. 100 μL of stop solution was added, followed by absorbance readings at 450 nm.

2.5.2.7 Microneutralization Assay

Serum samples collected on Days -1 and 31 had neutralizing antibody titers determined using the microneutralization assay. Briefly, individual samples were heat inactivated (56 °C for 30 ±5 min) and initially diluted 1:10 followed by seven two-fold serial dilutions (final dilution scheme 1:10 to 1:1280). Each dilution was mixed with a standard concentration of virus, incubated for 75 minutes (±15 mins) and added to a 96-well plate with a standard concentration of Vero E6 cells ($1x10^4$ – $1x10^5$ cells per well). These plates were incubated for 48 hours (±6 hours) at 37 (±2) °C with 5% CO2 (±1%). After incubation, plates were fixed with 80% cold acetone for a minimum of 30 minutes and cells were stained by anti-mouse SARS-CoV-2 nucleoprotein IgG (Cat: 40143-MM05, Sino Biological) followed by peroxidase-conjugated goat anti-mouse IgG (SeraCare). Wells were developed using ABTS Substrate Solution and the reaction stopped by acidification. The plates were read at 450 nm on a

spectrophotometer by microplate reader. The calculation for wells positive for at least 50% virus infection is determined using virus (VC) and cell (CC) control wells using the following calculation:

$$\frac{VC_{ODMean} + CC_{ODMean}}{2}$$

For each sample, neutralization was based on the last dilution that generated an OD value above (negative for neutralization) or below (positive for neutralization) this cut-off value. The highest dilution that is positive for neutralization is the estimated titer for the sample.

CHAPTER 3

HIGH THROUGHPUT SCREENING FOR SECOND GENERATION IMMUNOMODULATORS

3.1 Summary

Stimulation of the innate immune system is crucial in both effective vaccinations and immunotherapies. This is often achieved through adjuvants, molecules that usually activate pattern recognition receptors (PRRs) and stimulate two innate immune signaling pathways: the nuclear factor kappa-light-chain-enhancer of activated B-cells pathway (NF-B) and the interferon regulatory factors pathway (IRF). Here, we demonstrate the ability to alter and improve adjuvant activity via the addition of small molecule "immunomodulators". By modulating signaling activity instead of receptor binding, these molecules allow the customization of select innate responses. We demonstrate both inhibition and enhancement of the products of the NF-κB and IRF pathways by several orders of magnitude. Some modulators apply generally across many receptors, while others focus specifically on individual receptors. These modulators have a range of applications: from adjuvanticity in prophylactics to enhancement of immunotherapy.

3.2 Introduction

Vaccines are often heralded as one of the greatest triumphs of modern medicine and are a key defensive measure against infectious disease and cancer. Underneath the adaptive responses lies the stimulation of innate immune cells through pattern recognition elements. This is most often achieved via adjuvants – exogenous molecules which help stimulate innate immune pathways[215]. In vaccines, adjuvants require a careful balance between stimulation and tolerability – excess levels of activation often result in systemic inflammation and challenges

with reactogenicity[216; 217]. In immunotherapy, adjuvants face suppression from tumor microenvironments, weakening potential therapies resulting in the need to amplify interferon responses[218]. In each of these applications there is a need to improve adjuvant profiles by increasing or decreasing specific elements of innate signaling. Engineering individual adjuvants towards these unique circumstances, however, has proved quite challenging. Thus, we sought new approaches to modulate and tailor the immune response in the early stages of activation by altering signaling pathways.

Towards this goal, we hypothesized that manipulating the activity of two innate immune pathways, the nuclear factor kappa-light-chain-enhancer of activated B-cells pathway (NF-κB) and the interferon regulatory factors pathway (IRF), could be used to modulate innate immune stimulation[35; 219]. Signaling in these pathways begins with the binding of pattern recognition receptors (PRRs) ¬¬– a common target for adjuvants and vaccine activity[220]. When activated, these pathways develop many aspects of innate immunity: from cytokine responses to antigen presentation[221]. However, collectively, NF-κB and IRF contain more than 100 unique proteins within their signaling network providing many potential areas beyond the PRRs for manipulation[222].

Rather than search for novel agonists for these pathways, we explored the potential to manipulate the signaling activity of existing ligands through the addition of small molecules we term "immunomodulators". This approach differs from prior use of small molecules in vaccine adjuvants as other high throughput screens identify small molecules that exhibit immunostimulatory activity[223–225]. Previously, we demonstrated the possibility of modulation via a selective NF-κB inhibitor, SN50. When combined with CpG, a potent TLR9 agonist, SN50 reduced the systemic inflammatory cytokines TNF-α and IL-6 while improving antigen-specific antibody titers[182; 183]. To expand upon these results, we developed a multi-step high throughput screening approach to study a library of 3,000 small molecule modulators in combination with a wide array of existing PRR agonists. We observed significant changes

of transcription factor activity, cytokine expression, and co-stimulatory molecules in our in vitro screens. Modulators inhibited and enhanced both NF-κB and IRF, resulting in different activation profiles across all PRRs. Surprisingly, some modulators demonstrated activity that was broadly general across many receptors, whereas others were only effective against one or a small subset of receptors. Throughout our screening process, we developed tools to quantitatively score and select the top performing combinations of agonist and modulator with the goal of applying these toward vaccination.

Lastly, we explored the translation of our modulators to an in vivo setting. We identified two noteworthy classes of modulators: modulators that reduce proinflammatory cytokines and modulators that enhance antibody levels.

3.3 Results and Discussion

3.3.1 NF-κB and IRF Transcription Factor Activity Altered by Immunomodulators in a Primary Screen

To identify new adjuvants, we conducted a high throughput screen to examine differing levels of innate immune cell NF-κB and IRF activity after treatment with immunomodulators in combination with PRR agonists. We chose RAW-Dual macrophages so that both IRF and NF- κB could be measured in parallel[226; 227]. For our primary screen, we explored a tar-

Library	**Vendor**	**Number**
General Inhibitors	Selleck Chemicals	2796
NF-κB Inhibitors	Selleck Chemicals	40
NF-κB Inhibitors	MedChem Express	206
Tolerance Compounds	Various	105
Total		3141

Table 3.1: Compounds Explored in Primary Screen

geted library of small molecules: 246 NF-κB and IRF inhibitors and 2,901 pathway specific inhibitors sourced from commercial vendors (Table 3.1). Many of the included compounds were previously studied, a few even receiving FDA approval for various therapeutic applications. We hypothesized this library had an increased likelihood of modulating our desired immune signaling pathways. We tested this library's modulation of 13 PRR agonists, with the majority being toll-like receptors (TLRs) (Table 3.2)[33]. We included this wide range of agonists to better understand trends in modulator activity across similar or distinct PRRs and signaling pathways.

Agonist	**Target**	**NF-κB**	**IRF**	**Conc (μg/mL)**
Pam_2CSK_4	TLR2/1	X		0.1
Pam_3CSK_4	TLR2/6	X		0.1
poly(I:C)	TLR3		X	1
MPLA	TLR4	X	X	0.25
LPS	TLR4	X	X	0.1
Flagellin	TLR5	X	X	1
Imiquimod	TLR7	X	X	2.5
TL8-506	TLR8		X	0.1
CpG ODN 1826	TLR9	X	X	0.5
3'3'-cGAMP	STING		X	10
Tri-DAP	NOD1	X		25
MDP	NOD2	X		10
mIFN-β	IFNAR1/2	X	X	0.0083

Table 3.2: Agonists Explored in Primary Screen

To screen this initial library for activity in modulating NF-κB and IRF activity, we seeded cells in 384 well plates using high throughput robotics. Immunomodulator compounds were added in DMSO, via pin-drop, to a final concentration of 10 μM ($< 0.05\%$ DMSO vol/vol).

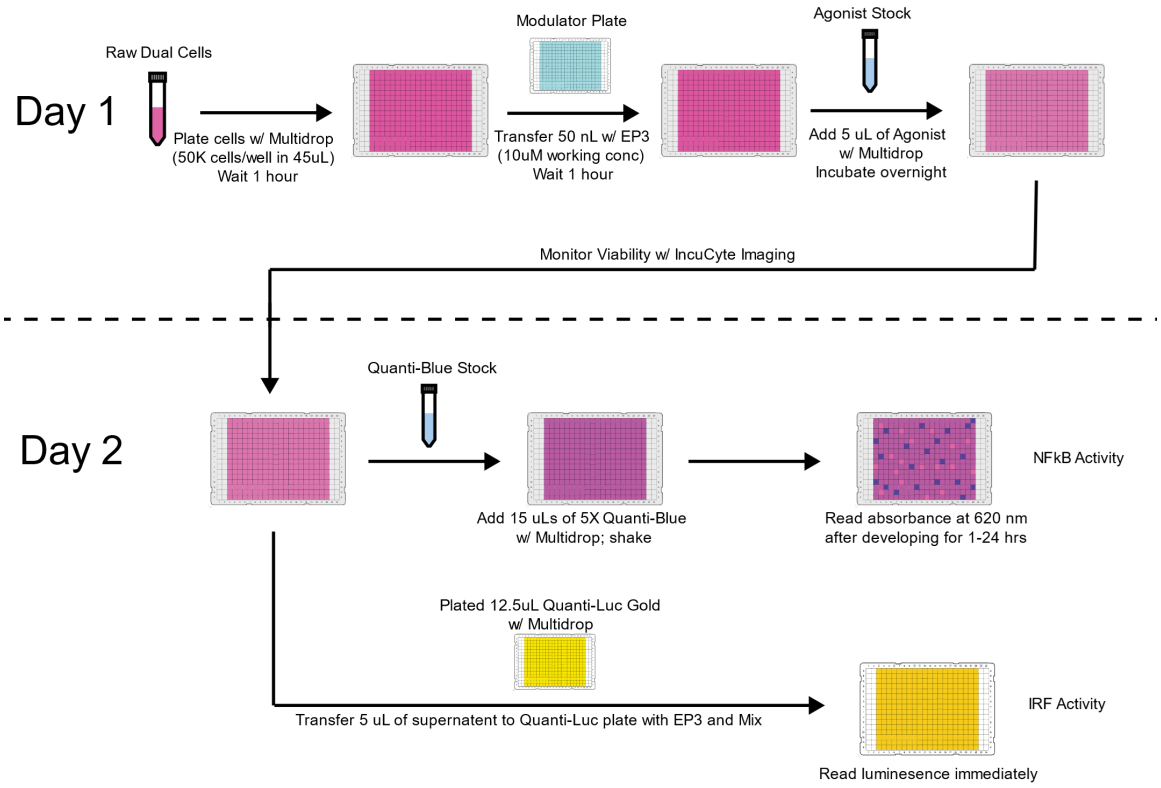

Figure 3.1: Schematic of High-Throughput Screening Workflow for Primary Screen

Following 1 h incubation at 37 C, one of fourteen PRR agonists was added to approximately the EC50 for each agonist. Cells were incubated with agonists and modulators for 24 h and supernatant was drawn for simultaneous analysis. To ensure consistent and quality results, we optimized this workflow including: cell seeding density, incubation time, agonist concentration, liquid handling, reagent volume, and plate uniformity (Figure 3.1)[228; 229].

Our initial screening approach presented unique challenges regarding this assay optimization and analysis. Most high throughput screens seek to either maximize or minimize a desired output[223–225]. As such, a typical result might report enhancement as a fold-change above a baseline. In our primary screen, we anticipated finding inhibition of both immune pathways. However, we were surprised to see for the 13 agonists studied, addition

of different modulators produced either enhancement or inhibition - sometimes ranging over 100-fold in both directions compared to agonist alone controls (Figure 3.2).

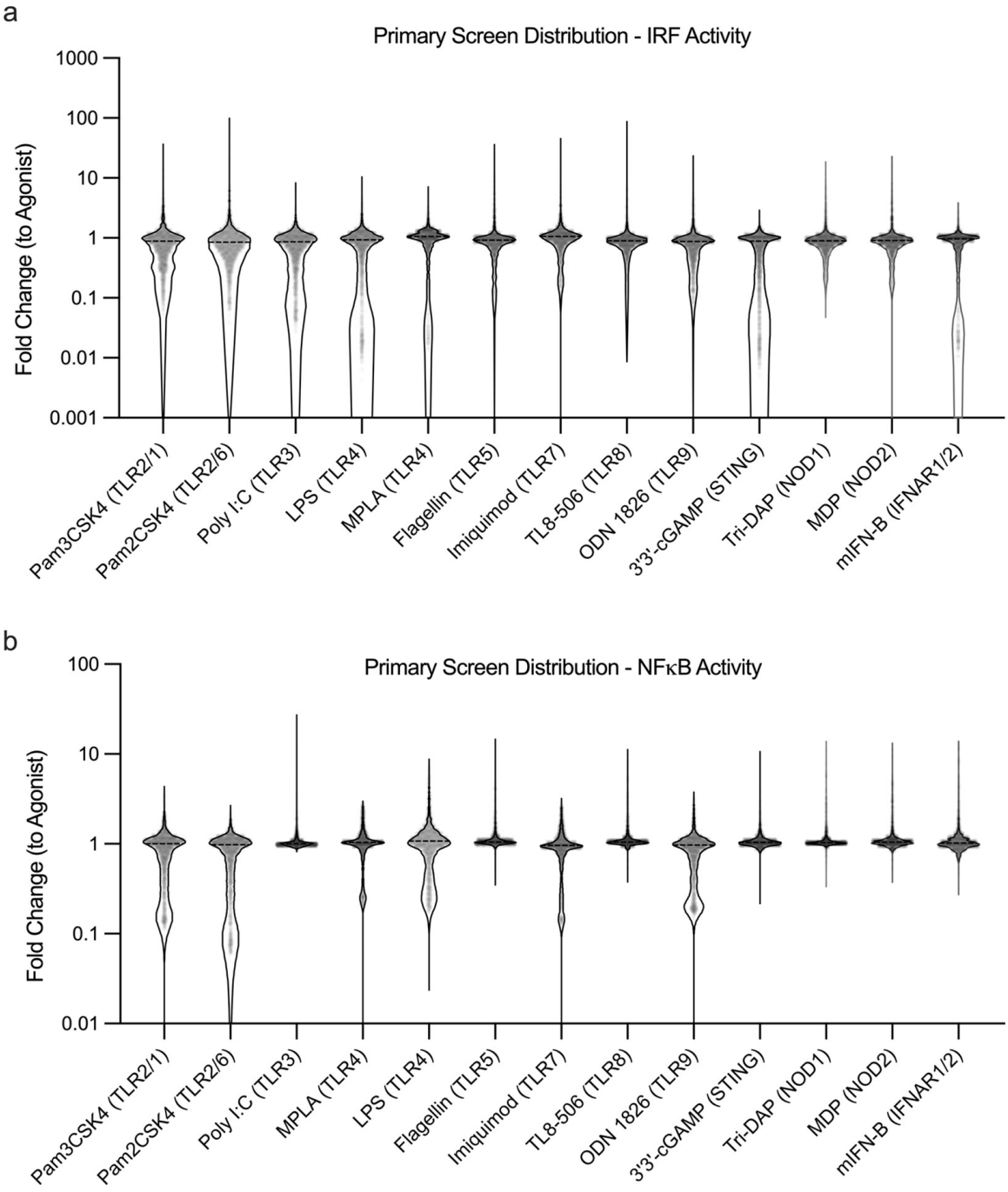

Figure 3.2: RAW Dual cells transcription factor activity for (A) IRF, and (B) NF-κB 24 hours after addition of modulator + agonist. Modulator (N = 3147) + agonist (N = 13) activity reported as a fold change compared to agonist alone activity. Inhibition and enhancement over multiple orders of magnitude is observed.

3.3.2 Classifying Immunomodulators on PRR Agonist Trends

Having successfully completed our primary screen, we began to study additional aspects of modulator activity with the goal of identifying optimal modulators for further study. First, we ensured that modulators alone do not exhibit inherent stimulation of either NF-κB or IRF, but rather that only combinations of modulator and agonist lead to variation in transcription factor activity (Figure 3.3A). Compounds that significantly activated either pathway on their

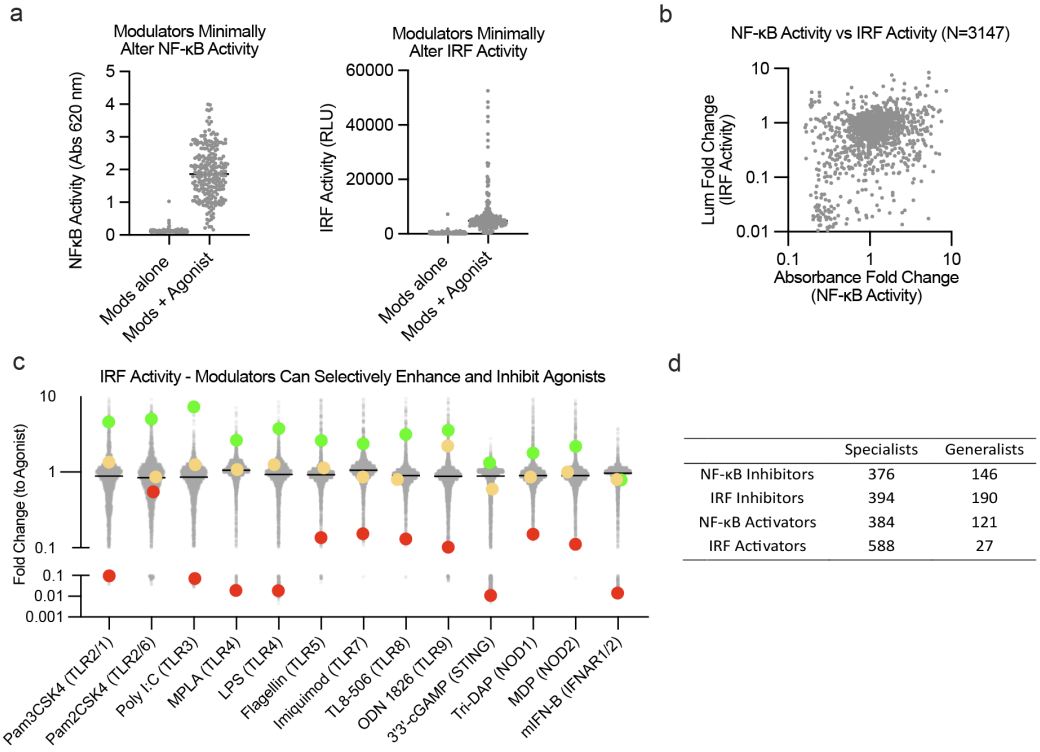

	Specialists	Generalists
NF-κB Inhibitors	376	146
IRF Inhibitors	394	190
NF-κB Activators	384	121
IRF Activators	588	27

Figure 3.3: A) Modulators (N=3147) alone show little inherent activity in either NF-κB or IRF transcription factors. B) Modulation of transcription factor for NF-κB with LPS shown to act independently of IRF transcription factor modulation ($R^2 = 0.0409$) C) Modulators demonstrate different trends across agonists: general enhancers (green), general inhibitors (red), or specialist activity (yellow) D) Table summary of specialist modulators (active with only one agonist) and generalist modulators (active with 12-13 agonists)

own were removed from further study (<1% of the library). Upon comparing NF-κB and IRF transcription activity, we observed little correlation between the two ($R^2 = 0.0409$),

indicating these pathways can be studied independently with our assay (Figure 3.3B). This modulation persists even when using potent agonists with high levels of activity. For example, modulation of 3'3'-cGAMP, a STING agonist, showed a fivefold increase in IRF activity - a result which surprised us as very few molecular entities have achieved higher activation of STING than 3'3'-cGAMP[230]. The balance of measuring large degrees of both inhibition and enhancement tested the limit of the assay's dynamic range – an issue that persisted throughout our various screening efforts.

A key observation from this larger data set was that modulators act either specifically or generally. For example, modulator X enhances IRF for TLR4 while other PRRs' activities remain unaffected. Conversely, modulator Y enhances IRF for all receptors. To identify each type of modulation, we classify immunomodulators that are specific to a few receptors as "specialists" and modulators that affect nearly all receptors as "generalists" (Figure 3.3C, D). Further, some modulators enhanced one PRR for a particular pathway and yet inhibited another PRR for the same pathway. We see wide distributions across each receptor/pathway, with some agonists showing greater statistical significance due to a larger dynamic range. Monitoring distributions across similar PRR targets revealed a correlation in their activity. For instance, modulation of MPLA and LPS, both TLR4 agonists, showed similar trends across NF-κB and IRF activity. Modulation of Pam_2CSK_4 (TLR1/2), Pam_3CSK_4 (TLR2/6), and other NF-κB dominant agonists also have degrees of correlation.

3.3.3 Removal of Inactive and Undesirable Modulator/Agonist Combinations

We sought to identify high modulatory compounds while removing inactive or toxic modulator/agonist combinations. We first designed a high throughput method to filter toxic modulators by measuring viability. As a proxy of viability, we used live cell imaging combined with digital analysis to create confluency masks. After applying our viability masks, we identified compounds with the highest likelihood of altering IRF and NF-κB responses.

To focus on high value PRR/modulator pairings, we also removed PRR agonists based on a lower Z-factor cutoff score.

In this down selection stage, we did not yet prioritize enhancement or inhibition, but sought only to remove compounds that had minimal effects on PRR agonist activity. To discern the relative level of activity, we employed principal component analysis on the dataset to quantitatively compare levels of variance between the compounds[231]. This dataset included both NF-κB and IRF distributions from eight agonists for a total of 16 variables. PC1 and PC2 accounted for 49% of the variation within our dataset. We sought to move forward only compounds that had major changes to immune response, so we created a circle with a radius of 1.75 PCA units centered on the origin. We rationalized this because, when using PCA, datapoints centered around the origin contain the least amount of variability. We retained compounds outside this radius - reducing the number of immunomodulators from 3,147 to 720 (Figure 3.4). This numerical cutoff was chosen to maximize the number of

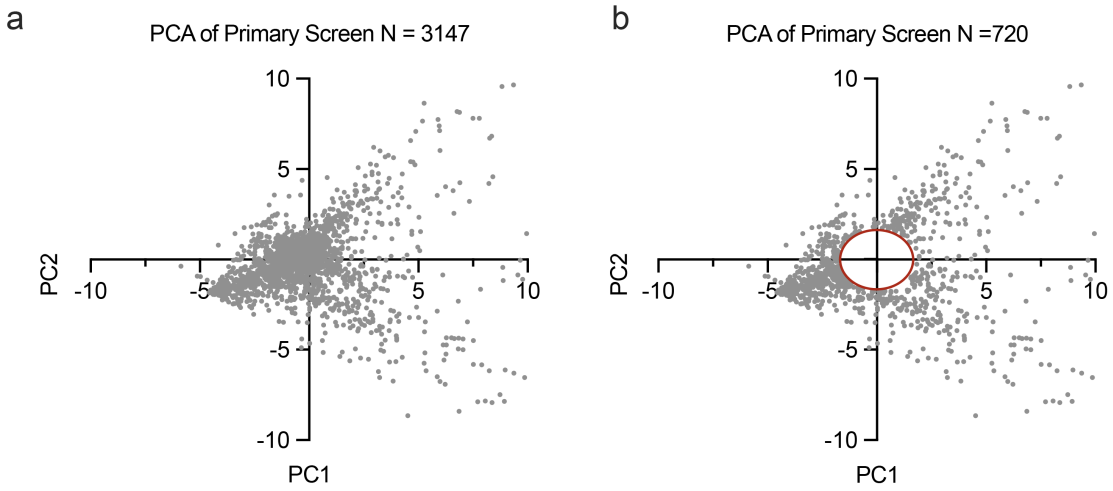

Figure 3.4: Downselection of immunomodulators via principal component analysis. A) Principal component analysis with IRF and NF-κB transcription factor data from all modulators (N=3147) and high z-factor agonists (N=8). B) Compounds with minimal variability were removed by creating a circle centered on the origin with radius 1.75.

dynamic modulators compared in higher cost multiplexed cytokine responses which we sought

to correlate with tolerability and efficacy. These 720 compounds composed our secondary library for further screening analysis, preserving the high degree of pathway modulation (Figure 3.5).

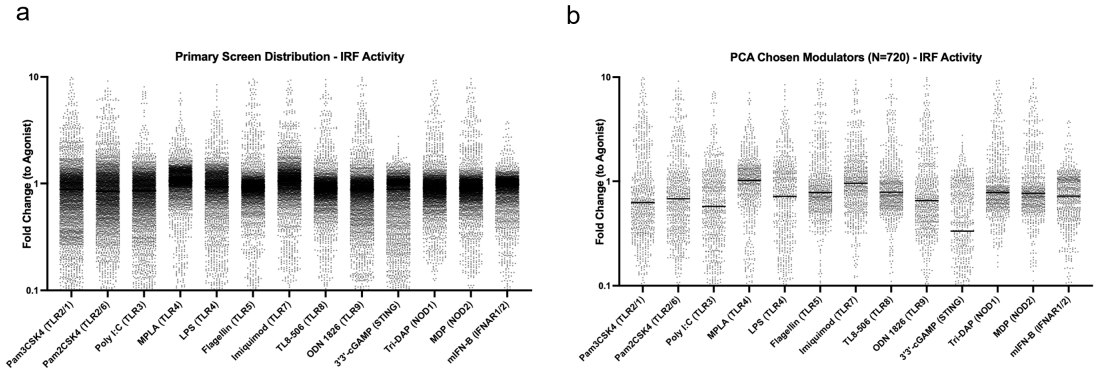

Figure 3.5: Verification of PCA down-selection analysis. A) Full primary screen distribution (N=3147) for IRF transcription factor activity. B) Distribution of Modulators chosen by PCA cutting analysis (N=720) shows retention of tails of NF-κB and IRF distributions and a significant reduction of modulators around a fold change of 1.

3.3.4 Cytokine Expression Changed by Immunomodulators in a Secondary Screen

Our next goal was to determine how the modulators would alter the cytokine response of innate immune cells to identify compounds for use in in vivo experiments. Cytokines and chemokines are secreted signaling proteins induced by adjuvants to regulate adaptive immunity[232]. However, excessive production of certain cytokines by adjuvants results in tissue damage. This response is strongly correlated with vaccine tolerability[123; 233]. To achieve the wide dynamic range necessary for modulators, in situ measurement, and multiplexed measurement, we employed the AlphaLISA assay[234–236]. As we narrowed our compounds, we sought to ensure their compatibility with human immune responses. Conveniently, human AlphaLISAs provided more multiplexed cytokines. As a result, we performed the screen with THP-1 monocytes. We measured the levels of six cytokines/chemokines in-

volved in inflammation, tolerability and adaptive responses - IL-12p40, IP-10, IL-1β, CCL4, TNF-α, and IFN-γ - accounting for a wide dynamic range and assay metrics[237]. TNF-α and IL-1β are endogenous pyrogens and there are multiple reports correlating them with induction of fever for vaccine tolerability[238]. TNF-α provided a baseline measure of generalized inflammation. Additionally, IL-1β is a measure of inflammation that is partially outside direct NF-κB regulation, unlike TNF-α, enabling us to differentiate compounds based on their pathways of inflammation[239]. We chose to study IFN-γ due it strong correlation with IRF pathway and its role as an antiviral type I interferon[240]. IL-12/23p40 activates NK cells, induces production of IFN-γ, and polarizes towards a Th1 and Th17 response[241]. IP-10 (CXCL10) is a chemoattractant for T cells and DC cells and correlated in adjuvants studies as an early signal of induction of strong responses[242]. Finally, CCL4 is a chemoattractant for monocytes and NK cells[243]. IP-10 and CCL4 were recently shown to correlate with tolerability issues[244]. This cytokine assay, the secondary screen, had an identical workflow as the primary screen until supernatant analysis. Cell supernatants were collected, and cytokines were measured in three, duplexed measurements (Figure 3.6). We optimized

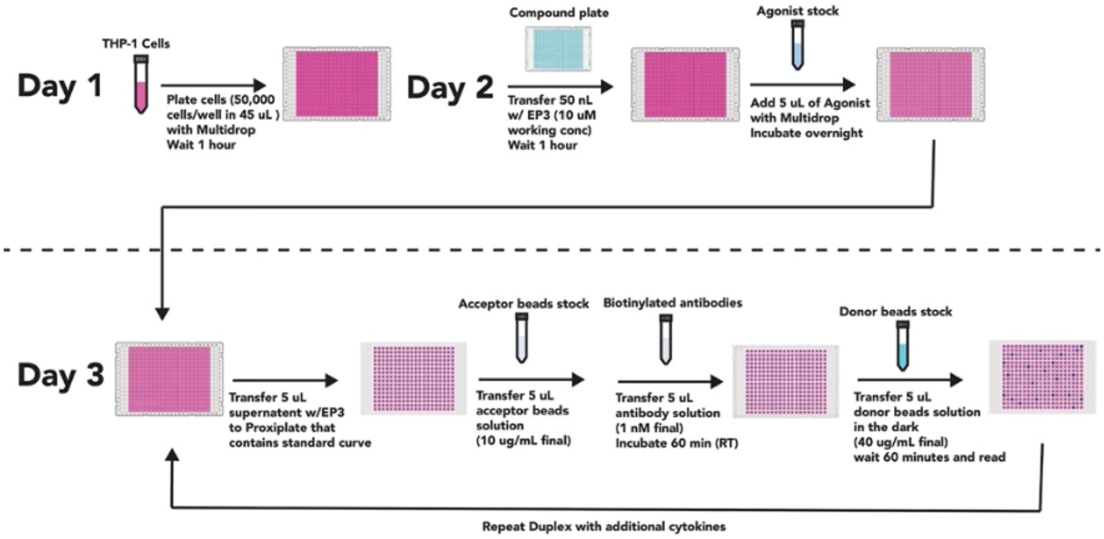

Figure 3.6: Cytokine screen workflow and optimization. Schematic representation of the AlphaPlex workflow

standard curve ranges, crosstalk correction factors, incubation times, and other parameters of the secondary screen to account for any differences between experiments. We stimulated cells with a subset of seven agonists from the primary screen. The distributions within cytokines varied based on the dynamic range and Z-factor obtained for each cytokine and agonist studied (Table 3.3). Modulators enhanced or inhibited cytokine production among

			Cytokine and Z-Factor					
Agonist	**Target**	**Conc.**	IL-1β	IL-12	IP-10	CCL4	TNF-α	IFN-β
Pam_3CSK_4	TLR2/1	0.1	0.51	0.67	0.23	0.82	0.68	-
Pam_2CSK_4	TLR2/4	0.1	-0.76	0.69	0.12	0.62	0.66	-
LPS	TLR4	0.1	0.69	0.32	0.50	0.67	0.71	-
Flagellin	TLR5	1	0.03	0.60	-0.19	0.57	0.71	-
R848	TLR7/8	10	0.79	0.88	0.87	0.56	0.61	-0.6
3'3'-cGAMP	STING	10	-	-	-	-	-0.69	-
poly(I:C)	TLR3	1	-	-	-	-	-	-

Table 3.3: Z-factor analysis of secondary screen. High throughput screening utilizes Z-factors as a proxy for statistical reliability of an assay, with $1.0 > Z > 0.5$ indicating an excellent assay and $0.5 > Z > 0$ indicating a marginal assay.

all six cytokines by several orders of magnitude (Figure 3.7). Similar to the primary screen, we observed that modulators could alter signals independent of one another (Figure 3.8A, B). Since each agonist produced differing levels of cytokine, sometimes near the limits of the standard curve, amending this assay for high-throughput analysis had limitations. Since the assays were multiplexed, dilution of individual wells or selection of other AlphaPlex excitation/emission profiles would increase cost and time significantly. This resulted in some compression of cytokine responses with lower or higher levels. Notably, IFN-γ which had a relatively low signal, and IP-10/CCL4 which had high signal and concentrations. Since we measure fold-change and reduce dimensionality in analysis, this approach is adequate to compare compounds within our dataset for down-selection. However, on account of these

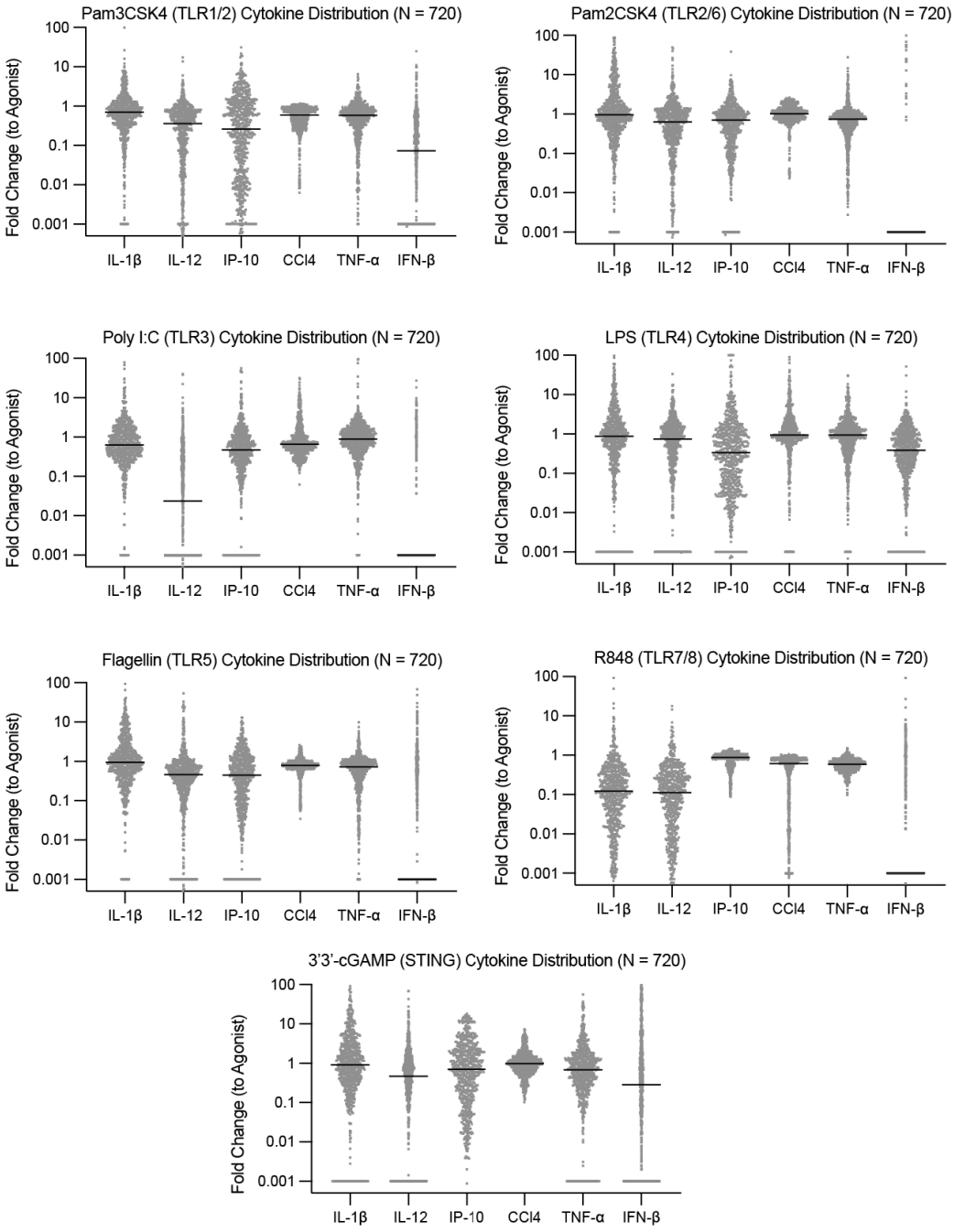

Figure 3.7: THP-1 cytokine distributions for TNF-α, IL-1β, IFN-β, IL-12/23 (p40), IP-10 (CXCL10), and CCL4 24 hour after addition of modulator + agonist. Modulator (N = 720) + agonist (N = 7) activity reported as a fold change compared to agonist alone activity. Inhibition and enhancement over multiple orders of magnitude is observed. Nondetectable measurements of cytokines were given a value of .001 fold change.

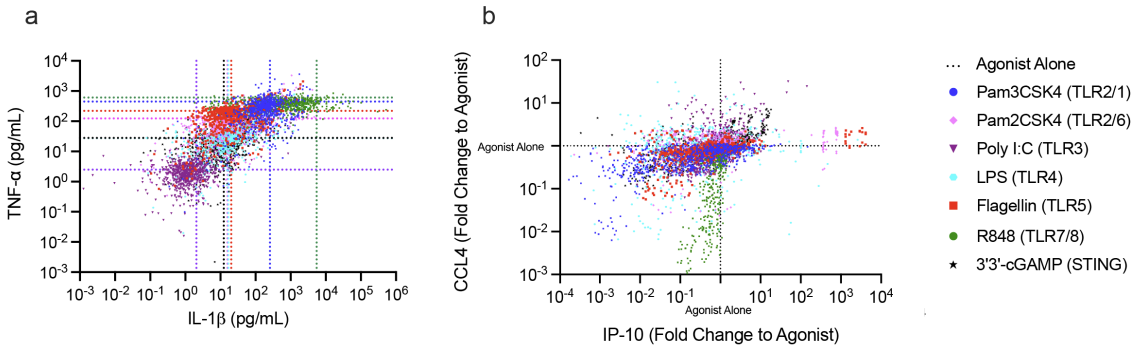

Figure 3.8: A) Concentrations of TNF-α and IL-1β (pg/mL) of each agonist + modulator combination. Dotted lines represent agonist alone secretion. Modulation allows for enhancement and inhibition independent of cytokines. B) Modulation of CCL4 and IP-10 of each agonist + modulator combination, represented as a fold change compared to agonist alone activity.

limitations, we caution the reader not to interpret any individual compound's cytokine response as equivalent to a typical ELISA assay with exacting parameters.

Similar to our primary screen, we observed that modulators alone do not natively affect or induce cytokine release, but rather the combination of agonist and modulator elicits a large increase or decrease in cytokine and chemokine production. Changes in cytokine activity did not always correlate with a corresponding level of change in the transcription factor activity for the same modulator. We did observe that, for the most active compounds, transcription factor activity correlated with an increase or decrease in cytokine response. For example, the strongest inhibitors of NF-κB also resulted in the lowest TNF-α levels. While the modulators can alter responses in unique patterns, they appear to do so with a generalized conservation of signalized pathways. When comparing agonists with similar profiles such as Pam2CS4K and Pam_3CSK_4, similar trends of enhancement and inhibition for each cytokine are observed.

To validate the effectiveness of our down-selection from the primary screen, we compared cytokine modulation between the selected compounds and an equivalent, random portion of the original primary screen library. We selected LPS as the agonist on account of its wide dynamic range. The secondary, down-selected library contained compounds with far

greater TNF-α range of activity compared to the random, equal in number primary screen compounds evaluated using an F test comparing Kurtosis of log-transformed TNF-α values supporting using NF-κB and IRF activity as a valuable down-selection tool (Figure 3.9).

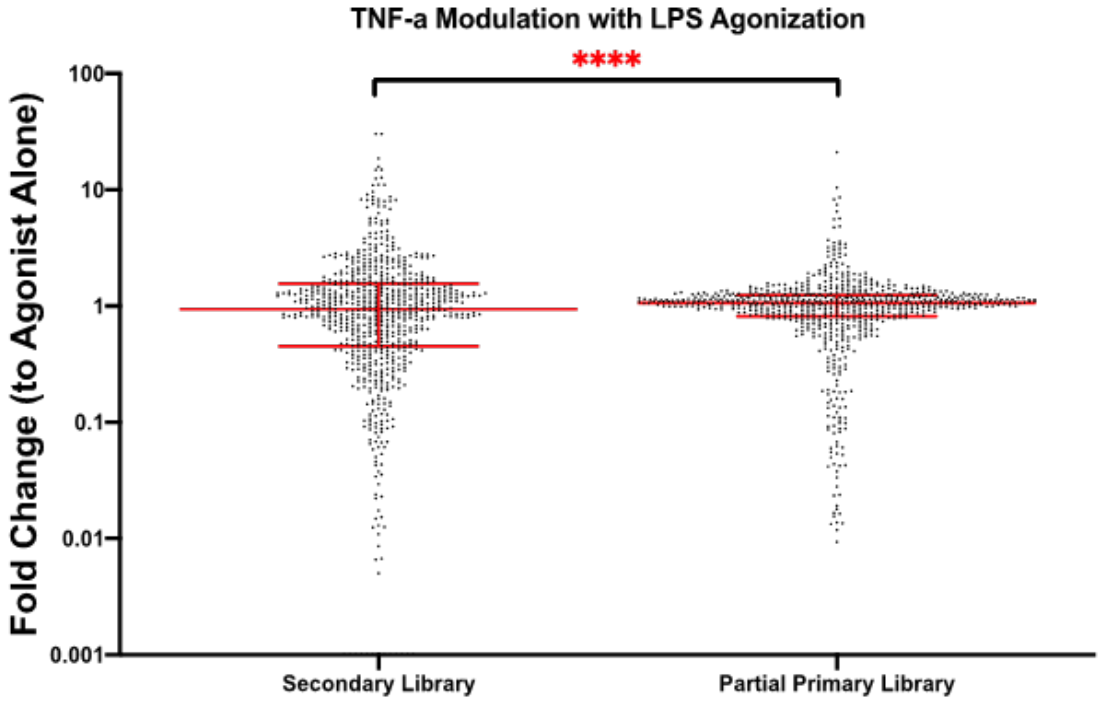

Figure 3.9: Secondary Library Shows Increased Immunomodulation. Comparison of 720 PCA selected compounds to 720 random subsection of primary screen TNF-α comparison from a subsection of the primary screen (N=720) and the secondary library (N=720) show a significant increase in modulators that deviate from a fold change of one, showing evidence in the effectiveness of the PCA down selection method. **** P $<$ .0001 Statistical analysis performed was a F Test to compare variance. Kurtosis of log-transformed primary screen: 6.884, secondary screen: 5.907.

3.3.5 Defining Cytokine Modulation via a Flexible, Quantitative Scoring System

With an increasing number of variables to consider when searching for desirable agonist and modulator combinations, we sought to develop a general framework to assist in the final down selection of modulators for testing in various in vivo applications. Since our previous

work focused on improving adjuvants for prophylactic vaccines, we developed our first scoring system to identify candidates for this use – creating a "cytokine score" as a quantitative metric. Modulator performance was quantified such that the "cytokine score" would preserve cytokine changes by normalizing each cytokine's and agonist's dynamic range[245]. Unlike our previous screen, we considered increases and decreases in cytokine responses separately when selecting molecules for vaccination studies. In a potential vaccine, a promising candidate would need to produce minimal systemic pro-inflammatory cytokines while increasing IFN-γ and chemokine production[123; 233]. Additionally, the score might prioritize the importance of one cytokine's modulation over another. To account for each of these issues, we assigned weighting variables of varying magnitudes to each cytokine depending on the desired modulatory effect (Table 3.4)[246].

	IL-1β	**IL-12**	**IP-10**	**CCL4**	**TNF-α**	**IFN-β**
Weight (Enhancer)	-0.5	1	1	0.5	-2	2
Weight (Inhibitor)	0.5	-1	-1	-0.5	2	0

Table 3.4: Weight Factors for Cytokine Score Generation

To account for differences in the dynamic range of all six cytokines, we normalized the data to ensure no single cytokines distribution would bias the results. Thus, cytokine responses were transformed to fit a range from -1 to 1 (Figure 3.10A). Because modulators acted on individual receptors with distinct responses, the first result from the vaccine scoring system is a "specialist" score for a specific agonist + modulator combination (Figure 3.10B). To then identify modulators which improved responses across multiple PRRs, the individual scores were summed to provide a "generalist" score across all agonists (Figure 3.10C).

The result of the cytokine scoring methodology created a spread amongst compounds ranging from 10 at the highest to nearly -20 at the lowest. Within the highest rated compounds for generalist modulators, the scoring system resulted in approximately 20 with scores between 6-10 from the total pool of 720 potential compounds. As a representation,

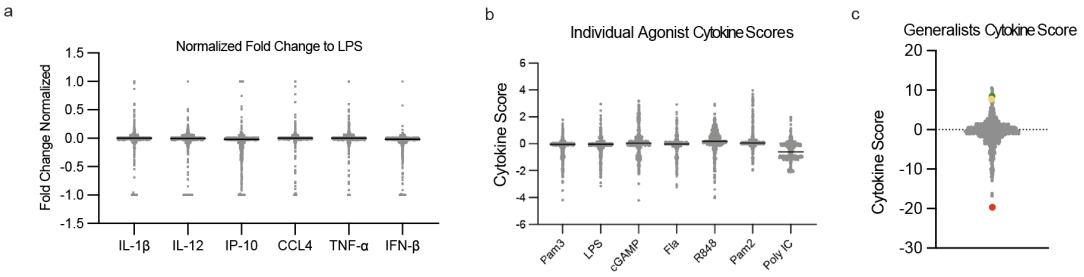

Figure 3.10: Cytokine score creation. A) Representative normalized cytokine distributions for one agonist, LPS (N=720) B) Cytokine score for each agonist (N=720), individual agonist cytokine scores are summed up to create the C) generalist cytokine score

we included one example compound to demonstrate the patterns observed for the individual modulators – PME-564 (Figure 3.11A). PME-564, a tyrosine kinase inhibitor, was one of the highest scoring compounds on our ranking system. Its high score can be attributed to a strong enhancement of IP-10 across most agonists and enhancement of IFN-γ and IL-12 for several agonists. PME-564 also decreased TNF-α expression across all agonists with notably high suppression for Pam_3CSK_4 and Resiquimod (R848) (Figure 3.11A). In selecting for a "generalist", we note that modulator activity is not exactly equal across all agonists. For example, comparing PME-564's enhancement of IP-10 and IFN-γ for Pam_3CSK_4, Pam_2CSK_4 vs cGAMP, there are nearly 2 orders of magnitude in difference. This suggests that depending on the application, a generalist might still have limitations vs specialist modulators for enhancing specific pathways. However, for suppression of inflammatory signals and thereby its ability to promote tolerability, this category of modulators was broadly general. Suppressing inflammatory cytokines, even partially, for nearly every PRR suggests these molecules might be used toward improved tolerability and broad use in improved vaccination or other immunotherapies.

In contrast to PME-564, we highlight PME-2988 (Figure 3.11B), which is a compound in our dataset with a strong negative cytokine score. This compound eliminated IL-12, IFN-γ, and IP-10 secretion across most receptors studied while simultaneously enhancing IL-1β and TNF-α secretion by nearly 100-fold. PME-2988 will not be useful as a vaccine

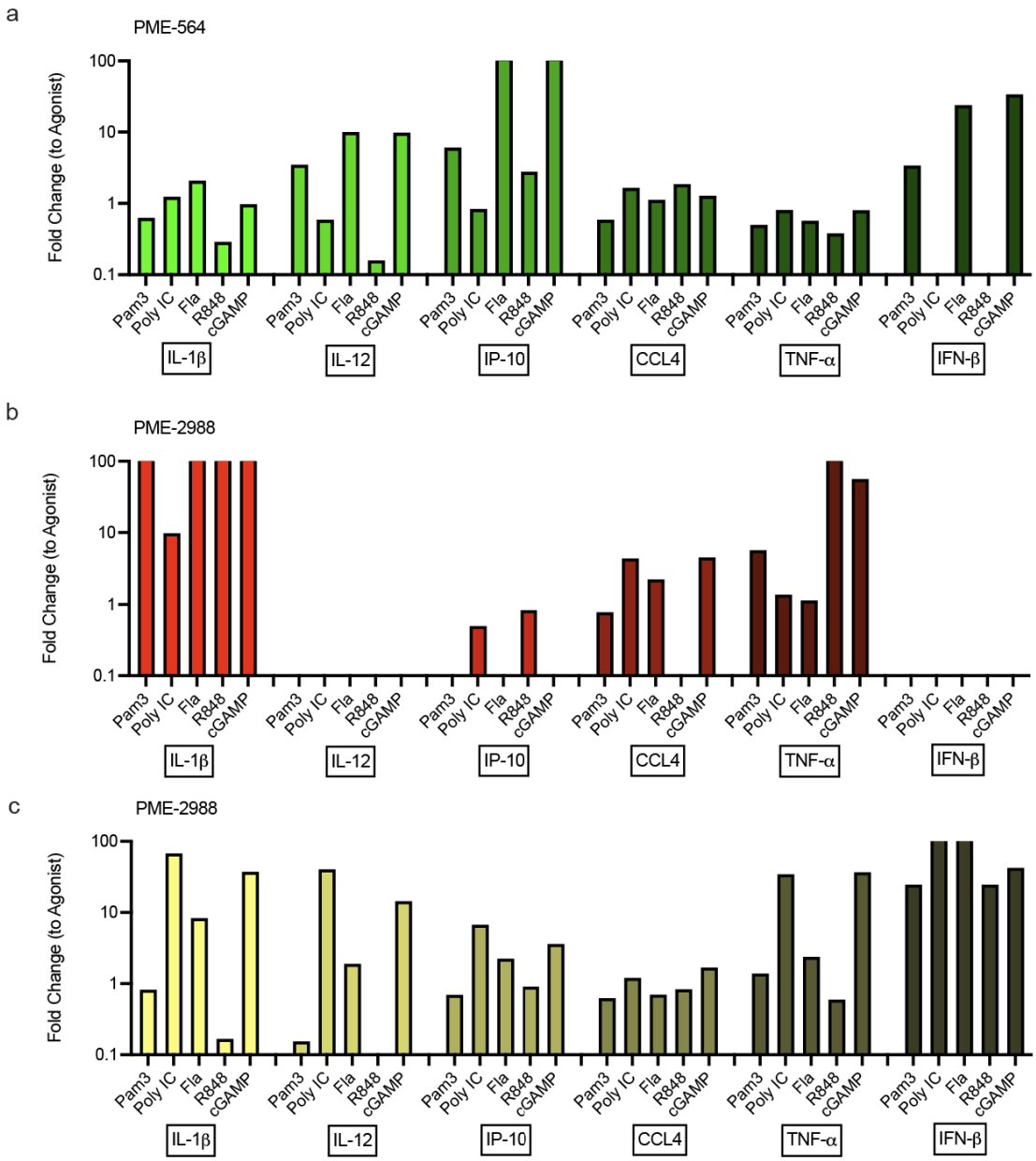

Figure 3.11: Demonstration of different cytokine scoring modulators. Cytokine production of a top vaccine score candidate, A) PME-564 (green), a negative score candidate, B) PME-2988 (red), and a candidate for additional applications, C) PME-2539 (yellow). Modulator + agonist activity reported as a fold change compared to agonist alone activity.

adjuvant, but its ability to radically alter secreted cytokines highlights the wide-ranging potential of modulators. This score is tailored to identify prophylactic vaccine adjuvants, but compounds within this dataset may be applicable for exploration in alternative appli-

cations. For instance, PME-2539 (Figure 3.11C), may warrant additional study in a cancer immunotherapy as it upregulates beneficial antitumor cytokines and chemokines[247; 248]. This compound can enhance TNF-α up to 36-fold using cGAMP and is shown to enhance IFN-γ secretion across all agonists studied. While further enrichment of cancer adjuvants is outside the scope of our current work, we seek to investigate these applications more in the future. We used the general cytokine score to identify a small subset of lead modulators of interest for preliminary in vivo studies. These compounds were also validated in murine bone marrow-derived dendritic cells (BMDCs).

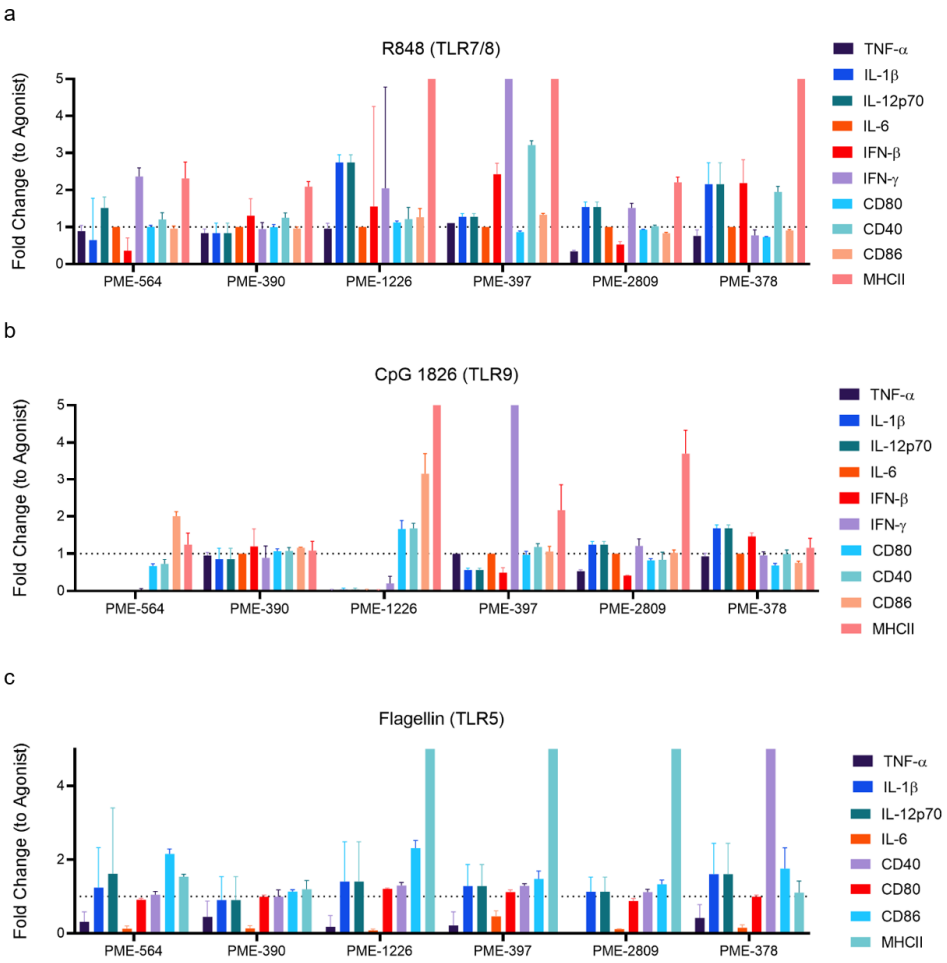

Figure 3.12: BMDC immunomodulation distribution of top candidates from cytokine score. Cytokines and cell surface markers were measured 24 hours after agonizing with A) R848, B) Flagellin, and C) CpG. Modulators show significant ability to lower inflammatory cytokines in primary cells as well enhance cell surface markers.

These immunomodulators altered cytokine production and cell surface markers in combination with multiple agonists (Figure 3.12). The foundation and simple mathematical nature of our scoring system allows us to apply this methodology to different areas of interest, albeit limited by the scope of the cytokine panel studied. Additionally, further screening efforts such as cell surface marker expression could be incorporated into this scoring system in the future. While we created a vaccine scoring system, a similar methodology could be tailored toward other applications, whether for inflammation therapeutics or cancer immunotherapy, control of immune pathways has potential in many immune-therapeutic spaces.

3.3.6 Surface Marker Expression Modulated and Measured via High-Throughput Flow Cytometry

We furthered our understanding of immunomodulation by measuring costimulatory and antigen presenting surface marker expression in innate immune cells. Innate cell activation and licensing results in the upregulated expression of surface proteins required to prime T cells. We chose to monitor the expression of three surface proteins, MHCII, CD86, and CD40 in THP-1 monocytes after treatment with adjuvant and immunomodulators. These molecules are all involved in the three signal paradigm for T cell priming[46; 47]. In the case of vaccines, the included extracellular antigen is phagocytosed and presented on MHCII molecules, serving as signal one when bound to the T cell receptor. The costimulatory molecules CD80 and CD86 engage CD28 on T cells, serving as signal two. CD40/CD40L interactions are also critical as the promote the secretion of cytokines by antigen presenting cells - this cytokine environment serves as signal three. While these molecules are expressed constitutively on innate cells, activation through adjuvants results in increased expression. This allows antigen presenting cells to better activate naïve T cells, initiating the adaptive response.

We developed a high throughput flow cytometry protocol to efficiently and accurately measure these surface markers in our THP-1 monocytes (Figure 3.13). As suspension cells,

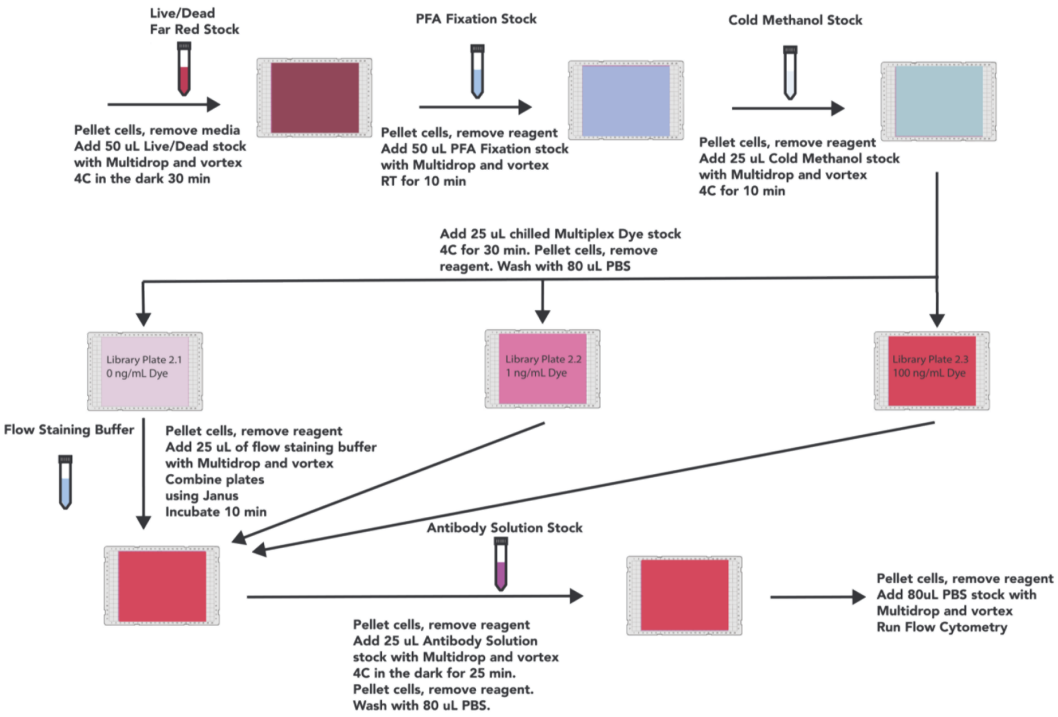

Figure 3.13: High-throughput flow cytometry staining workflow. Schematic representation of the staining procedures for THP-1 monocyte surface marker expression

THP-1s were more adaptable for flow cytometry use as they did not require physical or chemical detachment. THP-1 monocytes also exhibit similar expression trends of the markers we chose compared to their macrophage phenotype after PMA-differentiation[249]. We used the same 720 compound immunomodulator library and 7 agonist panel as the cytokine screen, treating THP-1 cells with immunomodulators for 1 hour before agonist addition. After an overnight incubation, cells were stained for viability before formaldehyde fixation and methanol permeabilization. Notably, we optimized our fixative to the minimum concentration that maintained cellular integrity, but maximized staining. Additionally, we fluorescently barcoded cells with three concentrations of an AF750-NHS ester dye: 0 ng/mL, 1 ng/mL, and 100 ng/mL[250]. This allowed for multiplexing three plates together before Fc blocking and surface marker staining with our antibody cocktail. This step reduces the reagents used and time spent on the cytometer by three-fold. When analyzing the data, the

samples from each plate can be demultiplexed based off fluorescent intensity of the multiplex dye (Figure 3.14).

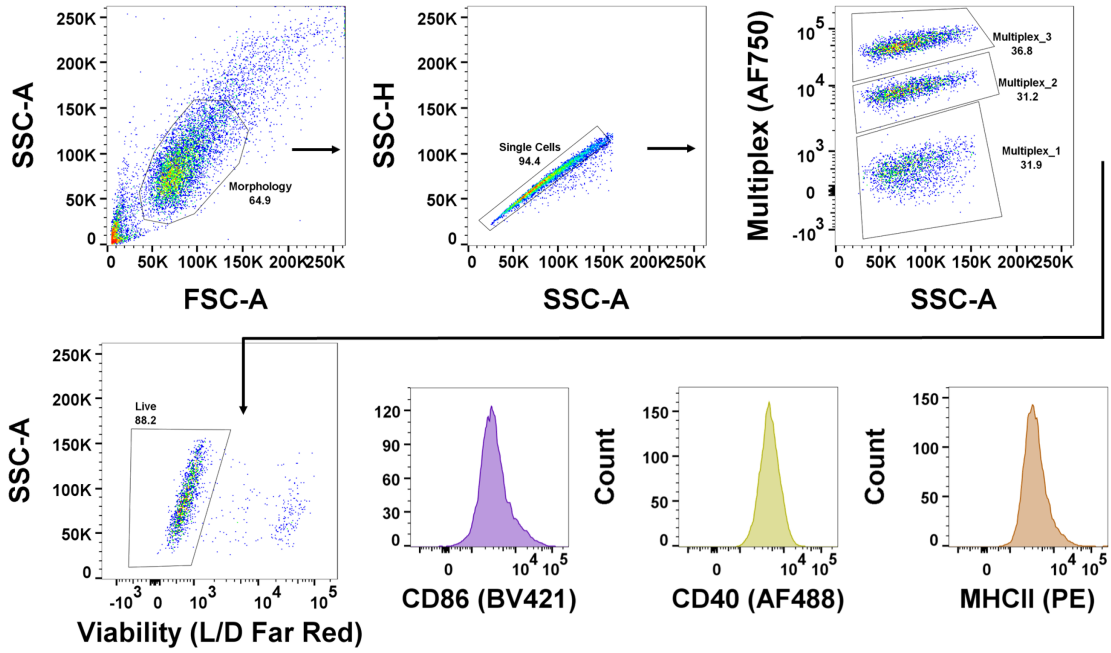

Figure 3.14: High-throughput flow cytometry gating strategy and fluorescent barcoding. After gating on morphology, individual samples can be distinguished through AF750 fluorescent intensity (0 ng/mL, 1 ng/mL, and 100 ng/mL). Dead cells are excluded before measuring the surface markers CD86, CD40, and MHC-II for median fluorescent intensity.

As with cytokines, modulators enhanced or inhibited surface marker expression across all agonists studied, albeit over a smaller total range (Figure 3.15). We did not see a large amount of downregulation, due to the lower basal rate of expression of these markers. Interestingly, we observed changes in the fluorescence in the wavelengths of the markers studied, even without the addition of staining antibodies. We assume that some of our compounds have inherent fluorescent properties or are significantly altering the autofluorescence of the THPs. We removed these compounds, and those that exhibited cytotoxicity in >2 out of the 7 agonists studied. After pruning these compounds, our library shrunk from 720 to 448 compounds.

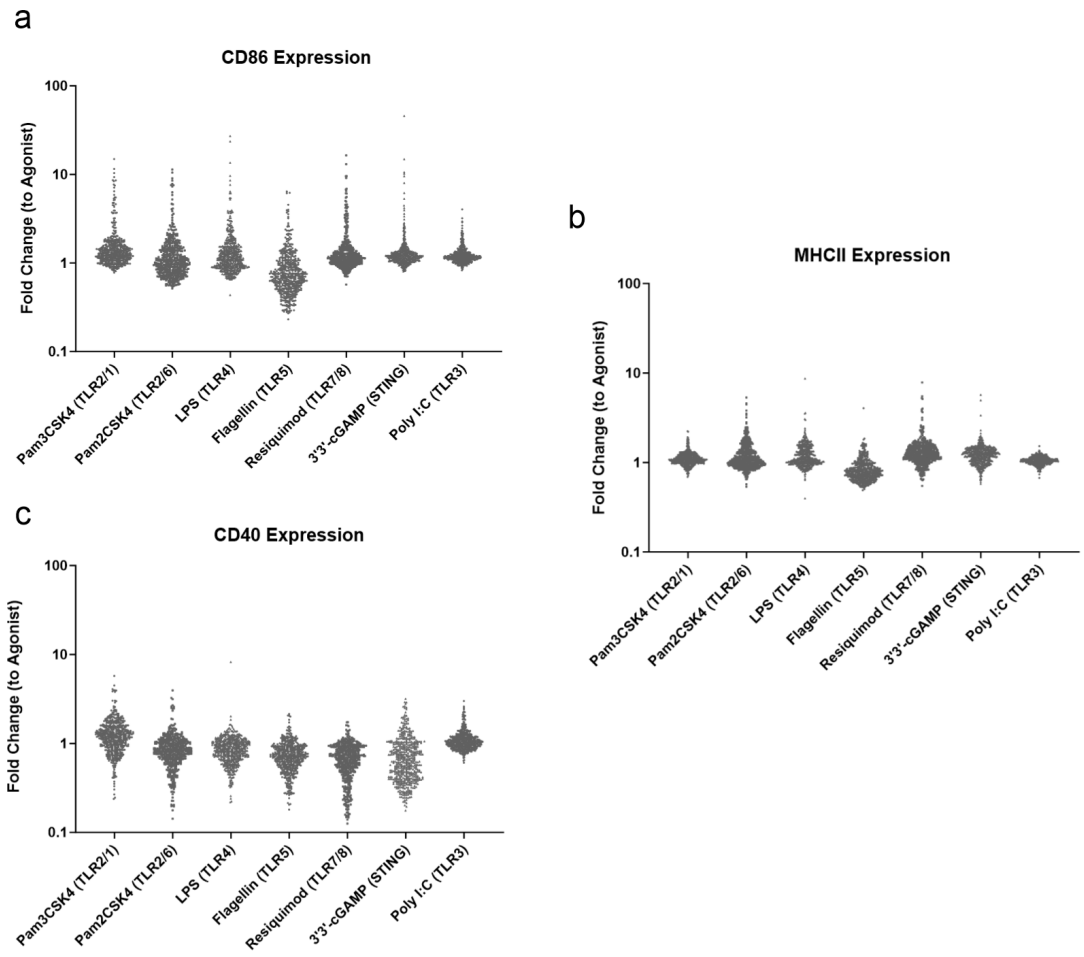

Figure 3.15: Distributions of surface marker modulation in secondary screen. THP-1 cells show modulated A) CD86, B) MHCII, and C) CD40 activity reported as a fold change compared to agonist alone activity across 448 compounds and 7 agonists. Inhibition and enhancement over multiple orders of magnitude is observed.

3.3.7 Defining Surface Marker Modulation via a Quantitative Scoring System

With our prior scoring system demonstrating success in identifying cytokine modulation, we applied the same methodologies in creating a scoring system for surface marker expression. As before, we transformed the data to fit a range between -1 and 1 in order to preserve as much expression level data as possible (Figure 3.16A). The surface marker scoring system

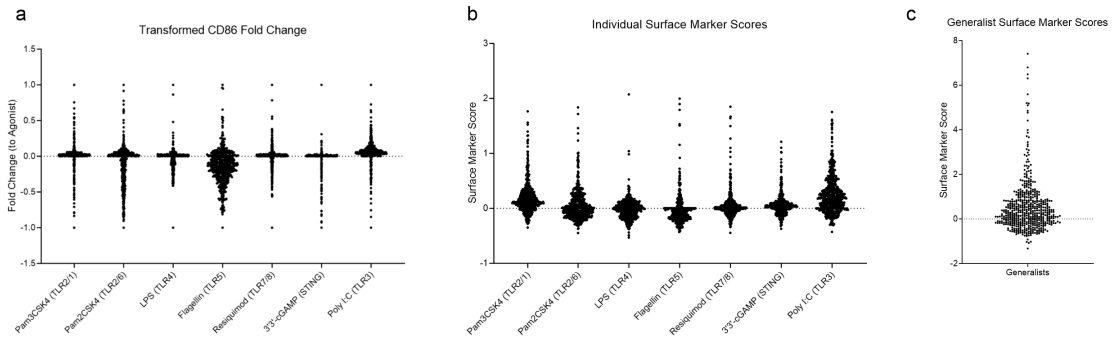

Figure 3.16: Surface marker score creation. A) Representative normalized surface marker distributions for one marker, CD86 B) Surface marker score for each agonist, individual agonist surface marker scores are summed up to create the C) generalist surface marker score.

was altered in two key ways from the cytokine scoring system due to the nature of the screen. First, we weighted the individual markers equally as we did not expect there to be a biological benefit in upregulating a singular marker. For a prophylactic vaccine, we desired to see an increase in all of these markers. Thus, modulators exhibiting an increased fold change over the agonist alone were given a weight of +1 while modulators exhibiting a decreased fold change were given a weight of -1. The second alteration to the scoring system applies to modulators with a decreased fold change. Since the THP-1 cells expressed a low basal level of cytokines, we believed compounds that exhibited only a small decrease in surface marker expression to be within the noise of our assay. Thus, modulators with a fold change of $0.8 < x < 1$, transformed to a normalized fold change of $-0.2 < x < 0$, were assigned a score of "0" for this marker, negating any "penalty" to the score. We once again created "specialist" scores as the modulators behaved differently across the agonists studied (Figure 3.16B). Summing these scores together gave the "generalist" score as a summary statistic for a modulator's ability to modify any adjuvant (Figure 3.16C).

3.3.8 Combining Cytokine and Surface Marker Scores into a "Vaccine Score"

We then sought to merge our scoring systems together into a combined, total vaccine score. We first compared the immunomodulator's generalist scores for each category on a single plot (Figure 3.17A). From this, we can see that the dynamic range of the cytokine scores are greater than that of the surface markers. Additionally, the surface markers have less negatively scoring compounds compared to the cytokine score. Nonetheless, we decided to equally weight the cytokines and surface markers and focused on creating a generalist vaccine score. We multiplied each score by 0.5 and combined these results into our final vaccine score (Figure 3.17B). Ideal candidates are likely in Quadrant 1 in the cytokine-surface marker XY

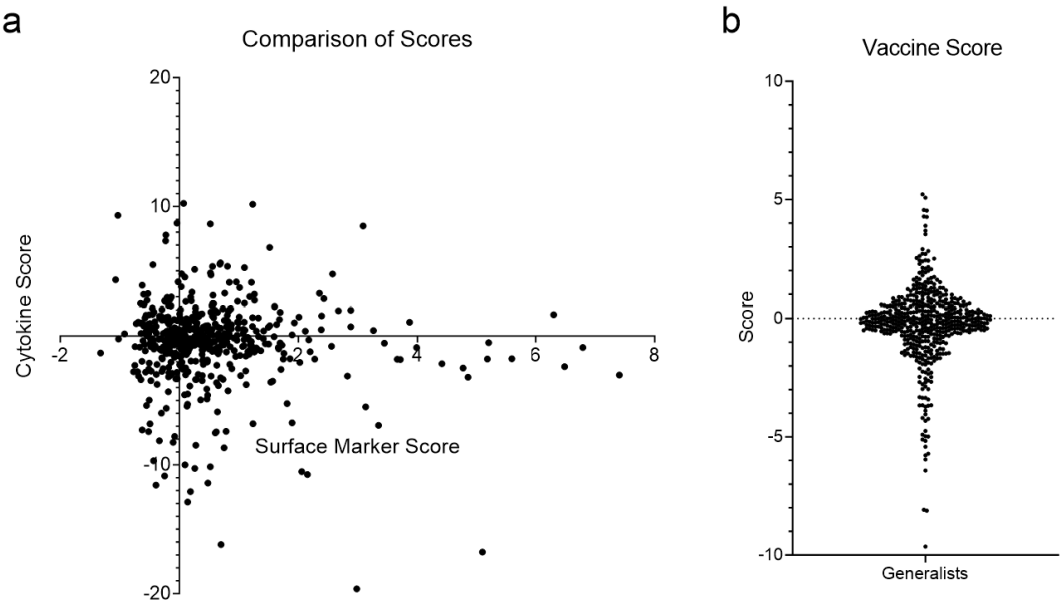

Figure 3.17: Combining cytokine and surface marker data into a vaccine score. A) Comparison of cytokine score and surface maker generalist score. B) Combined generalist vaccine score

plot, with a high positive score in both categories. We found top vaccine candidates to largely fit this description, with some potential bias towards the cytokine score due to its

higher scores. Overall, however, this framework provides a general quantitative metric that allows for easy downselection of our candidates.

3.3.9 Identified Candidates Improve Model Vaccination Responses in Mice

While in the process of making our scoring systems, we used our cytokine score to select modulators to test in a murine in vivo model of vaccination. We repeated the traditional prime-boost vaccination schedule as in our previous preliminary studies using ovalbumin as a model antigen[182; 183]. To test the generalist nature of the modulators, these subunit vaccinations were adjuvanted with a subset of the PRR agonists from our primary screen: R848 (TLR7/8), flagellin (TLR5), and CpG 1826 (TLR9). This subset was selected both for the previous use in vaccines and for a broader cross section of potential use in both subunit (R848, CpG) and as an approximation of whole bacterial (flagellin, CpG) vaccine products[251–253]. We chose a modulator dosage of 1.5 μmol, guided by our previous experience with small molecules and compound solubility limitations[183]. To improve formulation of these hydrophobic compounds, we used a 1:1 mixture of DMSO:Addavax as a vehicle. We monitored inflammatory cytokine levels one hour following initial injections and measured antigen specific antibody levels at two and four weeks post-boost.

Our goal, as previously, was to find compounds that would (a) increase tolerability of the vaccine formulation which we approximate using a simple metric of systemic cytokines 1 hr after injection and (b) improve antibody responses to the vaccination. We began by experimenting with PME-564, one of the highest performing compound from our generalist cytokine scoring system. The addition of this modulator resulted in an increased humoral response for all three agonists tested (Figure 3.18). Addition of PME-564 improved the antibody response for these adjuvants ranging from 2 to 6 fold over their agonist/antigen controls. This increase was remarkably consistent across all the agonists and persisted across both time points.

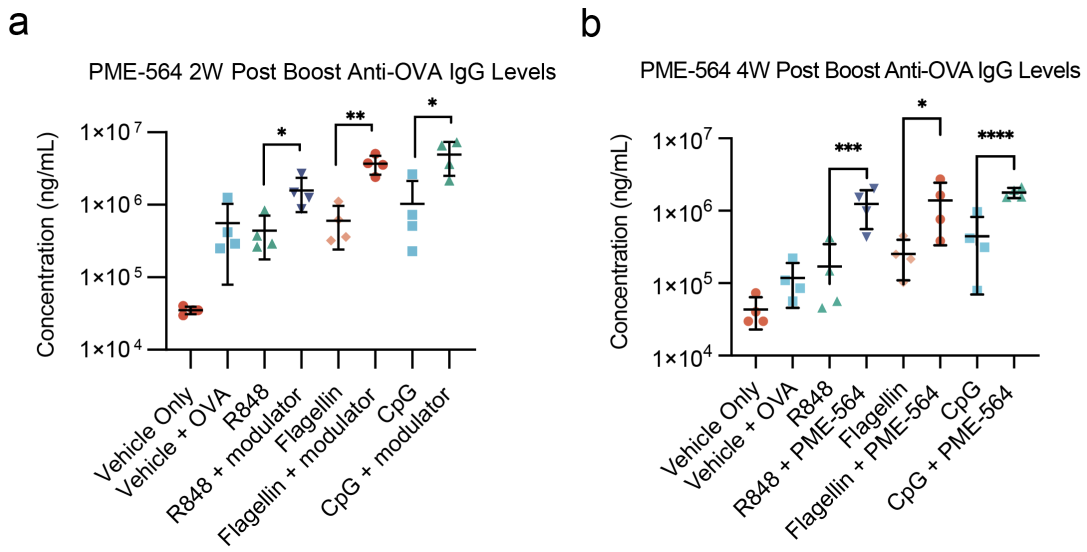

Figure 3.18: A top generalist increases antigen specific antibodies across multiple agonists. After a prime-boost vaccination with ovalbumin as a model antigen, agonist + PME-564 serum anti-OVA IgG antibody levels both A) two weeks post boost, and b) four weeks post boost (n = 4). Statistical analyses between agonist and agonist + PME-564 were performed by an unpaired t test. (* = $p < 0.05$, ** = $p < 0.01$, *** = $p < 0.001$, **** = $p < 0.0001$)

Emboldened by these positive results, we expanded our search to 5 more high scoring generalists following the same vaccination schedule as before (Figure 3.19). We observed that for the 5 modulators, compounds 2 (PME-1226) and 3 (PME-397) strongly decreased TNF-α for CpG 1 hour post injection. This decrease in systemic inflammatory cytokines is strongly correlated with improvement in clinical scoring, temperature drop, and weight-loss providing strong indications that these compounds could be used to improve the tolerability of CpG in further applications. Interestingly, there were similarities between the compounds that reduced inflammatory cytokines for CpG and for R848. However, as with our previous experiments, modulators were unable to completely remove the inflammatory nature of R848[182]. We hypothesize R848 diffuses rapidly away from the injection site due to its small molecular weight, inducing larger systemic effects. Yet compound 5 (PME-378) still reduced the inflammation to half the original formulation. No compounds showed statistically significant reduction in cytokines for flagellin, though compound 5 (PME-378) showed a decreasing

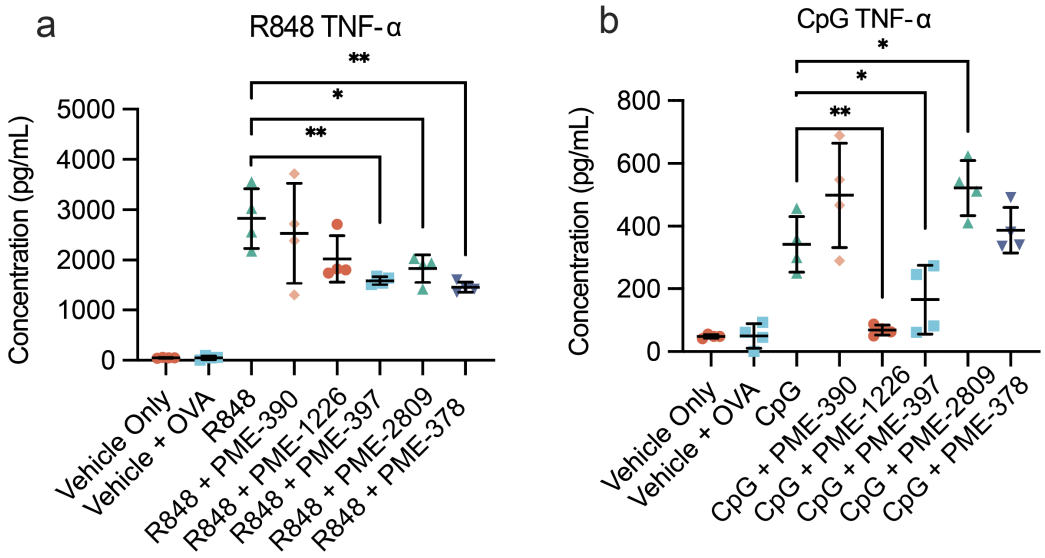

Figure 3.19: Generalist modulators decrease systemic cytokines with R848 and CpG. Systemic TNF-α levels 1 hour after vaccination with agonist, agonist + modulator, and vehicle (N=4) for R848 (TLR7/8) and CpG (TLR9). Statistical analyses between agonist + modulator groups and agonist alone were performed by a one-way ANOVA test. (* = $p < 0.05$, ** = $p < 0.01$

trend. Reduction of inflammatory cytokines did not result in an increase in antibody levels in most cases, but instead maintained a response similar to the agonist control.

We then explored modulators that scored highly in the combined vaccine score which added the surface marker expression data. We selected the top 5 scoring generalist immunomodulators and performed a similar prime-boost vaccination schedule as before, but with a singular adjuvant CpG 1826 and a more disease relevant antigen, hemagglutinin (HA) from an influenza A strain (Figure 3.20A). When observing systemic inflammatory cytokine data, we see a decrease in TNF-α 1 hour after injection in 3 out of the 5 modulators (Figure 3.20B). Additionally, when looking at antigen specific IgG antibodies two weeks post boost, we see a stark increase in production again for 3 out of the 5 modulators (Figure 3.20C). Two of the modulators, PME-2542 and PME-564, significantly decreased inflammatory cytokines while also boosting antibody responses. With this as the desired result, the inclusion

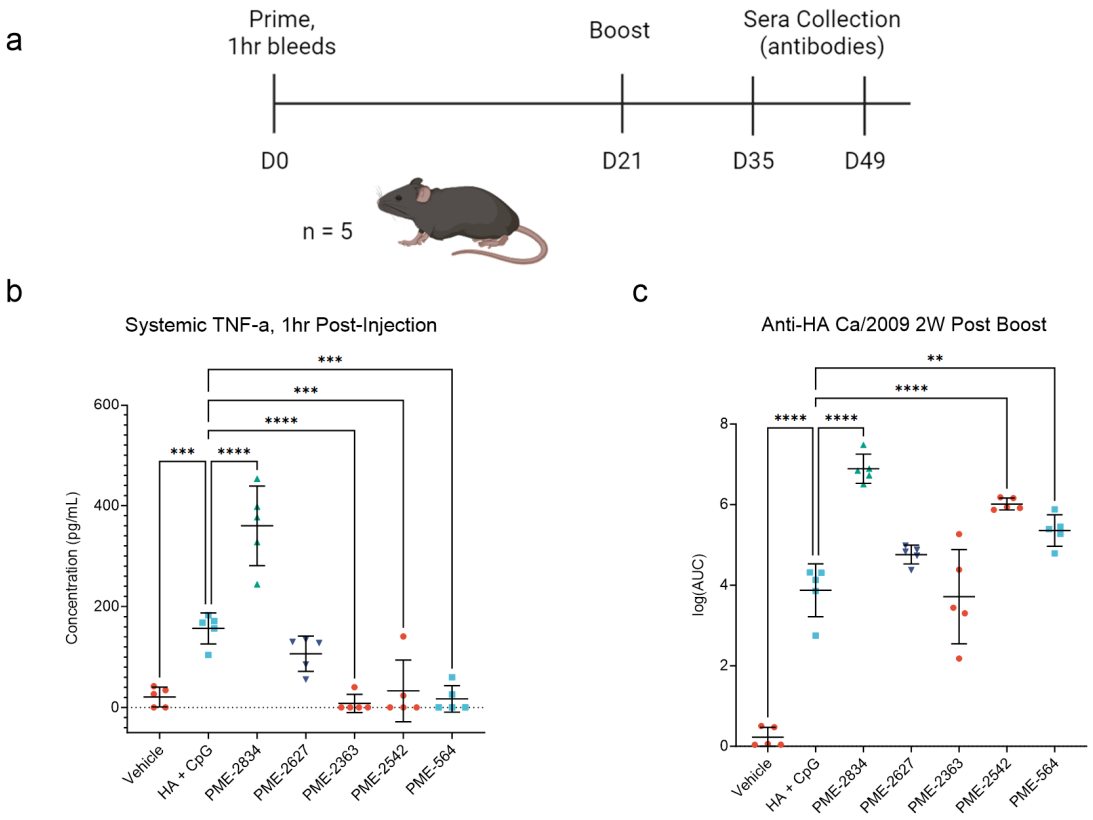

Figure 3.20: Immunomodulators selected by vaccine score outperform the cytokine score. A) Vaccination schedule schematic. B) Immunomodulators decreased systemic cytokines compared to CpG adjuvant alone one hour post injection. C) Immunomodulators increased antigen specific antibodies two weeks post boost. Statistical analyses between agonist + modulator groups and agonist alone were performed by a one-way ANOVA test. (* = $p < 0.05$, ** = $p < 0.01$, *** = $p < 0.001$, **** = $p < 0.0001$)

of the surface marker data served to increase the hit rate and versatility of our identified immunomodulators.

While these results are promising, we hypothesize that solubility and biodistribution of our modulators may limit their effectiveness in these formulations, and optimizing formulations for our lead candidates is an active area of investigation. Initial attempts at formulating antigen, agonist, and modulators in liposomal delivery systems diminished cytokine and antibody responses across both controls and treatments. Additional in vivo screening of candidate modulators is needed to further prove the efficacy of our quantitative scor-

ing systems. While there is much more that can be learned both about the immunological mechanism and the application to specific therapies of these modulators, our efforts here focused on the screening and down-selection of novel compounds with an extensive PRR library. With the identification of new compounds with new properties, we plan to examine the biological mechanism and potential for application in future studies.

3.3.10 Discussion

Our results demonstrated that modulators can be identified which operate with generality – improving the antigen specific antibody response more than 5-fold when used with multiple adjuvants. Conversely, modulators can also be selected which operate with specificity – matching with one adjuvant most successfully to lower systemic cytokines. The conclusion for this initial screen is that a ranking and assessment screen was sufficient to help identify modulators with a success rate in vivo of approximately 10-20% with just a cytokine screen, to almost 50% with both cytokine and surface marker expression data. While our in vivo results are preliminary for and much remains to be tested prior to use in clinical vaccines, modulators hold promise to enhance immune responses and mitigate side effects. At the same time, we want to highlight that this screening and selection process can be applied to modulatory outcomes for many immune-therapeutic applications beyond just vaccination.

Our study identifies a class of immunomodulators that can affect both innate and adaptive immunity. Many of these compounds have been previously used in alternative applications. For instance, our top compound, PME-564, has been used clinically in treatment against myelogenous leukemia. It inhibits the activity of multiple kinases, but it has previously demonstrated interaction with Lyn kinase. Lyn is a Src-family kinase whose roles in innate signaling extend throughout the innate system[254]. TLR pathways are partially regulated by Lyn as the kinase is membrane bound and associated with the TLR/MyD88 complex. In pDCs, Lyn promotes the trafficking of CpG from the extracellular space to internal endo-

somes - altering the production of proinflammatory cytokines and Type I IFNs[255]. Adding a Lyn inhibitor in combination with a TLR agonist may regulate proinflammatory cytokines and chemokines that we measured in our high throughput screens. While these previous studies support our findings, no Src or Lyn inhibitors had ever been combined with adjuvants in the context of vaccines. Another top modulator, PME-2834, is a pan-WNK kinase inhibitor and was originally discovered through work on hypertension[256]. Recently, WNK kinases have been implicated in a diverse array of signaling pathways, including NF-κB[257]. We posit this finding highlights the value of an empirical screening approach to the discovery of new modulators of innate signaling. Thus, we believe existing libraries can be used to explore additional applications for drugs with known indications.

3.4 Conclusion and Future Directions

Adjuvants and immune potentiators can enhance the immunogenicity of vaccines and immune therapies and are critical for effective clinical translation. Yet, there are currently few ways to control reactogenicity and tolerability or to enhance and suppress inflammatory and stimulatory responses. In this work, we present a high-throughput screen which identifies a new family of compounds, we term immunomodulators, that work in combination with traditional adjuvants as signal amplifiers/suppressors. We created a set of selection criteria for identifying molecules which themselves elicit minimal response, but when combined with a PRR stimulating adjuvant, result in changes to the immune response of more than an order of magnitude. This differs from traditional adjuvant discovery, in which small molecules are screened for their inherent ability to agonize receptors. With our approach, we expand innate responses to PRRs, discovering new phenotypes with unique signaling profiles. We screened molecules via a series of in vitro assays; first examining the modulators' ability to alter NF-κB and IRF expression signatures, then examining their ability to alter cytokine response. We developed a ranking system to identify potential lead compounds for use in

vivo. Through this series of down selecting primary and secondary screens, we identified a landscape of immunomodulators that can both enhance and suppress cytokine production and antigen presentation surface marker expression. Using the ranking system, we identified key modulators that lowered systemic inflammatory cytokines and increased antibody responses in vaccination experiments.

We have shown how quantitative and data-driven approaches can predict high performing adjuvant candidates. Taking this a step forward, our current and future work integrates machine learning and big data approaches into the discovery process[258]. To date, there has been little use of machine learning in the context of adjuvant discovery. We used the transcription factor activity from the primary screen as our training input, focusing on individual agonists as distinct databases (Figure 3.21A). This dataset pales in size (n = 3147)

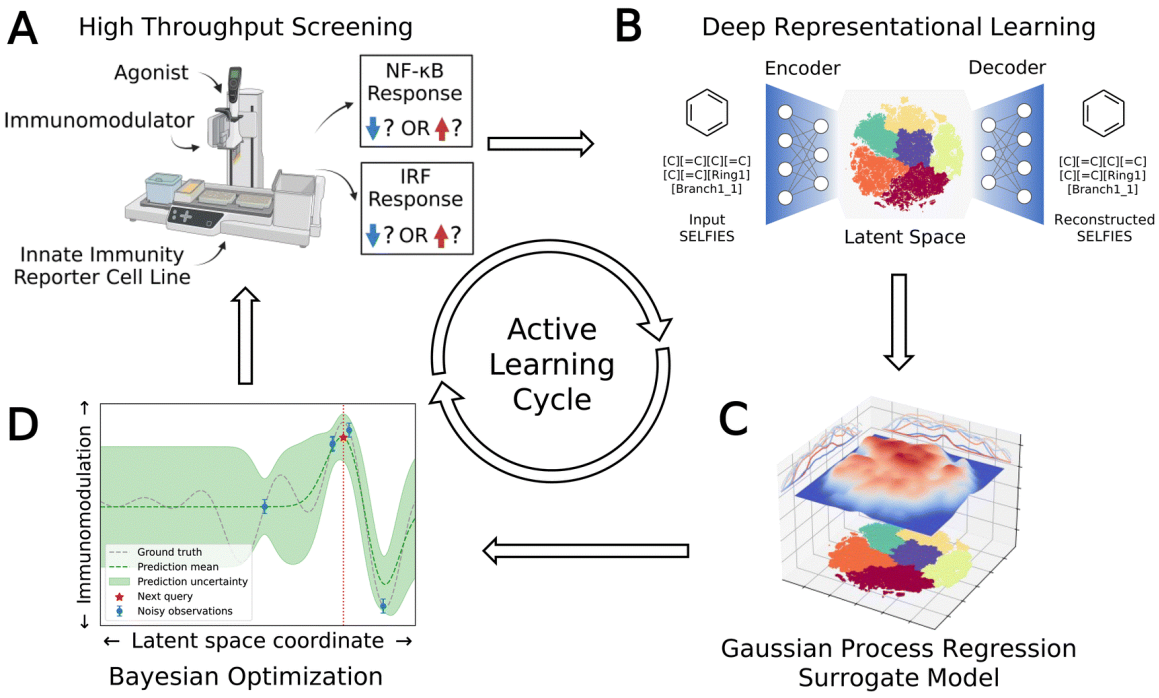

Figure 3.21: Data-driven active learning framework for immunomodulator discovery. A) Wet-lab screening of NF-κB and IRF activity. B) Encoding of immunomodulator candidates into a low-dimensional latent space. C) Training of Gaussian process regression model from experimental NF-κB and IRF transcription factor data. D) Prediction of new top immunomodulator candidates using Bayesian optimization for the next round of wet-lab screening

compared to the computationally screened library (n = 139,998). A variational autoencoder (VAE) was used to embed all immunomodulator candidates into a low-dimensional latent space (Figure 3.21B). The wet-lab transcription factor data was used to train a supervised Gaussian process regression (GPR) model (Figure 3.21C). This model was then interrogated using Bayesian optimization to select a subset of 720 immunomodulator candidates to test in another round of high-throughput screening (Figure 3.21D). This active learning model was repeated four times, for a total of a new 2,880 compounds screened for NF-κB and IRF activity. After sampling only 2% of the in silico library, we found new immunomodulator candidates that greatly increased IRF activity and decreased NF-κB activity, even above immunomodulators in our primary screens. In our estimation, using this in vitro/in silico machine learning cycle reduced the experimental time and financial cost needed to perform the screen by tenfold. This methodology of combining in silico libraries and machine learning algorithms allows for greater throughput of experimentation.

We also anticipate broadening the scope of our screening efforts to alter more aspects of the immune response. Controlling T cell polarization and activity following vaccination is an area of active research. Alum is known to boost a T_H2 response, but this is often ineffective against viral infections[108]. CpG ODNs can polarize towards T_H1 responses, which can be beneficial in protecting against some infectious diseases[96]. Finally, STING agonists can elicit T_H17 responses which might be beneficial in developing long term memory respones, especially against *Mycobacterium tuberculosis*[259]. With such a limited number of adjuvants currently in approved vaccines, selecting an adjuvant that meets the criteria of low reactogenicity, high efficacy, and now, a desired T_H response, is nearly impossible. We demonstrated the ability to alter cytokine expression from innate immune cells following activation with adjuvants. This cytokine milieu is critical in polarizing CD4 helper T cell responses. Thus, we believe are immunomodulators could alter the T_H states elicited by current adjuvants. Additionally, we believe we could unlock new intermediate pheno-

types that are currently not well described by traditional T_H subtypes. T_H subtypes are traditionally categorized by the effector cytokines produced by the activated T cells. Measuring all these parameters complicates high-throughout screening. Instead, we propose T_H polarization could be classified by the five master transcription factors, T-bet, GATA-3, RORγT, Bcl-6, and FoxP3[119]. Expression of these transcription factors was once thought to be mutually exclusive, but recent studies show that co-expression of transcription factors is possible[120; 121]. We have designed a miniaturized T-cell:BMDC co-culture assay to monitor T cell polarization by measuring relative levels of transcription factors via qPCR measurements. BMDCs will be treated with agonists, ovalbumin, and with or without immunomodulator and incubated overnight to allow for activation and cytokine expression. We will then add naïve CD4 T cells that have been immunomagnetically isolated from OT-II transgenic mice. These mice have engineering TCRs that are specific to the OVA 323-339 peptide, allowing us to see a large degree of activation compared to wild-type T cells. Following a multi-day incubation, cells will be lysed and mRNA captured before cDNA synthesis and qPCR readout. This assay will allow for monitoring of how modulators change the phenotypes of naïve CD4 T cells compared to activation with agonist alone.

Overall, with these screening efforts we have furthered our understanding and evidence of immunomodulation for vaccine adjuvants. In future work, we plan to explore both the mechanistic details of how chemically distinct modulators can achieve general patterns of altered immune response. In parallel, we plan to explore how these identified compounds can be used to improve current vaccines, vaccine candidates, or immune therapies. A host of potential approaches could be enabled by employing modulators alongside current technologies including: expanding therapeutic window by increasing tolerability, increasing the overall efficacy via improved humoral responses, altering specific cytokine/chemokine responses to adjust temporal responses of vaccination.

3.5 Materials and Methods

3.5.1 NF-κB and IRF Transcription Factor Screening

RAW-Dual cells (InvivoGen) were plated at 50,000 cells per well in 45μL of DMEM with 5% HI FBS from col 2-23 in clear flat bottom 384 well plates (Greiner Bio-One). Cells attached at room temperature for 1 h. 50 nL of 10 mM modulator libraries were added by Janus G3 via pintool to experimental wells (cols 3-22) for a final concentration of 10 μM. Following 1 hour incubation, 5 μL of PRR agonist was added via a MultiDrop Combi liquid handler (col 3-23). Cells were incubated at 37C and 5% CO2 overnight. 20 hours later, 12.5 μL of QuantiLuc Plus was plated in an opaque, white 384 well plate. 5 μL of RAW-DUAL cell supernatant was then added via Multi-Drop Combi Liquid handler before measuring luminescent values on a BioTek Synergy NEO2 plate reader as soon as plate was completed. QuanitLuc Plus contains a stabilizer which reduces signal decay, allowing for comparable values throughout the read. In parallel, 15 μL of 5X concentrated QuantiBlue was added directly to the remaining cell supernatant in the RAW-Dual cell plate. Absorbance values were measured at varying time intervals at 620 nm. These samples were incubated so that the PRR agonist control reported an absorbance signal of approximately 1 A.U.

3.5.2 Viability Monitoring

Viability was monitored after overnight modulator addition by monitoring confluency via IncuCyte imaging. Two sets of parameters were used to create a confluency mask over all imaged wells. Modulators were considered toxic if both sets of confluency masks were $<$ 70% of those of resting cells. Confluency masks were quantified using IncuCyte software. This methodology was validated with select library plates using a traditional CellTiter Glo assay (Promega). A more detailed description can be found in SI Appendix, Supplementary Information Text.

3.5.3 THP-1 Cell Culture

THP-1 cells were purchased from ATCC and were cultured in RPMI 1640 with 10% Biotin free HI-FBS and 1% P/S at 37C and 5% CO2. Cells were maintained between 0.2-1.0 x 10¬6 cells/mL and were not differentiated.

3.5.4 Cytokine Level Screening

THP-1 cells were seeded at 50,000 cells per well in 45 μL of biotin-free RPMI + 5%HI-FBS in clear 384 well plates. Following 24 h incubation, 50 nL of 10 mM modulator libraries were added by Janus G3 via pintool to experimental wells (cols 3-22) for a final concentration of 10 μM. After 1 hour, 5 μL of agonist was added via a MultiDrop Combi liquid handler (col 3-23). The following day, 5 μL of supernatant was transferred to white low volume ProxiPlates (Perkin Elmer). According to AlphaPlex protocol, 10 μL of a prepared acceptor bead (10 μg/mL final conc), biotinylated antibody (1 nM final conc) mixture was added via liquid handler to the cell supernatant. After 1hr incubation at RT, 5 μL of donor beads (40 μg/mL final conc) were added in the dark. After an additional 1hr incubation, plates were read on a BioTek Synergy NEO2 plate reader with AlphaPlex filters for europium (615 nm) and terbium (545 nm) emission. A separate plate was run each day containing a standard curve of known analyte for interpolation purposes.

3.5.5 BMDC Cytokine and Surface Marker Expression

Bone marrow was harvested from 6-week-old C57BL/6 mice and differentiated into dendritic cells (BMDCs) using supplemented culture medium: RPMI 1640 (Life Technologies), 10% HIFBS (Sigma-Aldrich), Recombinant Mouse GM-CSF (carrier-free)(20 ng/ml; BioLegend), 2 mM l-glutamine (Life Technologies), 1% antibiotic- antimycotic (Life Technologies), and 50μM β-mercaptoethanol (Sigma-Aldrich). After 6 days of culture, BMDCs were plated

at 100,000 cells per well and incubated with modulator (10μM). After 1 hour, agonist was added. Cells were incubated for 24 hours at 37°C and 5% CO2. Supernatant cytokines were measured using LEGENDplex™ Mouse Inflammation Cytokine Kit (BioLegend). Cells were pelleted, washed, Fc blocked, and stained with the following antibodies/reagents at the recommended manufacturer's concentrations: CD11c-AF700 (N418), CD40-APC (3/23), I-A/I-E-AF488 (M5/114.15.2), CD86-BV605 (GL-1), CD80-PE (16-10A1), Live/Dead Fixable Blue. Data was acquired on a NovoCyte Penteon and analyzed via FlowJo 10.8.1.

3.5.6 Flow Cytometry Surface Marker Screening

THP-1 cells were seeded at 50,000 cells per well in 45 μL of biotin-free RPMI + 5%HI-FBS in clear 384 well v-bottom plates. Following 1 h incubation, 50 nL of 10 mM modulator libraries were added by Janus G3 via pintool to experimental wells (cols 3-22) for a final concentration of 10 μM. After 1 hour, 5 μL of agonist was added via a MultiDrop Combi liquid handler (col 3-23). After 16 h incubation, cells were pelleted at 300 x g and aspirated before addition of 50 μL of Live/Dead Far Red (Thermo Fisher) was added via a MultiDrop Combi liquid handler, vortexed to mix, and incubated in the dark at 4C. Cells were pelleted and aspirated before addition of 50 μL of 0.5% paraformaldehyde fixative (Sigma) and incubated at room temperature for 10 min. Cells were pelleted at 750 x g from here onwards, and aspirated before addition of 25 μL of chilled methanol via MultiDrop Combi. Cells were vortexed and incubated at 4C for 10 min. 25 μL of either 0 ng/mL, 1 ng/mL, or 100 ng/mL of chilled AlexaFluor750-NHS ester (Thermo Fisher) in PBS was added followed by incubation at 4C for 30 min. Cells were pelleted, washed twice with 80 μL of PBS, and aspirated before resuspension in 25 μL of flow staining buffer (BioLegend) containing 5% FcX TruStain (BioLegend) to block Fc receptors. The three different intensities of fluorescent barcoding were then combined into a singular plate. After 10 min incubation, cells were pelleted, aspirated, and then resuspended in 25 μL of antibody stock solution containing the following

antibodies: CD86-BV421 (IT2.2), CD40-AF488 (5C3), HLA-DR-PE (L243). After 25 min of incubation at 4C, cells were pelleted, washed with 80 μL of PBS, and resuspended in 80 μL of PBS. Data was acquired using a BD LSRFortessa with HTS attachment and analyzed via FlowJo 10.8.1.

3.5.7 Animals

All animal procedures were performed under a protocol approved by the University of Chicago Institutional Animal Care and Use Committee (IACUC). 6-to-8-week-old C57/B6 female mice were purchased from the Jackson laboratory. All vaccinations were administered intramuscularly in the left hind leg. Blood was collected from the submandibular vein at time points indicated.

3.5.8 Vaccinations

VacciGrade Ovalbumin and Addavax was purchased from InvivoGen. VacciGrade CpG ODN 1826, ultrapure flagellin, and VacciGrade R848 were purchased from InvivoGen. Modulators were purchased through Selleck Chemicals.

Mice were lightly anesthetized with isoflurane and injected intramuscularly in the hind leg with an injection volume of 50 μL containing antigen, adjuvant, and a DMSO/Addavax combination. Antigen dose was as follows: OVA (100 μg), HA (10 μg). Agonist doses per mouse were as follows: Flagellin, 10 μg; R848, 50 μg; CpG, 50 μg. Modulators were added at 1.5 μmol.

3.5.9 Plasma cytokine analysis

Blood was collected from mice at specified time points in 0.2 mL of heparin-coated collection tubes (VWR Scientific). Plasma was isolated via centrifugation 2000xg at 4C for 15 min. Samples were collected and stored at -80C until use. Plasma was analyzed using

Bio-Legend's LEGENDPlex Mouse Inflammation Cytokine Panel (13-Plex) according to the manufacturer's protocol. Samples were analyzed using a NovoCyte Flow Cytometer. Data were analyzed using LEGENDplex Data Analysis Software Suite and GraphPad Prism.

3.5.10 Antibody quantification

Mice were vaccinated with indicated formulations. Blood was collected at time points indicated in 0.2 mL heparin-coated collection tubes (VWR Scientific). Plasma was isolated via centrifugation 2000xg at 4C for 15 min. Samples were collected and stored at -80 °C until use. Anti-ovalbumin antibody levels were analyzed using an anti-OVA IgG ELISA kit (Chondrex) according to the specified protocol. For influenza antibody levels, titers were performed by coating Nunc MaxiSorp ELISA plates (BioLegend) with 100 μL of 2 μg/mL hemagglutinin protein indicated (Sino Biological) overnight at 4C. Plates were washed and blocked with 150 μL 2% (w/v) BSA in PBST for 1hr at RT. Following wash, samples were serially diluted tenfold in blocking buffer for a total volume of 100 μL and incubated for 2hr at RT. Following wash, 100 μL of goat anti-mouse IgG HRP conjugate (Invitrogen) diluted 1:10,000 in 0.4% BSA buffer was incubated for 1hr at RT. Following wash, 100 μL of 1-Step Ultra TMB was incubated for 4.5min before stopping with 50 μL of 2 M sulfuric acid. ELISA plates were analyzed using a Multiskan FC plate reader (Thermo Fisher) and absorbance was measured at 450 nm with 620 nm correction. Area under the curve measurements were approximated with Riemann sums. Data were analyzed using GraphPad Prism.

CHAPTER 4

APPLYING LEAD COMPOUNDS TOWARDS INFLUENZA VACCINES

4.1 Summary

Effective vaccination responses require sufficient activation of innate immunity, which, in turn, initiates adaptive immunity. Innate immune activation in current vaccines often requires adjuvants to generate a robust response. Immunostimulatory adjuvants bind pattern recognition receptors (PRRs) on antigen presenting cells (APCs), eliciting cytokine and surface marker upregulation. Here, we manipulate adjuvant activity via secondary "immunomodulators" to improve the activated state of APCs. We demonstrate enhanced expression of co-stimulatory molecules involved in antigen presentation and activation of adaptive immunity. These immunomodulators were also proven to alter the induced cytokine profiles in our previous studies. We combined top scoring immunomodulators with a variety of commercial vaccines to find a suitable disease model. We selected influenza and identified immunomodulators that improved vaccine tolerability, durability, and efficacy. These immunomodulators increased protection against live viral challenge for both a model CpG adjuvanted subunit vaccine and a commercial inactivated whole pathogen vaccine.

4.2 Introduction

Vaccines are one of modern medicine's greatest marvels – they are estimated to save millions of lives globally every year[62]. Vaccines require cross talk between innate immunity and adaptive immunity to achieve sufficient protection against pathogens. To increase innate immune cell activation, helper molecules, termed adjuvants, are included in some vaccine formulations[16]. Immunostimulatory adjuvants bind pattern recognition receptors (PRRs)

on innate cells, resulting in a signaling cascade that causes and upregulation in cytokine expression and surface marker expression. These adjuvants are particularly useful in boosting the immune responses in lower-responding populations, like infants and the elderly[260]. These populations are at heightened risk for influenza and respiratory disease but are also uniquely sensitive to vaccine reactogenicity[261]. Elderly patients present with "inflammaging", characterized as an increasing proinflammatory state with age[262]. Thus, this balance between activation and reactogenicity is critical in adjuvant design.

We previously demonstrated the ability to alter adjuvanticity with small molecule "immunomodulators" [182; 183; 263]. We conducted a variety of high-throughput screening assays to assess alterations in transcription factory activity, cytokine expression, and . The modulators were immunologically inert, demonstrating little inherent activity. But when combined with traditional adjuvants and PRR agonists, the immunomodulators significantly altered innate immune cell activation. Here, we furthered our understanding of immunomodulation by applying our immunomodulators to disease relevant models.

We combined our cytokine and surface marker datasets to create an updated quantitative scoring system to select top candidate immunomodulators for testing in in vivo models. We first combined our immunomodulators with a variety of commercial vaccines in an attempt to choose a translational model that showcased our system well. Of those tested, influenza provided the best disease model from both an efficacy and impact standpoint. Historically, influenza has been one of the most pervasive infectious diseases and still exhibits a high global mortality burden of approximately 400,000 influenza-associated deaths annually from seasonal infections[264]. Influenza has also been the source of multiple pandemics. In the 20th century alone, there were three outbreaks now informally known for their presumed site of origin. The Spanish flu of 1918 is estimated to have resulted in the death of at least 17.4 million people, the Asian flu of 1955 at least 1.7 million people, and the Hong Kong flu of 1968 at least 2 million people[265]. Most recently, the Swine flu of 2009 is

estimated to have resulted in the death of between 100,000 and 2 million people[266]. Even in developed countries, seasonal influenza is still a significant health concern. In the United States, influenza and pneumonia are the 13th leading cause of death, causing about 42,000 deaths in 2021[267]. Clearly, while seasonal influenza vaccinations exist, their limited efficacy can be improved.

We began with adjuvanted subunit influenza vaccines as a model system to demonstrate the potential of our immunomodulators. We identified two immunomodulators that increased protection to a viral challenge compared to the adjuvanted subunit vaccine alone. Finally, we combined these immunomodulators with Fluzone, a commercial, quadrivalent, inactivated whole pathogen influenza vaccine. Modulators increased the durability of the antibody response elicited by these vaccines. The modulators also increased protection to a homologous live viral challenge compared to Fluzone alone.

4.3 Results and Discussion

4.3.1 Combining Immunomodulators with Commercial Vaccines to Determine a Suitable Disease Model

We sought to select the best disease model to showcase our immunomodulator platform. With a partnership with a local pharmacy, we were able to purchase a subset of vaccines

Vaccine	**Disease**	**Adjuvant**	**Modulators**
Shingrix	Shingles	$AS01_B$	TLR4 Specialists
Typhim Vi	Typhoid Fever	None/Self	TLR4 Specialists
Heplisav-B	Hepatitis B	CpG 1018	Generalists
Fluzone	Influenza	None/Self	Generalists
MMR	Mumps, Measles, Rubella	None/Self	Generalists

Table 4.1: Commercial Vaccines Studied with Immunomodulators

approved for human use from VaccineShop. These vaccines were primarily manufactured by Sanofi Pasteur, but also included product from Merck, GSK, and Pfizer. We selected the following vaccines, listed in Table 4.1, for testing in mice. Each of these vaccines were administered at approximately 1/10th the human dose, combined with 1.5 μmol of immunomodulator in 30% DMSO. We followed our prime-boost model, monitoring systemic inflammatory cytokines one hour after injection and antigen-specific antibodies two weeks post boost.

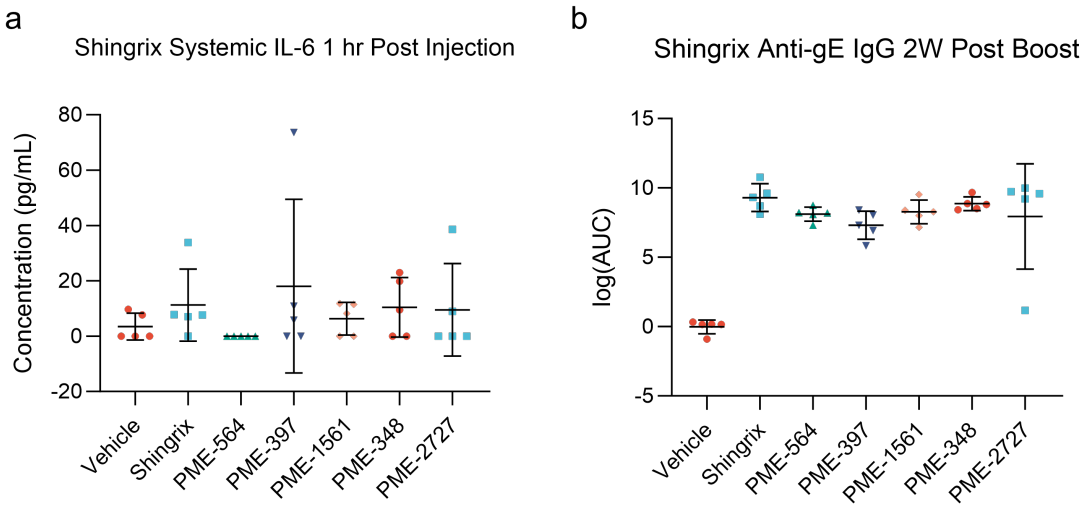

Figure 4.1: Cytokine and Antibody Modulation of Shingrix Vaccine. A) Systemic IL-6 expression 1 hr post injection. B) Antigen-specific antibody titers measured 2 weeks post boost

The first vaccine studied, Shingrix, is an adjuvanted subunit varicella zoster vaccine to prevent shingles. It contains one of the newest approved adjuvants $AS01_B$. This adjuvant is notorious for causing strong reactogenicity, but is quite efficacious[268]. $AS01_B$ contains the TLR4 ligand MPL and the saponin QS-21. Thus, we decided to combine immunomodulators that scored highly in the TLR4 specialist scoring system. We did not see a substantial amount of systemic inflammatory cytokines with the vaccine alone (Figure 4.1A). This is not surprising, however, as $AS01_B$ is known to be less reactogenic in rodents[269]. Additionally, we see high titers for the vaccine alone, with the addition of our immunomodulators having

little impact (Figure 4.1B). Thus, we decided not to study this vaccine further, though reducing the dose further could allow us to observe effects on antibody immunomodulation.

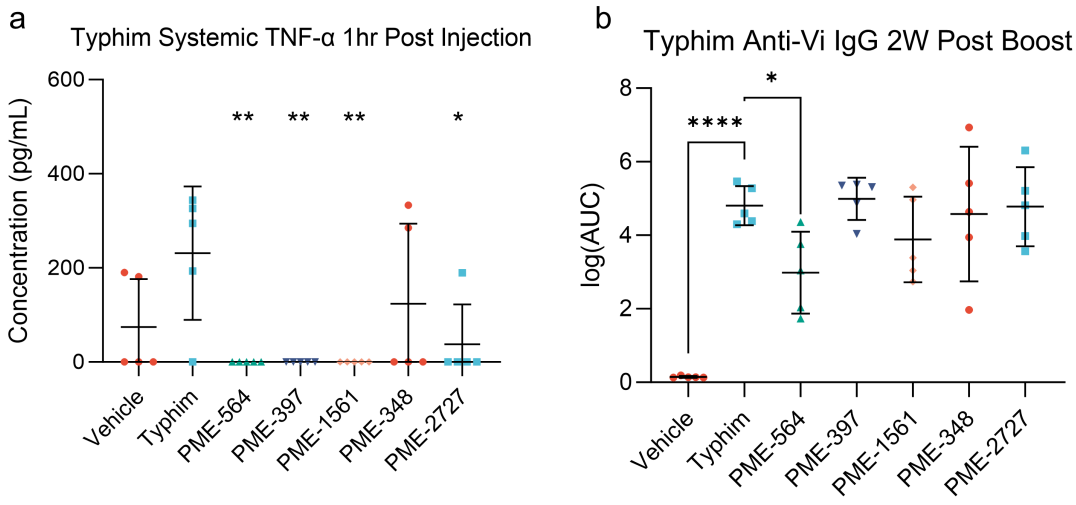

Figure 4.2: Cytokine and Antibody Modulation of Typhim Vi Vaccine. A) Systemic TNF-α is reduced in most modulator cases compared to Typhim Vi alone. B) Antigen specific antibody titers are maintained or decreased two weeks post boost. Statistical analyses between the Typhim group and Typhim with modulators were performed by a one-way ANOVA test. (* = $p < 0.05$, ** = $p < 0.01$, *** = $p < 0.001$, **** = $p < 0.0001$)

Next, we studied Typhim Vi, a polysaccharide antigen vaccine to prevent typhoid fever. This vaccine does not contain an exogenous adjuvant, only the bacterial polysaccharide, which may have some immunostimulatory effects. Thus, we again combined the same TLR4 specialist modulators as we explored with the Shingrix vaccine. With Typhim Vi, we did see a mild degree of cytokine induction one hour after injection. Four out of the five modulators significantly reduced systemic TNF-α (Figure 4.2A). Three of these modulators reduced this inflammatory cytokine to basal levels. The elicited antibody response, however, was not improved in any of the modulator cases (Figure 4.2B). In fact, PME-564 actually reduced antigen specific antibodies. As we had seen the opposite result in previous studies, we decided not to further study this vaccine.

We then explored Heplisav, an adjuvanted subunit vaccine against Hepatitis B. This

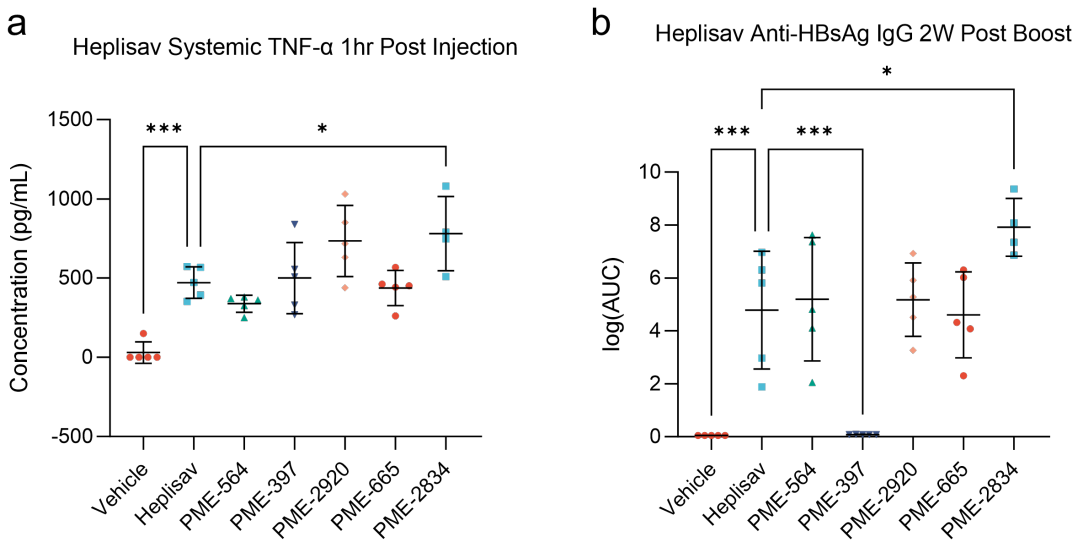

Figure 4.3: Cytokine and Antibody Modulation of Heplisav Vaccine. A) Systemic TNF-α is reduced in most modulator cases compared to Heplisav alone. B) Antigen specific antibody titers are modulated two weeks post boost. Statistical analyses between the Heplisav group and Heplisav with modulators were performed by a one-way ANOVA test. (* = $p < 0.05$, ** = $p < 0.01$, *** = $p < 0.001$)

vaccine also contains a recently approved adjuvant, CpG 1018. Unfortunately, we did not include CpG, or any TLR9 agonist, in our secondary screen as THP-1 monocytes do not high express TLR9. Without a specialist category for this adjuvant, we decided to combine this vaccine with high scoring generalists. None of our immunomodulators showed a decrease in TNF-α post injection. In fact, PME-2834 increased production of this inflammatory cytokine (Figure 4.3A). This was unexpected, as we have seen reduction of CpG 1018 induced cytokines when combining this adjuvant with the immunomodulator honokiol as seen in Chapter 2. The majority of our work with CpG, however, has been with ODN 1826 in mice, not the more human specific ODN 1018. This shift in sequence could explain some of these differences. When comparing antibody titers, we observe that PME-2834, the modulator that increased TNF-α, was the only modulator to increase antibody titers (Figure 4.3B). Interestingly, PME-397 reduced cytokines to undetectable levels, a phenomenon not observed with any other vaccine and modulator combination. The rest of the modulators had no

significant changes in antibody levels, however, the data are quite variable in these groups. Taken together, we decided to not further investigate this vaccine.

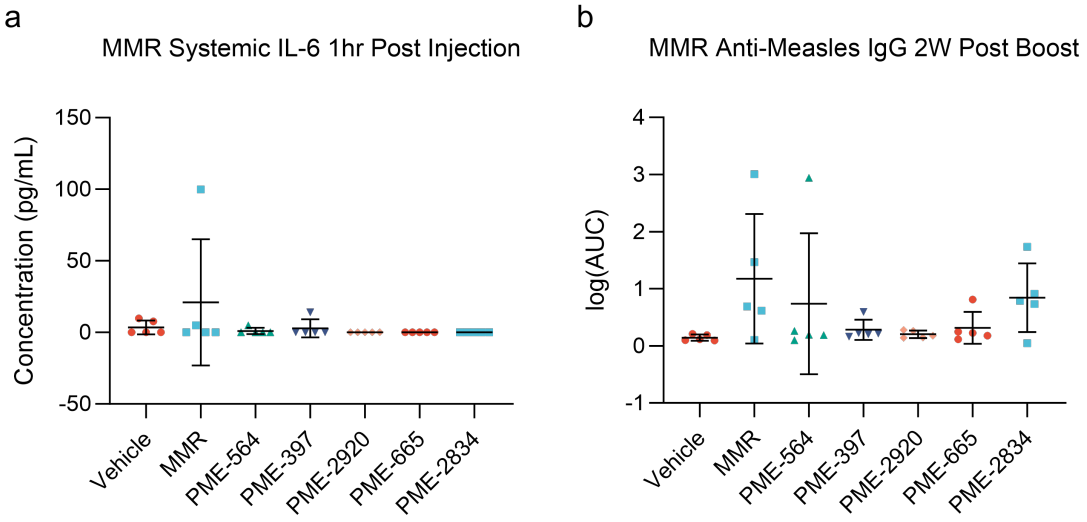

Figure 4.4: Cytokine and Antibody Modulation of MMR Vaccine. A) Systemic IL-6 is minimal in all vaccine cases. B) Antigen specific antibody titers are maintained or decreased two weeks post boost.

The penultimate vaccine studied was MMR, a live attenuated, whole pathogen vaccine against measles, mumps, and rubella. This vaccine should have many different endogenous PRRs from the viruses, so we included top scoring generalist modulators with these vaccines. We did not, however, see any significant inflammatory cytokine expression, or antigen specific antibody production with this vaccine (Figure 4.4A,B). Perhaps a higher dose of this vaccine was required, or theses viruses are adapted to humans and inefficient in a mouse model. Regardless, we did not continue to investigate this vaccine.

The last vaccine studied was Fluzone, a quadrivalent, inactivated whole pathogen vaccine to protect against seasonal influenza infections. The composition of Fluzone changes each year depending on the predicted mutation patterns, but it always contains an H1N1 influenza A strain, an H3N2 influenza A strain, a Yamagata-lineage influenza B strain, and a Victoria-lineage influenza B strain. We began by testing the 2022-2023 formulation with the following

strains: A/Victoria/2570/2019 (H1N1), A/Darwin/9/2021 (H3N2), B/Phuket/3073/2013 (Yamagata), and B/Michigan/01/2021 (Victoria). Again, because this is a whole pathogen vaccine, we decided to use high scoring generalist immunomodulators. Similar to MMR, we did not see strong inflammatory cytokine induction even though this vaccine contains whole pathogens. We assumed the presence of PAMPs would cause a substantial amount of innate immune activation. This vaccine, however, is a split-virus vaccine that has been disrupted via Triton X-100, and then ultrapurified via filtration. This results in significant concentration of the main target antigen, hemagglutinin, and substantially removes other viral components. We can still observe a significant reduction in TNF-α 1 hour after injection with the addition of most of our immunomodulotors (Figure 4.5A). Most striking, however, is the large increase in antigen specific antibodies. We tested for antibodies against the hemagglutinin glycoprotein (HA) from the H1N1 strain. We see a very significant improvement in antibody

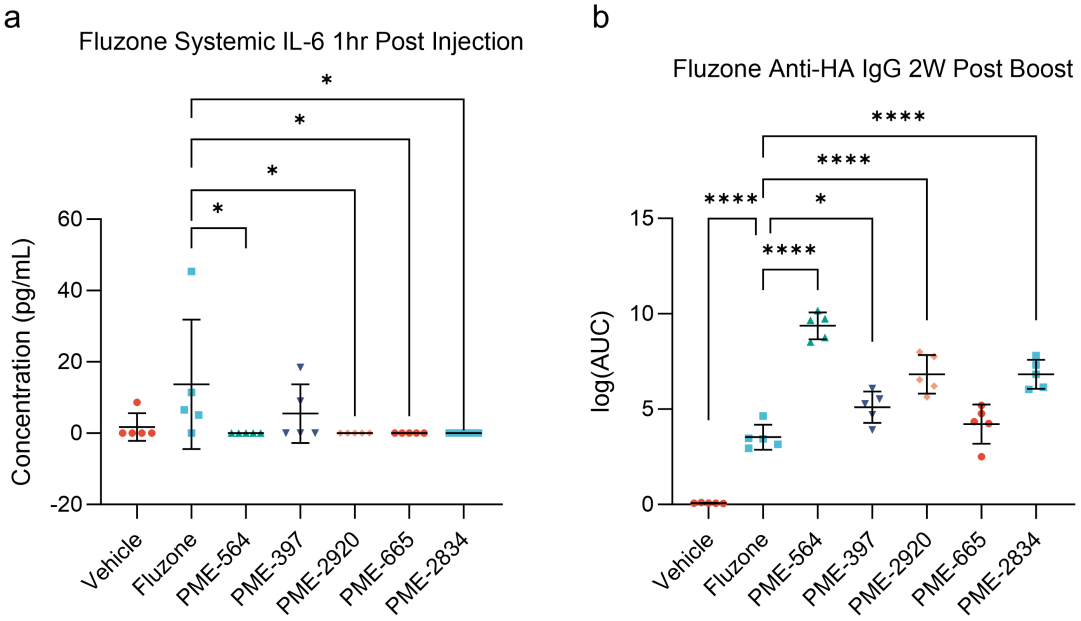

Figure 4.5: Cytokine and Antibody Modulation of Fluzone Vaccine. A) Systemic IL-6 is reduced in most modulator cases compared to Fluzone alone. B) Antigen specific antibody titers are maintained or increased two weeks post boost. Statistical analyses between Fluzone groups and Fluzone with modulator groups were performed by a one-way ANOVA test. (* = $p < 0.05$, ** = $p < 0.01$, *** = $p < 0.001$, **** = $p < 0.0001$)

production, especially with PME-564, and the second best modulator, PME-2834 (Figure 4.5B). We can also increase the cytokine production by adding CpG 1826 to Fluzone, which elicits high concentrations of TNF-α. When adding our initial dose of PME-564, 1.5 μmol, we see a significant decrease in inflammatory cytokines. Adding one-tenth the of the immunomoudlator does not significantly reduced inflammatory cytokines, however, indicating that this process is dose dependent (Figure 4.6A). This trend can also be observed in the increase in antibody production. The addition of CpG does significantly improve antibody titers above that of Fluzone alone. The high dose of PME-564 further increases antibodies produced by CpG and Fluzone, but the low dose of PME-564 does cause the same significant increase (Figure 4.6B).

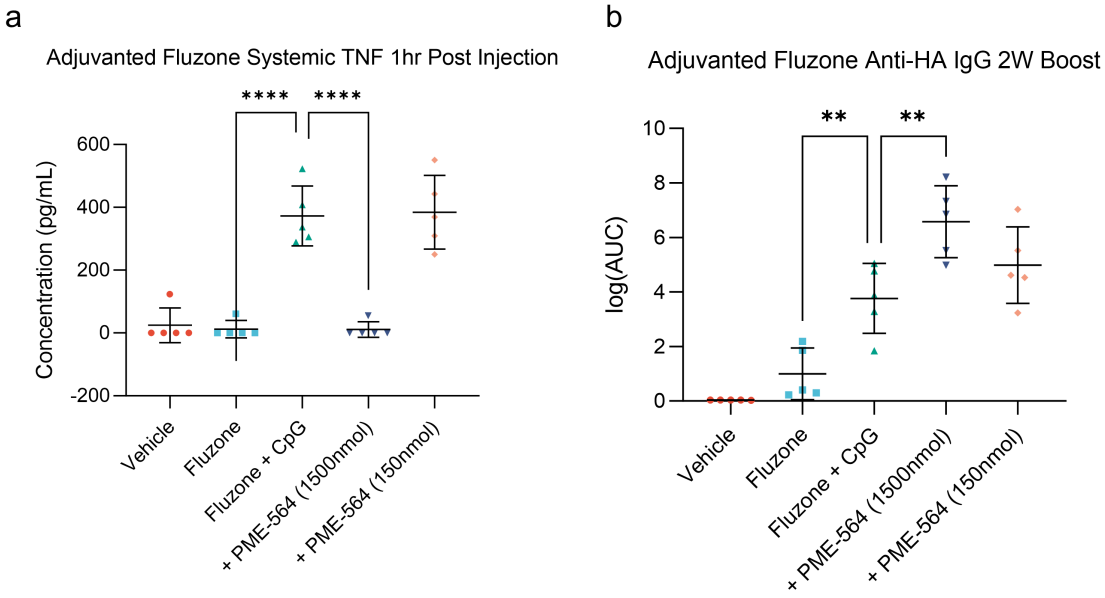

Figure 4.6: Cytokine and Antibody Modulation of Fluzone Vaccine Adjuvanted with CpG 1826. A) Systemic TNF-α is reduced with the addition of 1.5 μmol of PME-564 compared to Fluzone and CpG. B) Antigen specific antibody titers are increased two weeks post boost with the addition of CpG to Fluzone, and increased with 1.5 μmol of PME-564. Statistical analyses between Fluzone/CpG groups and other vaccine groups were performed by a one-way ANOVA test. (* = $p < 0.05$, ** = $p < 0.01$, *** = $p < 0.001$, **** = $p < 0.0001$)

4.3.2 Exploring Top Scoring Modulators in a Model Influenza Vaccine

With influenza as our chosen disease model, we wanted to revert back to a simpler vaccine model than the whole pathogen, quadrivalent vaccine. With Fluzone, the differing antigens would complicate our mechanistic understanding of the antigen presentation process. In Chapter 3, we presented a CpG subunit vaccine with the hemagglutinin from A/California/07/2009, an H1N1 strain (Figure 3.20). Looking at this data, we decided to further study the modulators PME-564 and PME-2834. PME-564 served as an immunomodulator that reduced TNF-α and increased antibodies, while PME-2834 served as an immunomodulator the amplified TNF-α and increased antibodies. We hypothesized that a decrease in TNF-α would be preferred in a clinical vaccine, but decided to probe the possible responses if this cytokine was not controlled.

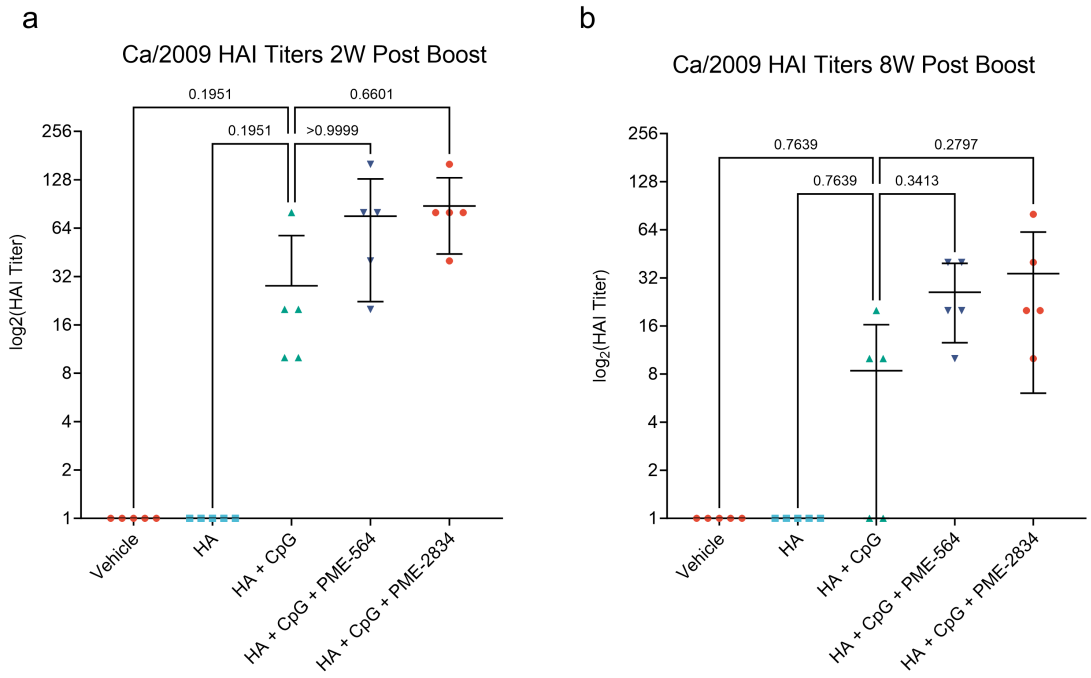

Figure 4.7: Functional Antibodies (HAI) in Ca/2009 Subunit Vaccine. Hemagglutinin inhibition assay to measure functionality of generated antibodies both A) two weeks post boost and B) eight weeks post boost. Data was analyzed using a Kruskal-Wallis test with Dunn's multiple comparisons. An HAI titer of >40 is considered protective

We performed hemagglutinin inhibition assays (HAI) on the sera two weeks post boost. HAI provides a proxy for neutralization, and shows antibody functionality as opposed to the mere binding shown by ELISA[270]. While the HAI titers trend higher in both the modulator vaccines compared to the adjuvanted control vaccine alone, these results are not significant (Figure 4.7A). In humans, however, an HAI titer of >40 is considered protective. Using this metric, only 1 out of 5 animals reported a protective HAI titer in the control vaccine group compared to 4 out of 5 animals in the PME-564 group and 5 out of 5 animals in the PME-2834 group. These antibodies also persist longer in the vaccines with modulator (Figure 4.7B). At this timepoint, none of the control vaccine animals reported a protective HAI titer. 2 out of 5 animals in each of the modulator groups, however, retained a protective HAI titer. These data suggest that, not only are the peak antibody responses greater with the addition of immunomodulator, but also this immunity is more durable than the control vaccine alone.

4.3.3 Immunomodulators Protect Mice from Live PR8 Challenge in a Subunit Vaccine

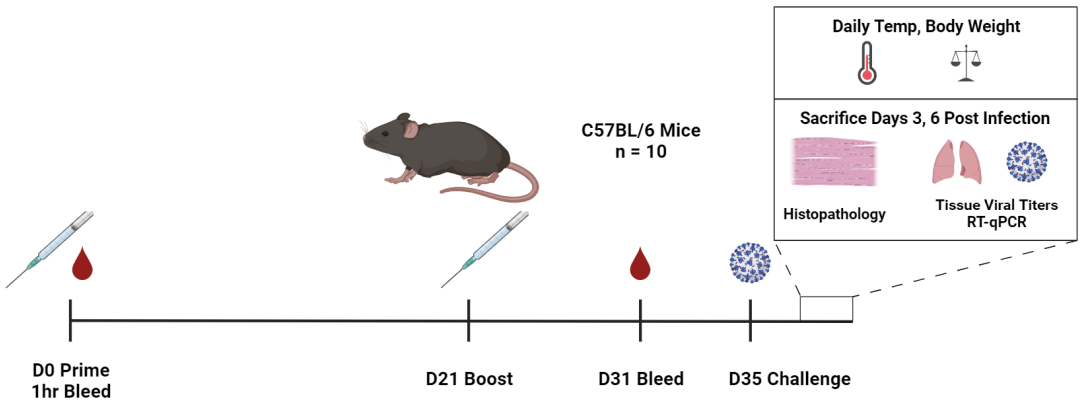

Figure 4.8: Experimental Timeline for PR8 Viral Challenge

With this promising data, we sought to test if modulators could protect mice against a

live viral challenge. We continued with a CpG adjuvanted HA subunit vaccine, but switched strains to A/Puerto Rico/8/1934/H1N1 as this strain is more aggressive in mouse models, requiring a lower amount of plaque forming units (PFUs) for a lethal dose[271]. We increased the number of animals from n = 5 per group to n = 10 per group to obtain endpoint measurements of disease severity at multiple timepoints. Mice were vaccinated in a prime-boost schedule, monitoring systemic inflammatory cytokines 1 hour post boost and antigen specific antibodies 10 days post boost. Two weeks post boost, mice were challenged with 1,000 LD50 of homologous A/Puerto Rico/8/1934/H1N1, attempting to mimic a very severe infection. Mice were monitored for temperature and body weights daily. At 3 and 6 days post infection (DPI), 5 mice were sacrificed in each group for histopathology measurements and viral load quantification via qPCR (Figure 4.8).

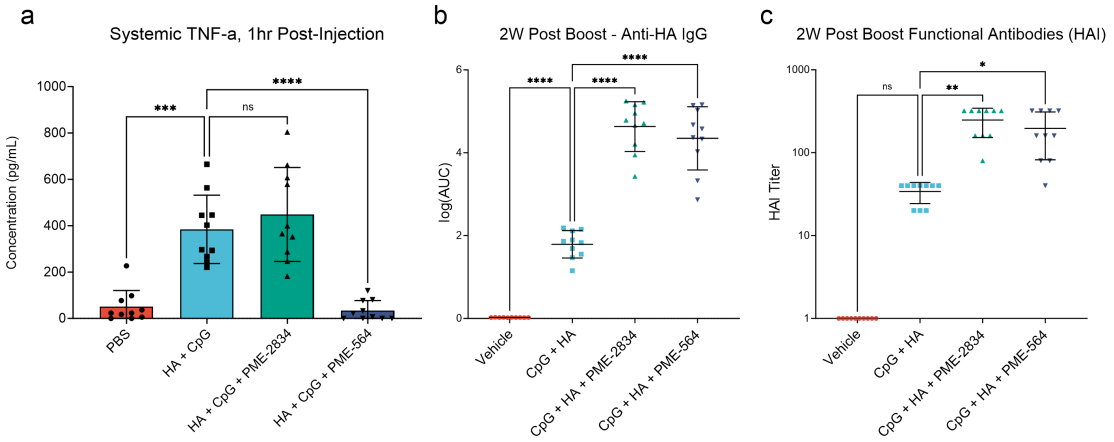

Figure 4.9: Cytokine and Antibody Responses Before PR8 Challenge. A) Systemic TNF-α elicited by CpG is reduced with the addition of PME-564, but not PME-2834. B) Antigen specific antibody response 10 days post boost. Both PME-564 and PME-2834 significantly increase antibody levels above the HA + CpG vaccine alone. C) Functional antibody measurements via HAI, both PME-564 and PME-2834 significantly increase HAI titers. Statistical analyses in A and B were performed by a one-way ANOVA test. Statistical analysis in C was performed by a Kruskal-Wallis test. (* = $p < 0.05$, ** = $p < 0.01$, *** = $p < 0.001$, **** = $p < 0.0001$)

We saw the same reduction in systemic inflammatory cytokines with PME-564 compared to the CpG adjuvanted control vaccine alone (Figure 4.9A). Additionally, antigen specific

antibodies were significantly higher in both modulator groups compared to the control vaccine (Figure 4.9B). The HAI titers for each modulator groups were also significantly higher compared to the control vaccine (Figure 4.9C). Mice began to severely lose weight starting at 2 days post infection. At 3 DPI, some of the mice in both modulator groups began to recover. At 3DPI and 4DPI, the weight change for the modulator groups were significantly lower than that of the control vaccine group (Figure 4.10A). The control vaccine did not elicit much protection from this high dose challenge. This is confirmed by the viral loads measured in the lungs at 3DPI. The modulator groups had significantly lower viral loads than that of the control vaccine (Figure 4.10B). The control vaccine group, however, did not have lower levels compared to the vehicle control.

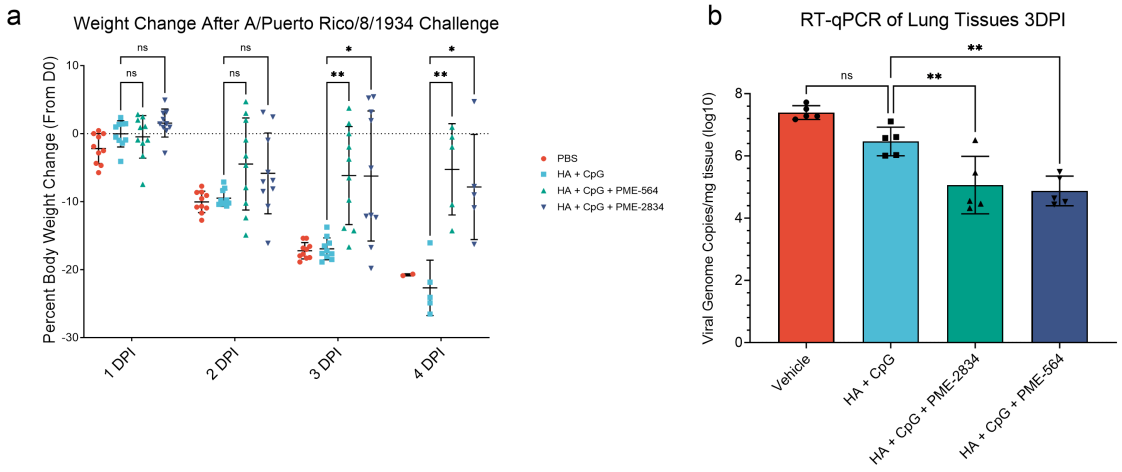

Figure 4.10: Weight Change and Viral Load After PR8 Challenge. A) Weight change plotted as a percentage change from day 0, pre-challenge weights. Modulator groups show reduced weight loss that is significant starting at 3DPI. B) Lung viral loads as measured by RT-qPCR 3DPI. Modulator groups show reduced viral loads compared to control vaccine. Statistical analyses between modulator groups and control vaccine were performed by a two-way ANOVA test. (* = $p < 0.05$, ** = $p < 0.01$, *** = $p < 0.001$, **** = $p < 0.0001$)

4.3.4 Immunomodulators Protect Against Viral Challenge in a Commercial Influenza Vaccine

We next sought to replicate this increased protection from viral challenge, but now in the more complex commercial vaccine model. We selected Fluzone as our commercial vaccine. The 2022-2023 formulation, used in this study, contains the following strains: A/Victoria/2570/2019 (H1N1), A/Darwin/9/2021 (H3N2), B/Phuket/3073/2013 (Yamagata lineage), and B/Michigan/01/2021 (Victoria lineage). We followed the same experimental approach for the challenge as before. Mice were vaccinated in a prime-boost schedule, monitoring systemic inflammatory cytokines 1 hour post boost and antigen specific antibodies 10 days post boost. Two weeks post boost, mice were challenged with 10^5 PFU - a dose we determined from our own lethal dose testing. Mice were monitored for temperature and body weights daily. At 3 and 6 days post infection (DPI), 5 mice were sacrificed in each group for histopathology measurements and viral load quantification via qPCR.

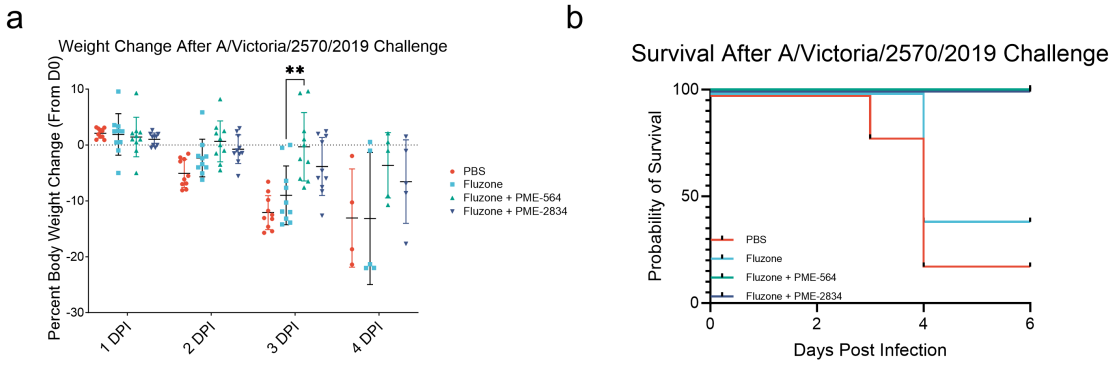

Figure 4.11: Weight Loss and Survival After A/Victoria/570/2019 Challenge. A) Weight change plotted as a percentage change from day 0, pre-challenge weights. Modulator groups show reduced weight loss that is significant starting at 3DPI. B) Survival curves from the n = 5 mice studied until 6 DPI. Statistical analyses between Fluzone + modulator groups and Fluzone alone were performed by a two-way ANOVA test. (* = $p < 0.05$, ** = $p < 0.01$

With Victoria/2570/2019 as a less potent strain than PR8, mice did not begin to lose much weight until 2DPI. By 3 DPI, both the vehicle control and Fluzone vaccine groups

demonstrated an average of 10% weight loss. PME-564, on average, maintained the weight of the mice, representing a significant change in body weight compared to Fluzone alone (Figure 4.11A). After sacrificing half of the animal cohort after 3 days, we see a large variation in body weight changes for the vehicle and Fluzone groups, indicating this study is limited by the viral strain lethality. Nonetheless, from the five animals observed through 6 DPI, we can see a drastic difference in the survival curves. At 3 DPI, one animal from the vehicle group required euthanasia, reaching the body weight threshold criteria. At 4 DPI, three more animals from the vehicle group, and three animals from the Fluzone group also required euthanasia (Figure 4.11B). Meanwhile, all animals in the Fluzone + modulator groups survived until the end of the study. This increase in survival, combined with the lessened body weight loss, indicate immunomodulators increased the protection of the Fluzone vaccine.

4.3.5 Immunomodulators Improve Vaccine Durability

We next probed whether immunomodulators could improve the durability of the vaccine response. Improved protection shortly after a booster vaccination is promising, yet these results

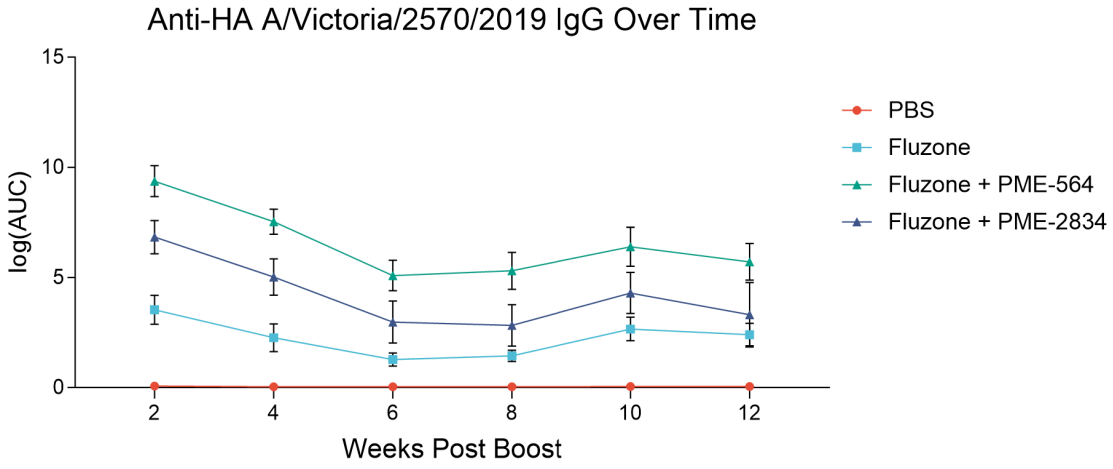

Figure 4.12: Monitoring Fluzone Induced IgG Over Time. Antibody titers were measured biweekly for three months post boost. Modulators improved antibody titers over Fluzone alone at all timepoints.

would have larger impact if this window of protection could be extended to later timepoints. We vaccinated mice in the same prime-boost format, but took biweekly bleeds for up to 12 weeks post boost, using Fluzone 22-23 as our vaccine. As before, we see an increase in anti-HA IgG against the H1N1 strain, A/Victoria/2570/2019 in immunomodulator-containing vaccines when measured at two weeks post boost (Figure 4.12). All Fluzone vaccinated groups show a decline in antibody levels at the same rate. This results in higher titers for modulator containing groups for a longer period of time. Additionally, titers appear to plateau and remain constant beginning around 8 weeks post boost.

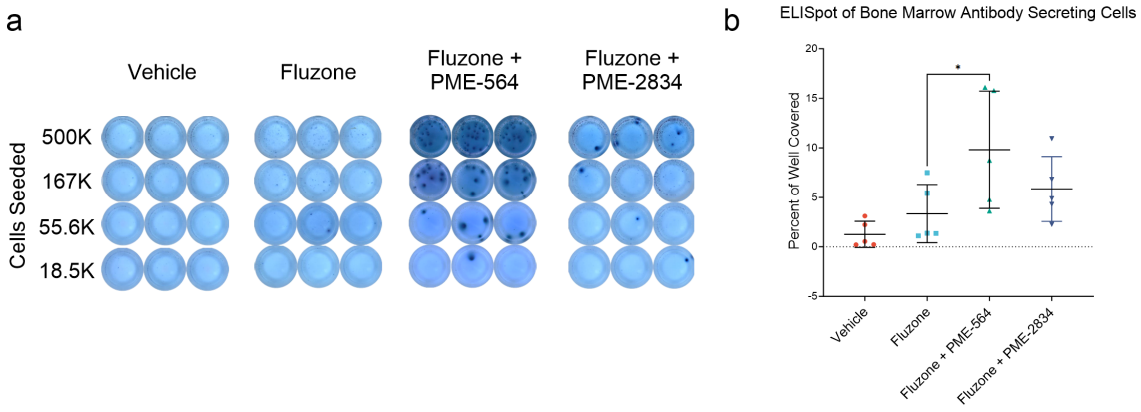

Figure 4.13: ELISpot for anti-HA IgG Producing ASCs. A) Representative ELISpot wells (in triplicate) of individual mice from each treatment group. B) Percent of well covered by spots of each treatment. PME-564 shows significant increase in well coverage. Statistical analyses between modulator groups and control vaccine groups were performed by a one-way ANOVA test. (* = $p < 0.05$, ** = $p < 0.01$)

As additional evidence to support this maintained level of antibodies at further timepoints when including immunomodulators, we performed an ELISpot assay to detect antibody secreting cells in the bone marrow. In a separate experiment with identical treatment groups, we sacrificed mice 8 weeks post boost to represent the plateaued period of the observed antibody titers. After polyclonally stimulating cells isolated from the bone marrow for 3 days, we performed an ELISpot assay, detecting cells secreting IgG against the HA from the H1N1 strain, A/Victoria/2570/2019. Representative images of ELISpot wells from a singular

mouse from each treatment group can be seen in Figure 4.13A. In analyzing the data, we reported the area of the well covered in spots. This better represents the total amount of antibody being produced as singular B cells secreting a large amount of antibody are better represented by this metric. We observed a significant increase in well coverage with the addition of immunomodulator (Figure 4.13B). This matches our long term antibody data, as PME-564 resutled in the highest antibody titers over time. PME-2834 seemed to high a slightly higher well coverage than Fluzone alone, but was not significant.

4.3.6 Exploring Mechanisms Behind Increased Protection

We next began to explore the mechanisms behind our top immunomodulator candidate, PME-564 before we further developed this molecule. We observe increased protection with the commercial influenza vaccines. While increases in antibodies can partially explain this observation, we sought to probe cellular responses in the form of antigen-specific CD8 T-cells. Cyototoxic CD8 T cells are especially important in preventing and combating severe infection, and can recognized conserved epitopes across multiple different influenza strains[272]. Mice were vaccinated with the commercial Fluzone 22-23 vaccine as previously described. Instead of selecting a singular immunodominant epitope, we decided to probe CD8 T cells across the entire hemagglutinin protein sequence from A/Victoria/2570/2019, the H1N1 strain from the seasonal Fluzone vaccine. To do so, we loaded empty H2-Kb MHCI tetramers with a pool of 139 15-mer peptides, with 11 amino acid overlaps. Ten days post boost, mice were sacrificed and splenocytes were processed for tetramer staining via flow cytometry. The flow gating strategy, including representative double staining on BUV737 and PE for the tetramers, can be seen in Figure 4.14. When added to Fluzone, PME-2834 significantly increased antigen-specific CD8 T cells compared to the Fluzone vaccine alone. PME-564 also showed a trend in this direction, though the statistics are close, but not significant (Figure 4.15A). When CpG is added to the Fluzone vaccine, this combination raises the percentage

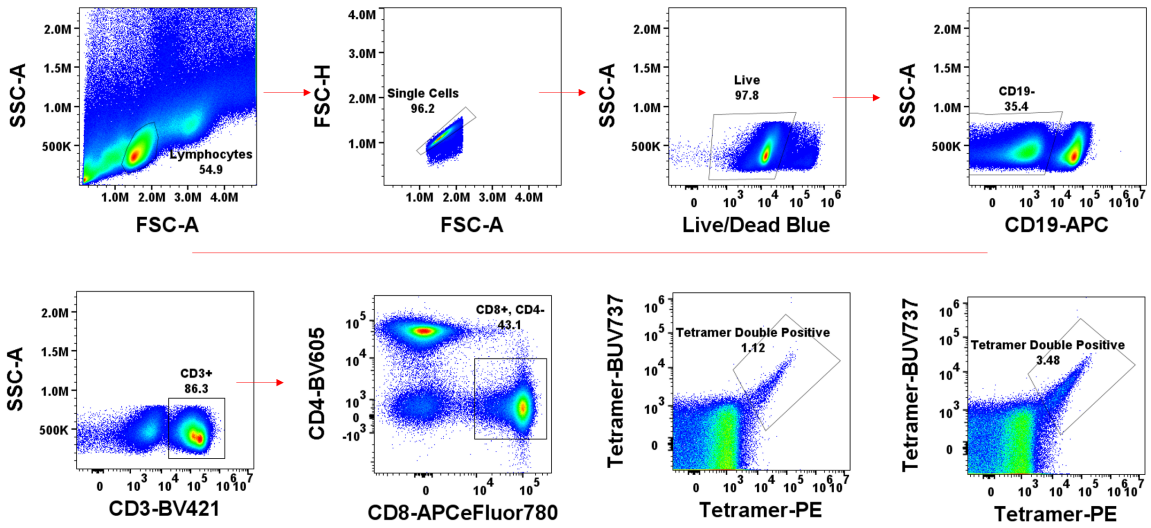

Figure 4.14: Flow Gating for Antigen-Specific CD8 T Cell Responses

of antigen-specific T cells. Neither immunomodulator caused an increase over this response, though PME-564 is again trending towards an increase (Figure 4.15B).

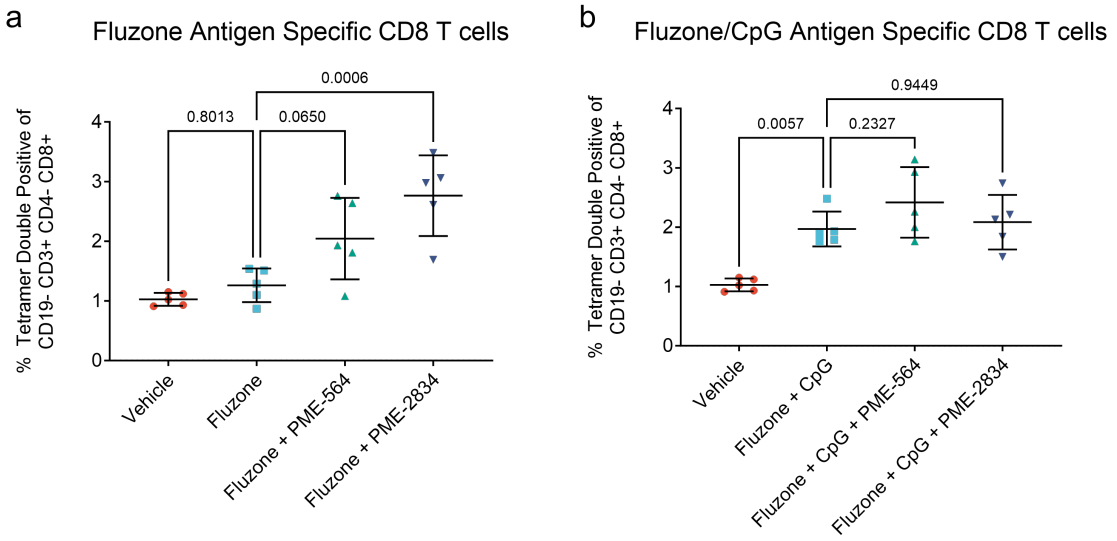

Figure 4.15: Immunomodulators Increase Antigen-Specific CD8 T Cells in Fluzone Vaccine. Splenocytes were isolated form vaccinated mice ten days post boost and processed for flow cytometry A) Without CpG, immunomodulators increase percentage of antigen specific CD8 T cells by hemagglutinin loaded tetramer double stains. B) CpG raises the baseline of the CD8 response with Fluzone. Immunomodulators do not further boost this response. Statistical analyses between Fluzone + modulator groups and Fluzone alone were performed by a one-way ANOVA test.

We demonstrated immunomodulators increased antigen-specific antibodies and antibody secreting cells at timepoints that were months post boost. We hypothesized that immunomodulators were impacting the germinal center (GC) response following vaccination. As small molecules, immunomodulators would be cleared from the organisms rather quickly, and thus would likely impact antigen presenting cells shortly after vaccination. Yet this modulation could have downstream effects on later functions in the immune response, including the germinal center reaction as this is a critical next step after innate and adaptive immunity are bridged. Thus, we performed an immunophenotyping study where we observed frequencies of various GC related cell types. We again employed Fluzone 22-23 as our vaccine, with and without the addition of PME-564. Mice were sacrificed eight days post boost and splenocytes were analyzed via flow cytometry. We primarily stained for germinal center B cells, T follicular helper cells, and plasmablasts. A representative gating strategy can be seen in Figure 4.16. We did not observe any significant difference in these cells populations

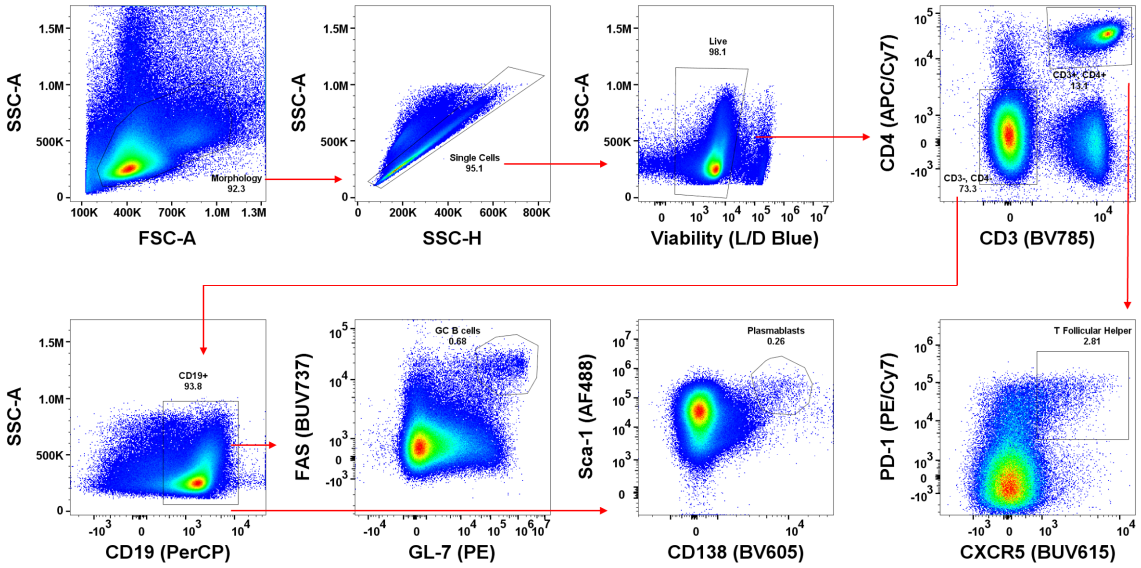

Figure 4.16: Flow Gating for Germinal Center Immunophenotyping

with the addition of PME-564, even though the cell populations were well characterized by our staining (Figure 4.17). There was a slight trend upwards in the amount of germinal center B cells elicited by PME-564, but these results were not significant. We hypothesize

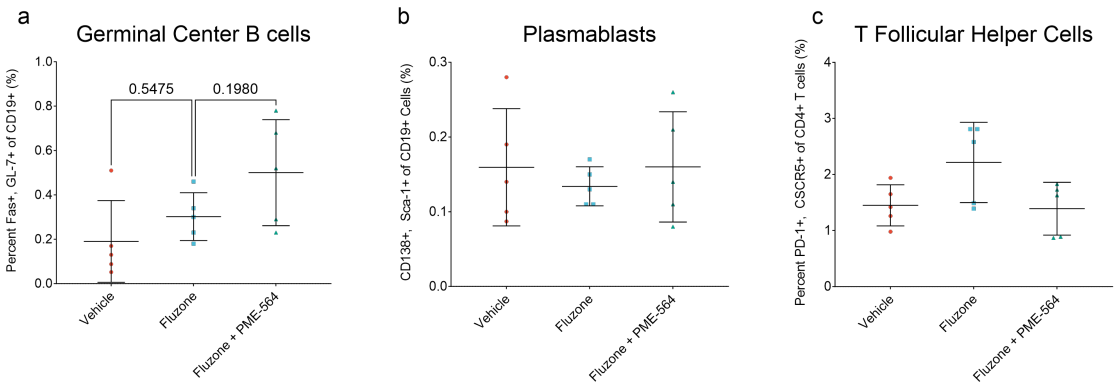

Figure 4.17: Immunomodulators Show Little Impact on Germinal Center Cell Populations. Splenocytes were isolated form vaccinated mice eight days post boost and processed for flow cytometry. No significant changes in either A) germinal center B cells, B) plasmablasts, or C) T follicular helper cells were observed. Statistical analyses between Fluzone + modulator groups and Fluzone alone were performed by a one-way ANOVA test.

that studying different timepoints would strengthen our understanding of the developing adaptive response. Perhaps immunomodulators prolong the GC reaction, allowing for an increased total output of antibody secreting cells that we observe at later timepoints in the immune response.

Finally, we probed the molecular mechanisms behind our immunomodulators. As mentioned previously, PME-564 inhibits the activity of multiple kinases, but we believe the Lyn kinase is the primary kinase responsible for the modulation of vaccine responses. Lyn is a Src-family with many roles in innate signaling and an emphasis on TLR pathways. TLR pathways are partially regulated by Lyn as through association with the TLR/MyD88 complex. We hypothesize that inhibiting Lyn activity has a strong affect on innate cell activation, resulting in the different phenotypes we see upon the addition of PME-564. To further study the importance of Lyn, we found a small subset of other commercially available small molecules that modulate Lyn activity. These include i) the Lyn inhibitor, XL228, which also has Abl and Src kinase activity, ii) the Lyn inhibitor, Sarcatinib, which has even broader kinase activity, and iii) the Lyn activator, MLR-1023, which is specific to only Lyn. We performed our typical prime-boost vaccination study with a model subunit vaccine consisting

of 50 μg of CpG 1826 and 100 μg of ovalbumin. 1.5 μmol of each of the immunomodulators were added to their respective groups. We see a significant reduction in systemic IL-6 one hour after injection with the use of PME-564 and one of the other Lyn inhibitors, XL228 (Figure 4.18A). Interestingly, we also see an increase in this cytokine with the addition of the Lyn activator MLR-1023. We did not see a significant difference with the addition of Sarcatinib, the immunomodulator with the broadest activity. These results also follow a similar trend for TNF-α, but the results are less significant across groups (Figure 4.18B).

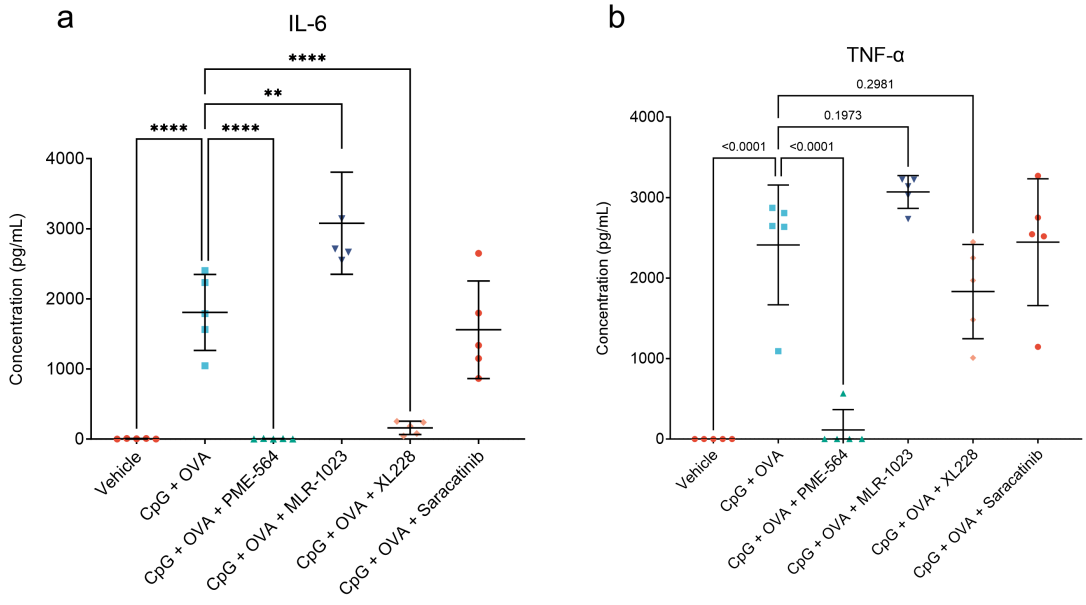

Figure 4.18: Lyn Modulators Affect Systemic Cytokine Expression After Vaccination. Lyn inhibitors (PME-546, XL228, Sarcatinib) and activator (MLR-1023) alter cytokine expression of A) IL-6 and B) TNF-α one hour after injection with a CpG adjuvanted subunit vaccine. Statistical analyses between modulator groups and vaccine alone were performed by a one-way ANOVA test. (* = $p < 0.05$, ** = $p < 0.01$), *** = $p < 0.001$, **** = $p < 0.0001$)

4.4 Conclusion and Future Directions

After testing top modulators with a variety of commercial vaccines, we identified combinations that drastically improved the efficacy and durability of these products. Most notably

was our ability to increase the protection of both whole pathogen and subunit influenza vaccines. With influenza as our disease model of choice, we seek to further develop PME-564 as a component of adjuvants for different vaccine platforms. We will continue to use inactivated whole pathogens (IAV) and hemagglutinin subunit vaccines, but will also expand our testing into mRNA vaccine systems. As an agonist, we will use a lipidated TLR7/8 agonist, INI-4001, developed by collaborators at the University of Montana[273]. These vaccine components will be formulated into vaccine components as either separate components or as chimeras. We also look to either suspend vaccines in oil-in-water emulsions, or directly integrate lipidated versions of these components into nanoparticles as in the case of mRNA vaccines. This development process will undergo multiple rounds of formulation, efficacy, and toxicity testing. A thematic overview can be seen in Figure 4.19.

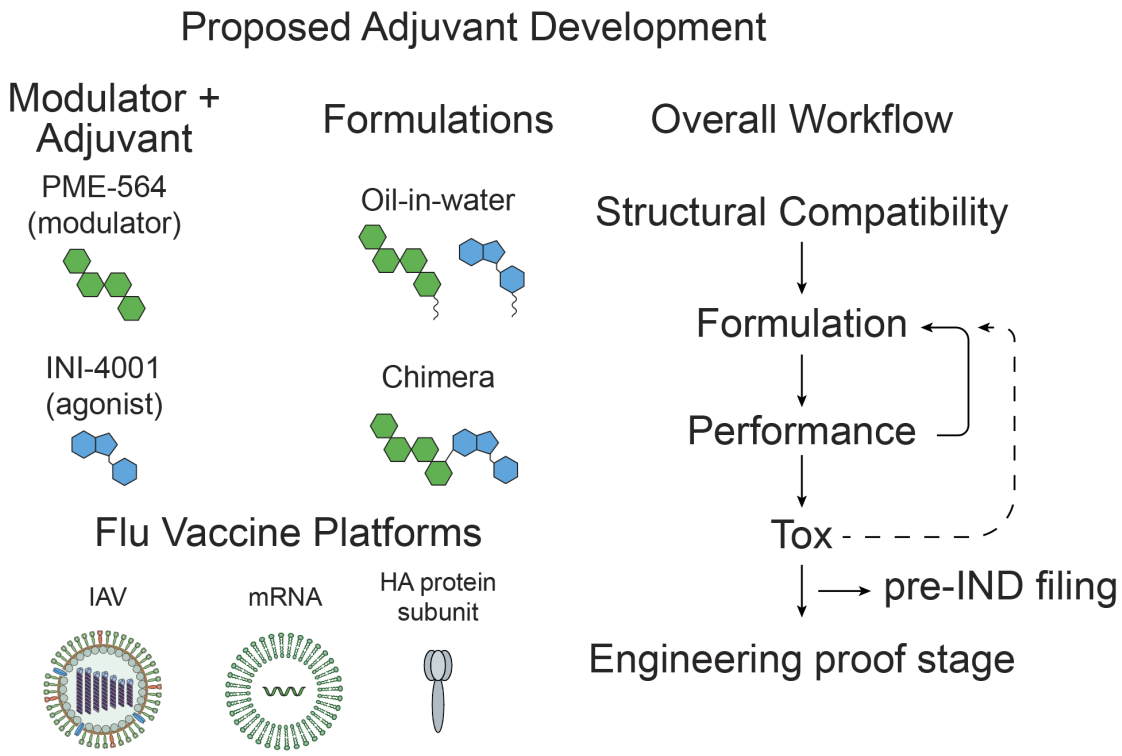

Figure 4.19: PME-564 Proposed Adjuvant Development Plan

We also plan to modify the structure of PME-564 to allow for chimeric attachment

while preserving, or even improving the Lyn inhibition activity. PME-564 was originally developed as a second generation Bcr-Abl inhibitor for the treatment of chronic mylogenous leukemia[274]. Thus, the modifications to PME-564 from prior compounds have been well documented in with their effects on Bcr-Abl binding. Lyn has only four amino acid substitutions in the key binding pocket domains compared to Bcr-Abl as they share large structural homology (Figure 4.20A)[275]. In examining the previous structure-activity relationships

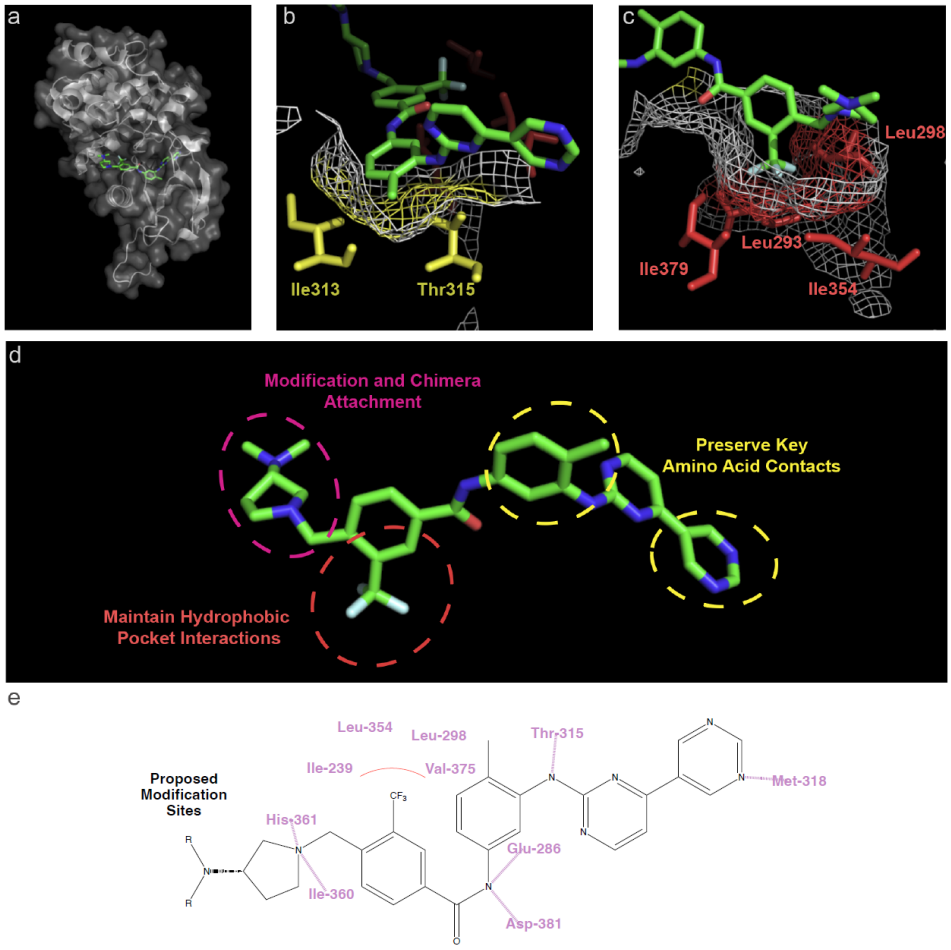

Figure 4.20: Analysis of PME-564 Binding in Lyn Active Site for Design of Derivatives. A) PME-564 (green) in the binding site of the Lyn kinase, modeled from the Bcr-Abl crystal structure. B) Key coordinating in the Lyn kinase binding pocket (yellow) coordinate PME-564. C) Tri-fluorogroup situated in the hydrophobic pocket of Lyn (red). D and E) Structure of PME-564 with sites of proposed modification indicated along with known interactions with Lyn kinase based on homology model with Bcr-Abl crystal structure.

and subsequent crystal structure of PME-564 bound to Bcr-Abl, it is clear that the piperazinylmethyl group was critical for the activity of both the precursor and PME-563[276]. Ile313 and Thr315 form close associations with this group limiting synthetic accessibility (Figure 4.20B). Similarly, the tri-fluorogroup was shown to increase activity more than 10-fold over the precursor, indicating that the phenyl ring and subsequent sections aniline are also essential for effective inhibition of the kinase (Figure 4.20C). Finally, the pyrrolidine was introduced. A series of substitutions of increasing size were placed here with modest alteration in activity indicating this site will provide an excellent spot to modify PME-564 for its formulation with INI-4001 in liposomes. The preservation of the cyclic amine is clear as it forms hydrogen bonds with both His-361 and Ile-360, but the second amine or subsequent elements extending off the ring do not interact in any direct with the protein. It is here that we propose to place our efforts in generating derivatives of PME-564 (Figure 4.20D,E).

We will continue to explore other top scoring immunomodulators in both vaccination and other applications. The data generated from this dissertation has already been used to identify molecules for various other projects inside the lab, from inflammasome activators to inducers of trained immunity. We strive to further understand and manipulate innate immunity in order to obtain fine control of cellular activation and signaling.

4.5 Materials and Methods

4.5.1 Animals

All animal procedures were performed under a protocol approved by the University of Chicago Institutional Animal Care and Use Committee (IACUC). 6-to-8-week-old C57/B6 female mice were purchased from the Jackson laboratory. All vaccinations were administered intramuscularly in the left hind leg. Blood was collected from the submandibular vein at time points indicated.

4.5.2 Vaccinations

Commercial vaccines were purchased from Vaccine Shop: Fluzone (Sanofi Pasteur), Heplisav-B (DYNAVAX), MMR-II (Merck), SHINGRIX (GlaxoSmithKline). Vaccines were formulated as 1/10th the human dose, and diluted, if needed, to 35 μL of PBS. Modulators were added at 1.5 μmol in 15 μL of DMSO. This resulted in a total of 50 μL with a 70% aqueous, 30% DMSO solution. Mice were lightly anesthetized with isoflurane and injected intramuscularly in the left hind leg.

For subunit vaccines, the formulation consisted of 10 μg of hemagglutinin (Sino Biological) and 50 μg of CpG 1826 (Adipogen) in 35 μL of PBS. Modulators were added at 1.5 μmol in 15 μL of DMSO.

4.5.3 Plasma Cytokine Analysis

Blood was collected from mice at specified time points in 0.2 mL of heparin-coated collection tubes (VWR Scientific). Plasma was isolated via centrifugation 2000xg at 4C for 15 min. Samples were collected and stored at -80°C until use. Plasma was analyzed using BioLegend's LEGENDPlex™ Mouse Inflammation Cytokine Panel (13-Plex) according to the manufacturer's protocol. Samples were analyzed using a NovoCyte Flow Cytometer. Data were analyzed using LEGENDplex™ Data Analysis Software Suite and GraphPad Prism.

4.5.4 Antibody ELISA Quantification

Blood was collected at time points indicated in 0.2 mL heparin-coated collection tubes (VWR Scientific). Plasma was isolated via centrifugation 2000xg at 4C for 15 min. Samples were collected and stored at -80 °C until use. Titers were performed by coating Nunc MaxiSorp ELISA plates (BioLegend) with 100 μL of 2 μg/mL of the indicated antigen (Sino Biological) overnight at 4C. Plates were washed and blocked with 150 μL 2% (w/v) BSA in PBST for

1hr at RT. Following wash, samples were serially diluted tenfold in blocking buffer for a total volume of 100 μL and incubated for 2hr at RT. Following wash, 100 μL of goat anti-mouse IgG HRP conjugate (Invitrogen) diluted 1:10,000 in 0.4% BSA buffer was incubated for 1hr at RT. Following wash, 100 μL of 1-Step Ultra TMB was incubated for 4.5min before stopping with 50 μL of 2M sulfuric acid. ELISA plates were analyzed using a Multiskan FC plate reader (Thermo Fisher) and absorbance was measured at 450 nm with 620nm correction. Area under the curve measurements were approximated with Riemann sums. Data were analyzed using GraphPad Prism.

4.5.5 Hemagglutinin Inhibition Assays

Hemagglutinin inhibition assays (HAI) were performed with recombinant antigen (Sino Biological). Hemagglutination titers (HA unit) were determined according to the following. Two-fold serial dilutions of 50 μL antigen in PBS were performed in duplicate to form a 12 point curve in a v-bottom plate (Corning). 50 μL of 0.75% turkey red blood cells (Lampire Biological) were added. Plates were mixed by tapping on all sides. Plates were incubated at room temperature for 30 min. Plates were then tilted 90 degrees for approximately 25 sec, or when non-agglutinated wells began to noticeably run. Samples were photographed and recorded as either completely, partially, or not agglutinated. An HA unit was determined to be the first antigen concentration that resulted in complete agglutination.

Next, HAI assays were performed with plasma collected at the indicated timepoints. Plasma samples were treated for any innate inhibitors via cholera filtrate treatment containing receptor destroying enzyme. Plasma samples were diluted 4-fold (6 μ of plasma, 18 μL of cholera filtrate) in cholera filtrate (Sigma-Aldrich), and incubated at 37C overnight. Cholera filtrate was then inactivated by further diluting with PBS for a total of ten fold dilution (addition of 36 μL of PBS). Samples were incubated at 56C for 30 min.

Plasma samples were serially diluted twofold in 25 μL to make an 8 point curve. Antigen

was prepared at a concentration of 4 HA units, and 25 μL was added to all sample and control wells. Plates were tapped to mix and incubated at room temperature for 30 min. Following incubation, 50 μL of 0.75% turkey red blood cells were added. Plates were tapped to mix and incubated at room temperature for a further 30 min. Plates were then tilted 90 degrees for approximately 25 sec, or when non-agglutinated wells began to noticeably run. Samples were photographed and recorded as either completely, partially, or not agglutinated. The HAI titer was reported at the maximum plasma dilution that showed no agglutination. Data were analyzed using GraphPad Prism.

4.5.6 Influenza Inoculation

Mice were anesthetized with isoflurane in a chamber before being placed in a split nose-cone system to allow multiple mice to be handled and intranasally inoculated with ease. Mice were inoculated intranasally via both nares with 40 μL of viral allantonic fluid containing 10^5 PFUs per mouse.

4.5.7 Influenza Challenge Animal Scoring and Monitoring

Mice were monitored once a day following influenza inoculation, with temperature and body weight measurements, and given a score according to the following criteria. **Score 0** (pre influenza inoculation): ambulatory and active, normal fur coat. **Score 1** (post influenza inoculation): mostly active, slightly ruffled fur coat, minimal weight loss. **Score 2** (post influenza inoculation): lethargic, but moves independently, ruffled coat, 5-10% weight loss. **Score 3** (post influenza inoculation): lethargic, but moves occasionally, ruffled coat, slightly increased breathing, 11-20% weight loss. **Score 4** (post influenza inoculation): hunched, ruffled coat, moves only when prompted, labored breathing, weight loss >20%. **Score 5** (post influenza inoculation): hunched, ruffled coat, does not move to stimulation, labored breathing, dehydration, weight loss >20%. **Score 6** (post influenza inoculation): death

Animals with a score of 2 were monitored every 12 hours. Animals with a score of 3 were monitored every 6 hours. Animals reaching a score of 2 were given supportive care in the form of Napa Nectar. Animals reaching a score of 3 were administered meloxicam subcutaneously, daily. Animals reaching a score of 3 were given supportive care in the form of DietGel 76A. Euthanasia Criteria: Each animal that reaches score 4 were promptly euthanized by CO2 asphyxiation. A 20% weight loss is the maximum IACUC recommendation. Infectious disease models often result in acute, moderately severe sections before resolution.

4.5.8 Viral Load Measurements by RT-qPCR

Lungs were harvested and split into both halves at days 3 and 6 post infection and placed in 1 mL of RNAprotect (Qiagen). Samples were flash frozen in liquid nitrogen and stored at -80C until processing. Samples were thawed and an approximately 30 mg section of the left lobe was cut and weighed. This tissue sample was placed in a PowerBead tube with 2.8 mm ceramic beads (Qiagen) with 600 μL of Buffer RLT from a RNEasy total RNA kit. Tissues were homogenized using a Qiagen PowerLyzer 24 at 3500 rpm for 2 x 45 sec cycles with a pause of 30 sec in between. Samples were then processed with a mini RNEasy kit according to the manufacturer's instructions. Total RNA was quantified in the eluate by Nanodrop. Following, viral genomes were quantified via a Luna Probe One-Step RT-qPCR mix (NEB) according to the manufacturer's instructions [277]. Primer and probes used were from the CDC's multiplex assay for respiratory viruses (IDT). Two sets of Influenza A primer pairs and a single probe were used as seen in Table 4.2. A total of 2 μL of RNEasy eluate was used for each sample. The assay was run on a BioRad CFX384 touch thermocycler. An eight point standard curve was created using known template copies of a conserved Influenza A matrix protein sequence. Data was analyzed via GraphPad Prism.

Description	Sequence 5' - 3'	Conc
InfA For1	CAA GAC CAA TCY TGT CAC CTC TGA C	0.4 μM
InfA For2	CAA GAC CAA TYC TGT CAC CTY TGA C	0.4 μM
InfA Rev1	GCA TTY TGG ACA AAV CGT CTA CG	0.6 μM
InfA Rev2	GCA TTT TGG ATA AAG CGT CTA CG	0.2 μM
InfA Probe	/FAM/TGC AGT CCT /ZEN/ CGC TCA CTG GGC ACG/3IABkFQ/	0.2 μM

Table 4.2: RT-qPCR Reagent Conditions for Influenza A Detection

4.5.9 Antibody Secreting Cell ELISPOTs

Mice were vaccinated with Fluzone as previously described. Eight weeks post boost, mice were sacrificed and both tibia and femurs were removed, cleaned, and placed in RPMI on ice. Bones were transferred to a petri dish containing 35% cold ethanol and further cleaned. Bones were washed sequentially in two more Petri dishes containing cold PBS. An 18G needle was used to pierce a hole in the bottom of a 0.5 mL microcentrifuge tube. Bones were cut and placed knee side down in this tube and nested into a 1.5 mL microcentrifuge with 100 μL of RPMI. Tubes were spun at 4500 x g for 15 sec. Pelleted bone marrow cells were resuspended and transferred to a 15 mL centrifuge tube and pelleted at 400 x g for 5 min. Supernatant was discarded and 3 mL of ACK lysis buffer (Gibco) was added and incubated at room temperature for 3 min. Following, cells were diluted with PBS up to 15mL and passed through a 70 μm filter before pelleting at 400 x g for 5 min. RBC lysed cells were then counted at resuspended in complete RPMI. Cells were plated in 100 mm dishes at a concentration of 1 M/mL. Cells were polyclonally stimulated with 1 μg/mL of R848 and 10 ng/mL of IL-2 for 3 days.

Two days later, ELISpot PVDF plates (Millipore Sigma) were activated with 15 μL of 35% ethanol for 1 min. Plates were then immediately washed five times with 200 μL of sterile

water. Plates were coated with 50 μL of 15 μg/mL A/Victoria/2570/2019 hemagglutinin and incubated overnight at 4C. After incubation, ELISpot plates were washed five times with 200 μL of sterile PBS. Plates were then blocked with 200 μL of complete RPMI for 30 min until cell plating.

The next day, following completion of the polyclonal stimulation, cells were collected and pelleted at 400 x g for 5 min. Cells were counted and resuspended at concentration of 2.5 M/mL in complete RPMI. Cells were plated at a top concentration of 500K cells per well in triplicate and serially diluted three fold in ELISpot plates with a final volume of 200 μL. Cells were incubated at 37 C overnight. Following incubation, the cells were removed, plates were washed, and an antigen specific ELISpot was performed using an Mouse IgG ELISpot Flex kit according to the manufacturer's instructions (Mabtech). After, plates were washed extensively with DI water and allowed to dry for a week protected from light at 4 C. When dried, plates were imaged using an ImmunoSpot ELISpot reader (C.T.L.). Well images were analyzed using the built-in ImmunoCapture Basic Count protocol, with the sensitivity adjusted from 80-200 to subtract background. Data were analyzed in GraphPad Prism.

4.5.10 T cell Tetramer Staining

Marker	**Fluorophore**	**Clone**	**Marker**	**Fluorophore**	**Clone**
Viability	Live/Dead Blue	N/A	CD3	BV421	17A2
CD4	BV605	RM4-5	CD8	APC-eFluor780	53-6.7
Tetramer	BUV737	N/A	CD19	APC	6D5
Tetramer	PE	N/A			

Table 4.3: Reagents Used for T Cell Tetramer Staining

Mice were vaccinated with Fluzone as previously described. Mice were sacrificed 10 days after boost vaccinations with spleens harvested and placed on ice. Spleens were turned into single cell suspension by dissociation with two frosted glass slides and passage through a

70-μm filter. Red blood cells were lysed with 2 mL ACK buffer (Gibco) for 3 min before diluting, pelleting, washing, and resuspending in 1 mL of RPMI media. Empty MHCI tetramers (TetramerShop) were loaded with PepMix™ Influenza A HA/H1N1/Victoria/2019 (JPT) according to the manufacturer's instructions. 2M cells were plated in flow staining buffer in a 96-well v-bottom plate and blocked for 10 min with Fc block (BioLegend) before proceeding with antibody staining. The above reagents were used at the manufacturer's recommended concentrations.

4.5.11 Germinal Center Immunophenotyping

Marker	**Fluorophore**	**Clone**	**Marker**	**Fluorophore**	**Clone**
Viability	Live/Dead Blue	N/A	CD4	APC/Cy7	GK1.5
CD3	BV785	17A2	CD19	PerCP	6D5
GL-7	PE	GL7	FAS	BUV737	Jo2
Sca-1	AF488	D7	CD138	BV605	281-2
PD-1	PE/Cy7	29F.1A12	CXCR5	BUV615	2G8

Table 4.4: Reagents Used for Germinal Center Staining

Mice were vaccinated with Fluzone as previously described. Mice were sacrificed 8 days after boost vaccinations with spleens harvested and placed on ice. Spleens were turned into single cell suspension by dissociation with two frosted glass slides and passage through a 70-μm filter. Red blood cells were lysed with 2 mL ACK buffer (Gibco) for 3 min before diluting, pelleting, washing, and resuspending in 1 mL of RPMI media. 2M cells were plated in flow staining buffer in 96-well v-bottom plate and blocked for 10 min with Fc block (BioLegend) before proceeding with antibody staining. The above reagents were used at the manufacturer's recommended concentrations.

REFERENCES

[1] Macfarlane Burnet. *Self and Not-Self: Cellular Immunology Book One*. CUP Archive, June 1969. Google-Books-ID: 3kg4AAAAIAAJ.

[2] P. Matzinger. Tolerance, danger, and the extended family. *Annual Review of Immunology*, 12:991–1045, 1994.

[3] C. A. Janeway. Approaching the asymptote? Evolution and revolution in immunology. *Cold Spring Harbor Symposia on Quantitative Biology*, 54 Pt 1:1–13, 1989.

[4] Stanley Cohen, Pierluigi E. Bigazzi, and Takeshi Yoshida. Similarities of T cell function in cell-mediated immunity and antibody production. *Cellular Immunology*, 12(1):150–159, April 1974.

[5] Jan Klein. *Natural History of the Major Histocompatibility Complex*. Wiley, 1986. Google-Books-ID: NQNrAAAAMAAJ.

[6] Sir Frank Macfarlane Burnet. *The Clonal Selection Theory of Acquired Immunity*. Vanderbilt University Press, 1959. Google-Books-ID: BV1BAAAAYAAJ.

[7] Kris De Smet and Roland Contreras. Human antimicrobial peptides: defensins, cathelicidins and histatins. *Biotechnology Letters*, 27(18):1337–1347, September 2005.

[8] Jason R. Dunkelberger and Wen-Chao Song. Complement and its role in innate and adaptive immune responses. *Cell Research*, 20(1):34–50, January 2010. Number: 1 Publisher: Nature Publishing Group.

[9] Damiana Álvarez Errico, Roser Vento-Tormo, Michael Sieweke, and Esteban Ballestar. Epigenetic control of myeloid cell differentiation, identity and function. *Nature Reviews Immunology*, 15(1):7–17, January 2015. Number: 1 Publisher: Nature Publishing Group.

[10] Carlos Rosales. Neutrophil: A Cell with Many Roles in Inflammation or Several Cell Types? *Frontiers in Physiology*, 9:113, February 2018.

[11] Amy D. Klion and Thomas B. Nutman. The role of eosinophils in host defense against helminth parasites. *Journal of Allergy and Clinical Immunology*, 113(1):30–37, January 2004. Publisher: Elsevier.

[12] Salvatore Chirumbolo. State-of-the-art review about basophil research in immunology and allergy: is the time right to treat these cells with the respect they deserve? *Blood Transfusion*, 10(2):148–168, April 2012.

[13] Ang Lin and Karin Loré. Granulocytes: New Members of the Antigen-Presenting Cell Family. *Frontiers in Immunology*, 8, 2017.

[14] Thomas A. Wynn, Ajay Chawla, and Jeffrey W. Pollard. Origins and Hallmarks of Macrophages: Development, Homeostasis, and Disease. *Nature*, 496(7446):445–455, April 2013.

[15] Bali Pulendran. The varieties of immunological experience: of pathogens, stress, and dendritic cells. *Annual Review of Immunology*, 33:563–606, 2015.

[16] Bali Pulendran, Prabhu S. Arunachalam, and Derek T. O'Hagan. Emerging concepts in the science of vaccine adjuvants. *Nature Reviews. Drug Discovery*, 20(6):454–475, 2021.

[17] Trine H. Mogensen. Pathogen Recognition and Inflammatory Signaling in Innate Immune Defenses. *Clinical Microbiology Reviews*, 22(2):240–273, April 2009.

[18] Danyang Li and Minghua Wu. Pattern recognition receptors in health and diseases. *Signal Transduction and Targeted Therapy*, 6(1):1–24, August 2021. Number: 1 Publisher: Nature Publishing Group.

[19] Bruno Lemaitre, Emmanuelle Nicolas, Lydia Michaut, Jean-Marc Reichhart, and Jules A Hoffmann. The Dorsoventral Regulatory Gene Cassette spätzle/Toll/cactus Controls the Potent Antifungal Response in Drosophila Adults. *Cell*, 86(6):973–983, September 1996.

[20] Fernando L. Rock, Gary Hardiman, Jackie C. Timans, Robert A. Kastelein, and J. Fernando Bazan. A family of human receptors structurally related to DrosophilaToll. *Proceedings of the National Academy of Sciences of the United States of America*, 95(2):588–593, January 1998.

[21] Nicholas Funderburg, Michael M. Lederman, Zhimin Feng, Michael G. Drage, Julie Jadlowsky, Clifford V. Harding, Aaron Weinberg, and Scott F. Sieg. Human -defensin-3 activates professional antigen-presenting cells via Toll-like receptors 1 and 2. *Proceedings of the National Academy of Sciences of the United States of America*, 104(47):18631–18635, November 2007.

[22] Elizabeth M. Long, Brandie Millen, Paul Kubes, and Stephen M. Robbins. Lipoteichoic Acid Induces Unique Inflammatory Responses when Compared to Other Toll-Like Receptor 2 Ligands. *PLoS ONE*, 4(5):e5601, May 2009.

[23] Katalin Karikó, Houping Ni, John Capodici, Marc Lamphier, and Drew Weissman. mRNA Is an Endogenous Ligand for Toll-like Receptor 3*. *Journal of Biological Chemistry*, 279(13):12542–12550, March 2004.

[24] Saurabh Chattopadhyay and Ganes C. Sen. dsRNA-Activation of TLR3 and RLR Signaling: Gene Induction-Dependent and Independent Effects. *Journal of Interferon & Cytokine Research*, 34(6):427–436, June 2014.

[25] Hongliang Fang, Yanfeng Wu, Xiaohui Huang, Wenying Wang, Bing Ang, Xuetao Cao, and Tao Wan. Toll-like Receptor 4 (TLR4) Is Essential for Hsp70-like Protein 1 (HSP70L1) to Activate Dendritic Cells and Induce Th1 Response. *The Journal of Biological Chemistry*, 286(35):30393–30400, September 2011.

[26] Beom Seok Park and Jie-Oh Lee. Recognition of lipopolysaccharide pattern by TLR4 complexes. *Experimental & Molecular Medicine*, 45(12):e66–e66, December 2013. Number: 12 Publisher: Nature Publishing Group.

[27] Sung-il Yoon, Oleg Kurnasov, Venkatesh Natarajan, Minsun Hong, Andrei V. Gudkov, Andrei L. Osterman, and Ian A. Wilson. Structural basis of TLR5-flagellin recognition and signaling. *Science (New York, N.Y.)*, 335(6070):859–864, February 2012.

[28] Nathaniel M. Green, Krishna-Sulayman Moody, Michelle Debatis, and Ann Marshak-Rothstein. Activation of Autoreactive B Cells by Endogenous TLR7 and TLR3 RNA Ligands. *The Journal of Biological Chemistry*, 287(47):39789–39799, November 2012.

[29] Jennifer M. Lund, Lena Alexopoulou, Ayuko Sato, Margaret Karow, Niels C. Adams, Nicholas W. Gale, Akiko Iwasaki, and Richard A. Flavell. Recognition of single-stranded RNA viruses by Toll-like receptor 7. *Proceedings of the National Academy of Sciences of the United States of America*, 101(15):5598–5603, April 2004.

[30] Wenduona Bao, Hong Xia, Yaojun Liang, Yuting Ye, Yuqiu Lu, Xiaodong Xu, Aiping Duan, Jing He, Zhaohong Chen, Yan Wu, Xia Wang, Chunxia Zheng, Zhihong Liu, and Shaolin Shi. Toll-like Receptor 9 Can be Activated by Endogenous Mitochondrial DNA to Induce Podocyte Apoptosis. *Scientific Reports*, 6(1):22579, March 2016. Number: 1 Publisher: Nature Publishing Group.

[31] Ali A. Ashkar and Kenneth L. Rosenthal. Toll-like receptor 9, CpG DNA and innate immunity. *Current Molecular Medicine*, 2(6):545–556, September 2002.

[32] Nadra J. Nilsen, Gregory I. Vladimer, Jørgen Stenvik, M. Pontus A. Orning, Maria V. Zeid-Kilani, Marit Bugge, Bjarte Bergstroem, Joseph Conlon, Harald Husebye, Amy G. Hise, Katherine A. Fitzgerald, Terje Espevik, and Egil Lien. A Role for the Adaptor Proteins TRAM and TRIF in Toll-like Receptor 2 Signaling. *The Journal of Biological Chemistry*, 290(6):3209–3222, February 2015.

[33] Takumi Kawasaki and Taro Kawai. Toll-Like Receptor Signaling Pathways. *Frontiers in Immunology*, 5, 2014.

[34] Lin Luo, Richard M. Lucas, Liping Liu, and Jennifer L. Stow. Signalling, sorting and scaffolding adaptors for Toll-like receptors. *Journal of Cell Science*, 133(5):jcs239194, December 2019.

[35] Ting Liu, Lingyun Zhang, Donghyun Joo, and Shao-Cong Sun. NF-B signaling in inflammation. *Signal Transduction and Targeted Therapy*, 2(1):1–9, July 2017. Number: 1 Publisher: Nature Publishing Group.

[36] Shao-Cong Sun. The non-canonical NF-B pathway in immunity and inflammation. *Nature Reviews Immunology*, 17(9):545–558, September 2017. Number: 9 Publisher: Nature Publishing Group.

[37] Andrea Oeckinghaus and Sankar Ghosh. The NF-B Family of Transcription Factors and Its Regulation. *Cold Spring Harbor Perspectives in Biology*, 1(4):a000034, October 2009.

[38] I. a. M. MacPhee, D. R. Turner, H. Yagita, and D. B. G. Oliveira. CD80(B7.1) and CD86(B7.2) Do not Have Distinct Roles in Setting the Th1/Th2 Balance in Autoimmunity in Rats. *Scandinavian Journal of Immunology*, 54(5):486–494, 2001. _eprint: https://onlinelibrary.wiley.com/doi/pdf/10.1046/j.1365-3083.2001.00998.x.

[39] P. A. van der Merwe, D. L. Bodian, S. Daenke, P. Linsley, and S. J. Davis. CD80 (B7-1) binds both CD28 and CTLA-4 with a low affinity and very fast kinetics. *The Journal of Experimental Medicine*, 185(3):393–403, February 1997.

[40] David M. Sansom, Claire N. Manzotti, and Yong Zheng. What's the difference between CD80 and CD86? *Trends in Immunology*, 24(6):313–318, June 2003. Publisher: Elsevier.

[41] David G. Schatz and Yanhong Ji. Recombination centres and the orchestration of V(D)J recombination. *Nature Reviews Immunology*, 11(4):251–263, April 2011. Number: 4 Publisher: Nature Publishing Group.

[42] Jr Charles A Janeway, Paul Travers, Mark Walport, and Mark J. Shlomchik. The generation of diversity in immunoglobulins. In *Immunobiology: The Immune System in Health and Disease. 5th edition*. Garland Science, 2001.

[43] Maxim N. Artyomov, Mieszko Lis, Srinivas Devadas, Mark M. Davis, and Arup K. Chakraborty. CD4 and CD8 binding to MHC molecules primarily acts to enhance Lck delivery. *Proceedings of the National Academy of Sciences*, 107(39):16916–16921, September 2010. Publisher: Proceedings of the National Academy of Sciences.

[44] Ronald N. Germain. T-cell development and the CD4–CD8 lineage decision. *Nature Reviews Immunology*, 2(5):309–322, May 2002. Number: 5 Publisher: Nature Publishing Group.

[45] Ludger Klein, Bruno Kyewski, Paul M. Allen, and Kristin A. Hogquist. Positive and negative selection of the T cell repertoire: what thymocytes see and don't see. *Nature reviews. Immunology*, 14(6):377–391, June 2014.

[46] K. J. Lafferty, I. S. Misko, and M. A. Cooley. Allogeneic stimulation modulates the in vitro response of T cells to transplantation antigen. *Nature*, 249(454):275–276, May 1974.

[47] J. M. Curtsinger, C. S. Schmidt, A. Mondino, D. C. Lins, R. M. Kedl, M. K. Jenkins, and M. F. Mescher. Inflammatory cytokines provide a third signal for activation of naive CD4+ and CD8+ T cells. *Journal of Immunology (Baltimore, Md.: 1950)*, 162(6):3256–3262, March 1999.

[48] Dipanjan Chowdhury and Judy Lieberman. Death by a thousand cuts: granzyme pathways of programmed cell death. *Annual Review of Immunology*, 26:389–420, 2008.

[49] John H. Russell and Timothy J. Ley. Lymphocyte-mediated cytotoxicity. *Annual Review of Immunology*, 20:323–370, 2002.

[50] T R Mosmann and R L Coffman. TH1 and TH2 Cells: Different Patterns of Lymphokine Secretion Lead to Different Functional Properties. *Annual Review of Immunology*, 7(1):145–173, 1989. _eprint: https://doi.org/10.1146/annurev.iy.07.040189.001045.

[51] D. R. Lucey. Evolution of the type-1 (Th1)-type-2 (Th2) cytokine paradigm. *Infectious Disease Clinics of North America*, 13(1):1–9, v, March 1999.

[52] Chen Dong and Richard A Flavell. Cell fate decision: T-helper 1 and 2 subsets in immune responses. *Arthritis Research*, 2(3):179–188, 2000.

[53] Masato Kubo. The role of IL-4 derived from follicular helper T (TFH) cells and type 2 helper T (TH2) cells. *International Immunology*, 33(12):717–722, November 2021.

[54] Taku Kouro and Kiyoshi Takatsu. IL-5- and eosinophil-mediated inflammation: from discovery to therapy. *International Immunology*, 21(12):1303–1309, December 2009.

[55] Bruce Glick, Timothy S. Chang, and R. George Jaap. The Bursa of Fabricius and Antibody Production. *Poultry Science*, 35(1):224–225, January 1956.

[56] Thomas H. Winkler and Inga-Lill Mårtensson. The Role of the Pre-B Cell Receptor in B Cell Development, Repertoire Selection, and Tolerance. *Frontiers in Immunology*, 9, 2018.

[57] David Nemazee. Mechanisms of central tolerance for B cells. *Nature Reviews Immunology*, 17(5):281–294, May 2017. Number: 5 Publisher: Nature Publishing Group.

[58] Gabriel D. Victora and Michel C. Nussenzweig. Germinal centers. *Annual Review of Immunology*, 30:429–457, 2012.

[59] Bruce Alberts, Alexander Johnson, Julian Lewis, Martin Raff, Keith Roberts, and Peter Walter. B Cells and Antibodies. In *Molecular Biology of the Cell. 4th edition.* Garland Science, 2002.

[60] Gestur Vidarsson, Gillian Dekkers, and Theo Rispens. IgG Subclasses and Allotypes: From Structure to Effector Functions. *Frontiers in Immunology*, 5:520, October 2014.

[61] Cynthia L. Schultz and Robert L. Coffman. Control of isotype switching by T cells and cytokines. *Current Opinion in Immunology*, 3(3):350–354, June 1991.

[62] Jenifer Ehreth. The global value of vaccination. *Vaccine*, 21(7-8):596–600, January 2003.

[63] Arthur Boylston. The origins of inoculation. *Journal of the Royal Society of Medicine*, 105(7):309–313, July 2012.

[64] Stefan Riedel. Edward Jenner and the history of smallpox and vaccination. *Proceedings (Baylor University. Medical Center)*, 18(1):21–25, January 2005.

[65] Theodore H. Tulchinsky. Maurice Hilleman: Creator of Vaccines That Changed the World. *Case Studies in Public Health*, pages 443–470, 2018.

[66] Alexander Hodgens and Rachana Marathi. Hepatitis B Vaccine. In *StatPearls*. StatPearls Publishing, Treasure Island (FL), 2023.

[67] D Goldblatt. Conjugate vaccines. *Clinical and Experimental Immunology*, 119(1):1–3, January 2000.

[68] Hasnat Tariq, Sannia Batool, Saaim Asif, Mohammad Ali, and Bilal Haider Abbasi. Virus-Like Particles: Revolutionary Platforms for Developing Vaccines Against Emerging Infectious Diseases. *Frontiers in Microbiology*, 12:790121, January 2022.

[69] Alex Schudel, David M. Francis, and Susan N. Thomas. Material design for lymph node drug delivery. *Nature Reviews. Materials*, 4(6):415–428, June 2019.

[70] Ennio De Gregorio, Elaine Tritto, and Rino Rappuoli. Alum adjuvanticity: Unraveling a century old mystery. *European Journal of Immunology*, 38(8):2068–2071, August 2008.

[71] Kate McKeage and Barbara Romanowski. AS04-adjuvanted human papillomavirus (HPV) types 16 and 18 vaccine (Cervarix®): a review of its use in the prevention of premalignant cervical lesions and cervical cancer causally related to certain oncogenic HPV types. *Drugs*, 71(4):465–488, March 2011.

[72] Surender Khurana, Elizabeth M. Coyle, Jody Manischewitz, Lisa R. King, Jin Gao, Ronald N. Germain, Pamela L. Schwartzberg, John S. Tsang, and Hana Golding. AS03-adjuvanted H5N1 vaccine promotes antibody diversity and affinity maturation, NAI titers, cross-clade H5N1 neutralization, but not H1N1 cross-subtype neutralization. *npj Vaccines*, 3(1):1–12, October 2018. Number: 1 Publisher: Nature Publishing Group.

[73] Derek T O'Hagan, Leonard R Friedland, Emmanuel Hanon, and Arnaud M Didierlaurent. Towards an evidence based approach for the development of adjuvanted vaccines. *Current Opinion in Immunology*, 47:93–102, August 2017.

[74] Arnaud M. Didierlaurent, Béatrice Laupèze, Alberta Di Pasquale, Nadia Hergli, Catherine Collignon, and Nathalie Garçon. Adjuvant system AS01: helping to overcome the challenges of modern vaccines. *Expert Review of Vaccines*, 16(1):55–63, January 2017. Publisher: Taylor & Francis _eprint: https://doi.org/10.1080/14760584.2016.1213632.

[75] Sarah Schillie. Recommendations of the Advisory Committee on Immunization Practices for Use of a Hepatitis B Vaccine with a Novel Adjuvant. *MMWR. Morbidity and Mortality Weekly Report*, 67, 2018.

[76] Linda Stertman, Anna-Karin E. Palm, Behdad Zarnegar, Berit Carow, Carolina Lunderius Andersson, Sofia E. Magnusson, Cecilia Carnrot, Vivek Shinde, Gale Smith, Gregory Glenn, Louis Fries, and Karin Lövgren Bengtsson. The Matrix-M™ adjuvant: A critical component of vaccines for the 21st century. *Human Vaccines & Immunotherapeutics*, 19(1):2189885.

[77] A. T. Glenny, C. G. Pope, Hilda Waddington, and U. Wallace. Immunological notes. XVII–XXIV. *The Journal of Pathology and Bacteriology*, 29(1):31–40, 1926. _eprint: https://onlinelibrary.wiley.com/doi/pdf/10.1002/path.1700290106.

[78] A. T. Glenny and Mollie Barr. The precipitation of diphtheria toxoid by potash alum. *The Journal of Pathology and Bacteriology*, 34(2):131–138, 1931. _eprint: https://onlinelibrary.wiley.com/doi/pdf/10.1002/path.1700340203.

[79] Harm HogenEsch, Derek T. O'Hagan, and Christopher B. Fox. Optimizing the utilization of aluminum adjuvants in vaccines: you might just get what you want. *npj Vaccines*, 3(1):1–11, October 2018. Number: 1 Publisher: Nature Publishing Group.

[80] Hok Hei Tam, Mariane B. Melo, Myungsun Kang, Jeisa M. Pelet, Vera M. Ruda, Maria H. Foley, Joyce K. Hu, Sudha Kumari, Jordan Crampton, Alexis D. Baldeon, Rogier W. Sanders, John P. Moore, Shane Crotty, Robert Langer, Daniel G. Anderson, Arup K. Chakraborty, and Darrell J. Irvine. Sustained antigen availability during germinal center initiation enhances antibody responses to vaccination. *Proceedings of the National Academy of Sciences of the United States of America*, 113(43):E6639–E6648, October 2016.

[81] Eva van Doorn, Heng Liu, Anke Huckriede, and Eelko Hak. Safety and tolerability evaluation of the use of Montanide ISA™51 as vaccine adjuvant: A systematic review. *Human Vaccines & Immunotherapeutics*, 12(1):159–169, September 2015.

[82] Jerome Aucouturier, Stephane Ascarateil, and Laurent Dupuis. The use of oil adjuvants in therapeutic vaccines. *Vaccine*, 24:S44–S45, April 2006.

[83] D. T. O'Hagan, G. S. Ott, E. De Gregorio, and A. Seubert. The mechanism of action of MF59 – An innately attractive adjuvant formulation. *Vaccine*, 30(29):4341–4348, June 2012.

[84] Phuong Nguyen-Contant, Mark Y. Sangster, and David J. Topham. Squalene-Based Influenza Vaccine Adjuvants and Their Impact on the Hemagglutinin-Specific B Cell Response. *Pathogens*, 10(3):355, March 2021. Number: 3 Publisher: Multidisciplinary Digital Publishing Institute.

[85] Sandra Morel, Arnaud Didierlaurent, Patricia Bourguignon, Sophie Delhaye, Benoît Baras, Valérie Jacob, Camille Planty, Abdelatif Elouahabi, Pol Harvengt, Harald Carlsen, Anders Kielland, Patrick Chomez, Nathalie Garçon, and Marcelle Van Mechelen. Adjuvant System AS03 containing -tocopherol modulates innate immune response and leads to improved adaptive immunity. *Vaccine*, 29(13):2461–2473, March 2011.

[86] Michael I. Hauser, David J. Muscatello, Annabel C. Y. Soh, Dominic E. Dwyer, and Robin M. Turner. An indirect comparison meta-analysis of AS03 and MF59 adjuvants in pandemic influenza A(H1N1)pdm09 vaccines. *Vaccine*, 37(31):4246–4255, July 2019.

[87] J. Freund and K. McDermott. Sensitization to Horse Serum by Means of Adjuvants. *Experimental Biology and Medicine*, 49(4):548–553, April 1942.

[88] Carolyn R. Casella and Thomas C. Mitchell. Putting endotoxin to work for us: monophosphoryl lipid A as a safe and effective vaccine adjuvant. *Cellular and molecular life sciences : CMLS*, 65(20):3231–3240, October 2008.

[89] G Ramon. Sur L'augmentation anormale de L'antitoxine chez les chevaux producteurs de serum antidiphtherique. *Bull. Soc. Centr. Med. Vet*, 101:227–234, 1925.

[90] C. R. Kensil, U. Patel, M. Lennick, and D. Marciani. Separation and characterization of saponins with adjuvant activity from Quillaja saponaria Molina cortex. *Journal of Immunology (Baltimore, Md.: 1950)*, 146(2):431–437, January 1991.

[91] Geert Leroux-Roels, Arnaud Marchant, Jack Levy, Pierre Van Damme, Tino F. Schwarz, Yves Horsmans, Wolfgang Jilg, Peter G. Kremsner, Edwige Haelterman, Frédéric Clément, Julian J. Gabor, Meral Esen, Annick Hens, Isabelle Carletti, Laurence Fissette, Fernanda Tavares Da Silva, Wivine Burny, Michel Janssens, Philippe Moris, Arnaud M. Didierlaurent, Robbert Van Der Most, Nathalie Garçon, Pascale Van Belle, and Marcelle Van Mechelen. Impact of adjuvants on CD4+ T cell and B cell responses to a protein antigen vaccine: Results from a phase II, randomized, multicenter trial. *Clinical Immunology*, 169:16–27, August 2016.

[92] Marie-Aleth Lacaille-Dubois. Updated insights into the mechanism of action and clinical profile of the immunoadjuvant QS-21: A review. *Phytomedicine*, 60:152905, July 2019.

[93] Tim Sparwasser, Thomas Miethke, Grayson Lipford, Katrin Borschert, Hans Häcker, Klaus Heeg, and Hermann Wagner. Bacterial DNA causes septic shock. *Nature*, 386(6623):336–337, March 1997. Number: 6623 Publisher: Nature Publishing Group.

[94] Hermann Wagner. Bacterial CpG DNA Activates Immune Cells to Signal Infectious Danger. In Frank J. Dixon, editor, *Advances in Immunology*, volume 73, pages 329–368. Academic Press, January 1999.

[95] William L. Heyward, Michael Kyle, Joseph Blumenau, Matthew Davis, Keith Reisinger, Martin L. Kabongo, Sean Bennett, Robert S. Janssen, Hamid Namini, and J. Tyler Martin. Immunogenicity and safety of an investigational hepatitis B vaccine with a Toll-like receptor 9 agonist adjuvant (HBsAg-1018) compared to a licensed hepatitis B vaccine in healthy adults 40–70 years of age. *Vaccine*, 31(46):5300–5305, November 2013.

[96] Rose S. Chu, Oleg S. Targoni, Arthur M. Krieg, Paul V. Lehmann, and Clifford V. Harding. CpG Oligodeoxynucleotides Act as Adjuvants that Switch on T Helper 1 (Th1) Immunity. *The Journal of Experimental Medicine*, 186(10):1623–1631, November 1997.

[97] J. R. Broach and J. Thorner. High-throughput screening for drug discovery. *Nature*, 384(6604 Suppl):14–16, November 1996.

[98] Ricardo Macarron, Martyn N. Banks, Dejan Bojanic, David J. Burns, Dragan A. Cirovic, Tina Garyantes, Darren V. S. Green, Robert P. Hertzberg, William P. Janzen, Jeff W. Paslay, Ulrich Schopfer, and G. Sitta Sittampalam. Impact of high-throughput screening in biomedical research. *Nature Reviews Drug Discovery*, 10(3):188–195, March 2011. Number: 3 Publisher: Nature Publishing Group.

[99] R. L. Miller, J. F. Gerster, M. L. Owens, H. B. Slade, and M. A. Tomai. Imiquimod applied topically: a novel immune response modifier and new class of drug. *International Journal of Immunopharmacology*, 21(1):1–14, January 1999.

[100] Sudhir Pai Kasturi, Mohammed Ata-Ur Rasheed, Colin Havenar-Daughton, Mathew Pham, Traci Legere, Zarpheen Jinnah Sher, Yevgeny Kovalenkov, Sanjeev Gumber, Jessica Huang, Raphael Gottardo, William Fulp, Alicia Sato, Sheetal Sawant, Sherry Stanfield-Oakley, Nicole Yates, Celia LaBranche, S. Munir Alam, Georgia Tomaras, Guido Ferrari, David Montefiori, Jens Wrammert, Francois Villinger, Mark Tomai, John Vasilakos, Christopher B. Fox, Steven G. Reed, Barton F. Haynes, Shane Crotty, Rafi Ahmed, and Bali Pulendran. 3M-052, a synthetic TLR-7/8 agonist induces durable HIV-1 envelope specific plasma cells and humoral immunity in non-human primates. *Science immunology*, 5(48):eabb1025, June 2020.

[101] Hiroki Ishikawa and Glen N. Barber. STING is an endoplasmic reticulum adaptor that facilitates innate immune signalling. *Nature*, 455(7213):674–678, October 2008.

[102] Lijun Sun, Jiaxi Wu, Fenghe Du, Xiang Chen, and Zhijian J. Chen. Cyclic GMP-AMP Synthase Is a Cytosolic DNA Sensor That Activates the Type I Interferon Pathway. *Science*, 339(6121):786–791, February 2013. Publisher: American Association for the Advancement of Science.

[103] Nathan Kelley, Devon Jeltema, Yanhui Duan, and Yuan He. The NLRP3 Inflammasome: An Overview of Mechanisms of Activation and Regulation. *International Journal of Molecular Sciences*, 20(13):3328, July 2019.

[104] M. L. Albert, B. Sauter, and N. Bhardwaj. Dendritic cells acquire antigen from apoptotic cells and induce class I-restricted CTLs. *Nature*, 392(6671):86–89, March 1998.

[105] Nader Yatim, Hélène Jusforgues-Saklani, Susana Orozco, Oliver Schulz, Rosa Barreira da Silva, Caetano Reis e Sousa, Douglas R. Green, Andrew Oberst, and Matthew L. Albert. RIPK1 and NF-B signaling in dying cells determines cross-priming of CD8 T cells. *Science (New York, N.Y.)*, 350(6258):328–334, October 2015.

[106] Mihai G. Netea, Jorge Domínguez-Andrés, Luis B. Barreiro, Triantafyllos Chavakis, Maziar Divangahi, Elaine Fuchs, Leo A. B. Joosten, Jos W. M. van der Meer, Musa M. Mhlanga, Willem J. M. Mulder, Niels P. Riksen, Andreas Schlitzer, Joachim L. Schultze, Christine Stabell Benn, Joseph C. Sun, Ramnik J. Xavier, and Eicke Latz. Defining trained immunity and its role in health and disease. *Nature Reviews Immunology*, 20(6):375–388, June 2020. Number: 6 Publisher: Nature Publishing Group.

[107] Z. K. Ballas, A. M. Krieg, T. Warren, W. Rasmussen, H. L. Davis, M. Waldschmidt, and G. J. Weiner. Divergent therapeutic and immunologic effects of oligodeoxynucleotides with distinct CpG motifs. *Journal of Immunology (Baltimore, Md.: 1950)*, 167(9):4878–4886, November 2001.

[108] Laura Bungener, Felix Geeraedts, Wouter Ter Veer, Jeroen Medema, Jan Wilschut, and Anke Huckriede. Alum boosts TH2-type antibody responses to whole-inactivated virus influenza vaccine in mice but does not confer superior protection. *Vaccine*, 26(19):2350–2359, May 2008.

[109] José Francisco Zambrano-Zaragoza, Enrique Jhonatan Romo-Martínez, Ma. de Jesús Durán-Avelar, Noemí García-Magallanes, and Norberto Vibanco-Pérez. Th17 Cells in Autoimmune and Infectious Diseases. *International Journal of Inflammation*, 2014:651503, 2014.

[110] Hongbo Shen and Zheng W. Chen. The crucial roles of Th17-related cytokines/signal pathways in M. tuberculosis infection. *Cellular & Molecular Immunology*, 15(3):216–225, March 2018. Number: 3 Publisher: Nature Publishing Group.

[111] I. V. Lyadova and A. V. Panteleev. Th1 and Th17 Cells in Tuberculosis: Protection, Pathology, and Biomarkers. *Mediators of Inflammation*, 2015:1–13, 2015.

[112] Selma Tuzlak, Anne S. Dejean, Matteo Iannacone, Francisco J. Quintana, Ari Waisman, Florent Ginhoux, Thomas Korn, and Burkhard Becher. Repositioning TH cell polarization from single cytokines to complex help. *Nature Immunology*, 22(10):1210–1217, October 2021.

[113] Casey T. Weaver, Laurie E. Harrington, Paul R. Mangan, Maya Gavrieli, and Kenneth M. Murphy. Th17: An Effector CD4 T Cell Lineage with Regulatory T Cell Ties. *Immunity*, 24(6):677–688, June 2006.

[114] A Corthay. How do Regulatory T Cells Work? *Scandinavian Journal of Immunology*, 70(4):326–336, October 2009.

[115] Shane Crotty. T Follicular Helper Cell Biology: A Decade of Discovery and Diseases. *Immunity*, 50(5):1132–1148, May 2019.

[116] Mark H. Kaplan. Th9 cells: differentiation and disease. *Immunological reviews*, 252(1):104–115, March 2013.

[117] Lei Jia and Changyou Wu. The biology and functions of Th22 cells. *Advances in Experimental Medicine and Biology*, 841:209–230, 2014.

[118] J. Zhang, A. I. Roberts, C. Liu, G. Ren, G. Xu, L. Zhang, S. Devadas, and Yufang Shi. A novel subset of helper T cells promotes immune responses by secreting GM-CSF. *Cell Death & Differentiation*, 20(12):1731–1741, December 2013. Number: 12 Publisher: Nature Publishing Group.

[119] Jinfang Zhu, Hidehiro Yamane, and William E. Paul. Differentiation of Effector CD4 T Cell Populations. *Annual review of immunology*, 28:445–489, 2010.

[120] Kenneth J. Oestreich and Amy S. Weinmann. Master regulators or lineage-specifying? Changing views on CD4+ T cell transcription factors. *Nature reviews. Immunology*, 12(11):799–804, November 2012.

[121] Bhalchandra Mirlekar. Co-expression of master transcription factors determines CD4+ T cell plasticity and functions in auto-inflammatory diseases. *Immunology Letters*, 222:58–66, June 2020.

[122] Nikolai Petrovsky. Comparative Safety of Vaccine Adjuvants: A Summary of Current Evidence and Future Needs. *Drug Safety*, 38(11):1059–1074, 2015.

[123] Lisa M. Christian, Kyle Porter, Erik Karlsson, and Stacey Schultz-Cherry. Proinflammatory cytokine responses correspond with subjective side effects after influenza virus vaccination. *Vaccine*, 33(29):3360–3366, June 2015.

[124] Andreas Eigler, Bhanu Sinha, Gunther Hartmann, and Stefan Endres. Taming TNF: strategies to restrain this proinflammatory cytokine. *Immunology Today*, 18(10):487–492, October 1997.

[125] George D. Kalliolias and Lionel B. Ivashkiv. TNF biology, pathogenic mechanisms and emerging therapeutic strategies. *Nature Reviews. Rheumatology*, 12(1):49–62, January 2016.

[126] Charles A. Dinarello. Overview of the IL-1 family in innate inflammation and acquired immunity. *Immunological reviews*, 281(1):8–27, January 2018.

[127] Christoph Schultheiß, Edith Willscher, Lisa Paschold, Cornelia Gottschick, Bianca Klee, Svenja-Sibylla Henkes, Lidia Bosurgi, Jochen Dutzmann, Daniel Sedding, Thomas Frese, Matthias Girndt, Jessica I. Höll, Michael Gekle, Rafael Mikolajczyk, and Mascha Binder. The IL-1, IL-6, and TNF cytokine triad is associated with post-acute sequelae of COVID-19. *Cell Reports Medicine*, 3(6):100663, June 2022.

[128] Rein Verbeke, Ine Lentacker, Stefaan C. De Smedt, and Heleen Dewitte. Three decades of messenger RNA vaccine development. *Nano Today*, 28:100766, October 2019.

[129] Rein Verbeke, Michael J. Hogan, Karin Loré, and Norbert Pardi. Innate immune mechanisms of mRNA vaccines. *Immunity*, 55(11):1993–2005, November 2022.

[130] Nathalie Garçon and Alberta Di Pasquale. From discovery to licensure, the Adjuvant System story. *Human Vaccines & Immunotherapeutics*, 13(1):19–33, September 2016.

[131] K. Lövgren and B. Morein. The requirement of lipids for the formation of immunostimulating complexes (iscoms). *Biotechnology and Applied Biochemistry*, 10(2):161–172, April 1988.

[132] Jenny M. Reimer, Karin H. Karlsson, Karin Lövgren-Bengtsson, Sofia E. Magnusson, Alexis Fuentes, and Linda Stertman. Matrix-M™ Adjuvant Induces Local Recruitment, Activation and Maturation of Central Immune Cells in Absence of Antigen. *PLoS ONE*, 7(7):e41451, July 2012.

[133] Martin F. Bachmann and Gary T. Jennings. Vaccine delivery: a matter of size, geometry, kinetics and molecular patterns. *Nature Reviews Immunology*, 10(11):787–796, November 2010. Number: 11 Publisher: Nature Publishing Group.

[134] Melissa A. Kachura, Colin Hickle, Sariah A. Kell, Atul Sathe, Carlo Calacsan, Radwan Kiwan, Brian Hall, Robert Milley, Gary Ott, Robert L. Coffman, Holger Kanzler, and John D. Campbell. A CpG-Ficoll Nanoparticle Adjuvant for Anthrax Protective Antigen Enhances Immunogenicity and Provides Single-Immunization Protection against Inhaled Anthrax in Monkeys. *The Journal of Immunology*, 196(1):284–297, January 2016.

[135] Susan N. Thomas, Efthymia Vokali, Amanda W. Lund, Jeffrey A. Hubbell, and Melody A. Swartz. Targeting the tumor-draining lymph node with adjuvanted nanoparticles reshapes the anti-tumor immune response. *Biomaterials*, 35(2):814–824, January 2014.

[136] Natalia Munoz-Wolf, Ross W. Ward, Claire H. Hearnden, Fiona A. Sharp, Joan Geoghegan, Katie O'Grady, Craig P. McEntee, Katharine A. Shanahan, Coralie Guy, Andrew G. Bowie, Matthew Campbell, Carla B. Roces, Giulia Anderluzzi, Cameron Webb, Yvonne Perrie, Emma Creagh, Ed C. Lavelle, and Sneak Peek Administrator.

Non-Canonical Inflammasome Activation Mediates the Adjuvanticity of Nanoparticles, February 2022.

[137] Moses O Oyewumi, Amit Kumar, and Zhengrong Cui. Nano-microparticles as immune adjuvants: correlating particle sizes and the resultant immune responses. *Expert review of vaccines*, 9(9):1095–1107, September 2010.

[138] Ragheb Al-Shakhshir, Fred Regnier, Joe L. White, and Stanley L. Hem. Effect of protein adsorption on the surface charge characteristics of aluminium-containing adjuvants. *Vaccine*, 12(5):472–474, January 1994.

[139] Rumiana Tenchov, Robert Bird, Allison E. Curtze, and Qiongqiong Zhou. Lipid NanoparticlesFrom Liposomes to mRNA Vaccine Delivery, a Landscape of Research Diversity and Advancement. *ACS Nano*, 15(11):16982–17015, November 2021. Publisher: American Chemical Society.

[140] Marco Maugeri, Muhammad Nawaz, Alexandros Papadimitriou, Annelie Angerfors, Alessandro Camponeschi, Manli Na, Mikko Hölttä, Pia Skantze, Svante Johansson, Martina Sundqvist, Johnny Lindquist, Tomas Kjellman, Inga-Lill Mårtensson, Tao Jin, Per Sunnerhagen, Sofia Östman, Lennart Lindfors, and Hadi Valadi. Linkage between endosomal escape of LNP-mRNA and loading into EVs for transport to other cells. *Nature Communications*, 10(1):4333, September 2019. Number: 1 Publisher: Nature Publishing Group.

[141] Sandeep T. Koshy, Alexander S. Cheung, Luo Gu, Amanda R. Graveline, and David J. Mooney. Liposomal Delivery Enhances Immune Activation by STING Agonists for Cancer Immunotherapy. *Advanced biosystems*, 1(1-2):1600013, February 2017.

[142] Xin Yang, Daniel Coriolan, Vanishree Murthy, Kelly Schultz, Douglas T. Golenbock, and Debbie Beasley. Proinflammatory phenotype of vascular smooth muscle cells: role of efficient Toll-like receptor 4 signaling. *American Journal of Physiology. Heart and Circulatory Physiology*, 289(3):H1069–1076, September 2005.

[143] Madhav V. Dhodapkar, Mario Sznol, Biwei Zhao, Ding Wang, Richard D. Carvajal, Mary L. Keohan, Ellen Chuang, Rachel E. Sanborn, Jose Lutzky, John Powderly, Harriet Kluger, Sheela Tejwani, Jennifer Green, Venky Ramakrishna, Andrea Crocker, Laura Vitale, Michael Yellin, Thomas Davis, and Tibor Keler. Induction of Antigen-Specific Immunity with a Vaccine Targeting NY-ESO-1 to the Dendritic Cell Receptor DEC-205. *Science Translational Medicine*, 6(232):232ra51–232ra51, April 2014. Publisher: American Association for the Advancement of Science.

[144] K. Mahnke, M. Guo, S. Lee, H. Sepulveda, S. L. Swain, M. Nussenzweig, and R. M. Steinman. The dendritic cell receptor for endocytosis, DEC-205, can recycle and enhance antigen presentation via major histocompatibility complex class II-positive lysosomal compartments. *The Journal of Cell Biology*, 151(3):673–684, October 2000.

[145] Yvette van Kooyk, Wendy W. J. Unger, Cynthia M. Fehres, Hakan Kalay, and Juan J. García-Vallejo. Glycan-based DC-SIGN targeting vaccines to enhance antigen cross-presentation. *Molecular Immunology*, 55(2):143–145, September 2013.

[146] Trevor Stack, Michael Vincent, Amir Vahabikashi, Guorong Li, Kristin M. Perkumas, W. Daniel Stamer, Mark Johnson, and Evan Scott. Targeted Delivery of Cell Softening Micelles to Schlemm's Canal Endothelial Cells for Treatment of Glaucoma. *Small*, 16(43):2004205, 2020. _eprint: https://onlinelibrary.wiley.com/doi/pdf/10.1002/smll.202004205.

[147] Beth A Tamburini, Matthew A Burchill, and Ross M Kedl. Antigen capture and archiving by lymphatic endothelial cells following vaccination or viral infection. *Nature communications*, 5:3989, June 2014.

[148] Qiong Xue, Yao Lu, Markus R. Eisele, Endah S. Sulistijo, Nafeesa Khan, Rong Fan, and Kathryn Miller-Jensen. Analysis of single-cell cytokine secretion reveals a role for paracrine signaling in coordinating macrophage responses to TLR4 stimulation. *Science Signaling*, 8(381):ra59, June 2015.

[149] Peter Deak, Bradley Studnitzer, Trevor Ung, Rachel Steinhardt, Melody Swartz, and Aaron Esser-Kahn. Isolating and targeting a highly active, stochastic dendritic cell subpopulation for improved immune responses. *Cell Reports*, 41(5):111563, November 2022.

[150] Jeffrey Alan Tomalka, Adam Nicolas Pelletier, Slim Fourati, Muhammad Bilal Latif, Ashish Sharma, Kathryn Furr, Kevin Carlson, Michelle Lifton, Ana Gonzalez, Peter Wilkinson, Genoveffa Franchini, Robert Parks, Norman Letvin, Nicole Yates, Kelly Seaton, Georgia Tomaras, Jim Tartaglia, Merlin L. Robb, Nelson L. Michael, Richard Koup, Barton Haynes, Sampa Santra, and Rafick Pierre Sekaly. The transcription factor CREB1 is a mechanistic driver of immunogenicity and reduced HIV-1 acquisition following ALVAC vaccination. *Nature Immunology*, 22(10):1294–1305, October 2021.

[151] Motohiko Kadoki, Ashwini Patil, Cornelius C. Thaiss, Donald J. Brooks, Surya Pandey, Deeksha Deep, David Alvarez, Ulrich H. von Andrian, Amy J. Wagers, Kenta Nakai, Tarjei S. Mikkelsen, Magali Soumillon, and Nicolas Chevrier. Organism-Level Analysis of Vaccination Reveals Networks of Protection across Tissues. *Cell*, 171(2):398–413.e21, October 2017.

[152] Jeffrey A. Tomalka, Mehul S. Suthar, Steven G. Deeks, and Rafick Pierre Sekaly. Fighting the SARS-CoV-2 pandemic requires a global approach to understanding the heterogeneity of vaccine responses. *Nature Immunology*, 23(3):360–370, March 2022.

[153] Adarsh Dave, Jared Mitchell, Kirthevasan Kandasamy, Han Wang, Sven Burke, Biswajit Paria, Barnabás Póczos, Jay Whitacre, and Venkatasubramanian Viswanathan. Autonomous Discovery of Battery Electrolytes with Robotic Experimentation and Machine Learning. *Cell Reports Physical Science*, 1(12):100264, December 2020.

[154] Brian Hie, Bryan D. Bryson, and Bonnie Berger. Leveraging Uncertainty in Machine Learning Accelerates Biological Discovery and Design. *Cell Systems*, 11(5):461–477.e9, November 2020.

[155] Andreas Mayr, Günter Klambauer, Thomas Unterthiner, Marvin Steijaert, Jörg K. Wegner, Hugo Ceulemans, Djork-Arné Clevert, and Sepp Hochreiter. Large-scale comparison of machine learning methods for drug target prediction on ChEMBL †Electronic supplementary information (ESI) available: Overview, Data Collection and Clustering, Methods, Results, Appendix. See DOI: 10.1039/c8sc00148k. *Chemical Science*, 9(24):5441–5451, June 2018.

[156] Matthew N. Davies, Jagadeesh Bayry, Elma Z. Tchilian, Janakiraman Vani, Melkote S. Shaila, Emily K. Forbes, Simon J. Draper, Peter C. L. Beverley, David F. Tough, and Darren R. Flower. Toward the Discovery of Vaccine Adjuvants: Coupling In Silico Screening and In Vitro Analysis of Antagonist Binding to Human and Mouse CCR4 Receptors. *PLoS ONE*, 4(11):e8084, November 2009.

[157] Jerome de Ruyck, Guillaume Brysbaert, Ralf Blossey, and Marc Lensink. Molecular docking as a popular tool in drug design, an in silico travel. *Advances and Applications in Bioinformatics and Chemistry*, Volume 9:1–11, June 2016.

[158] Kei Terayama, Masato Sumita, Ryo Tamura, and Koji Tsuda. Black-Box Optimization for Automated Discovery. *Accounts of Chemical Research*, 54(6):1334–1346, March 2021.

[159] John D Harding. Nonhuman Primates and Translational Research: Progress, Opportunities, and Challenges. *ILAR Journal*, 58(2):141–150, December 2017.

[160] Duxin Sun, Wei Gao, Hongxiang Hu, and Simon Zhou. Why 90% of clinical drug development fails and how to improve it? *Acta Pharmaceutica Sinica B*, 12(7):3049–3062, July 2022.

[161] Ramin Sedaghat Herati and E. John Wherry. What Is the Predictive Value of Animal Models for Vaccine Efficacy in Humans? *Cold Spring Harbor Perspectives in Biology*, 10(4):a031583, April 2018.

[162] Clare E. Bryant and Tom P. Monie. Mice, men and the relatives: cross-species studies underpin innate immunity. *Open Biology*, 2(4):120015, April 2012. Publisher: Royal Society.

[163] Michael Rehli. Of mice and men: species variations of Toll-like receptor expression. *Trends in Immunology*, 23(8):375–378, August 2002.

[164] Emma S. Winkler, Adam L. Bailey, Natasha M. Kafai, Sharmila Nair, Broc T. McCune, Jinsheng Yu, Julie M. Fox, Rita E. Chen, James T. Earnest, Shamus P. Keeler, Jon H. Ritter, Liang-I. Kang, Sarah Dort, Annette Robichaud, Richard Head, Michael J. Holtzman, and Michael S. Diamond. SARS-CoV-2 infection of human ACE2-transgenic

mice causes severe lung inflammation and impaired function. *Nature Immunology*, 21(11):1327–1335, November 2020. Number: 11 Publisher: Nature Publishing Group.

[165] Jorge L. Cervantes, Bennett Weinerman, Chaitali Basole, and Juan C. Salazar. TLR8: the forgotten relative revindicated. *Cellular & Molecular Immunology*, 9(6):434–438, November 2012. Number: 6 Publisher: Nature Publishing Group.

[166] Cristiana Guiducci, Mei Gong, Alma-Martina Cepika, Zhaohui Xu, Claudio Tripodo, Lynda Bennett, Chad Crain, Pierre Quartier, John J. Cush, Virginia Pascual, Robert L. Coffman, and Franck J. Barrat. RNA recognition by human TLR8 can lead to autoimmune inflammation. *Journal of Experimental Medicine*, 210(13):2903–2919, November 2013.

[167] Zhenyi Hu, Hiromi Tanji, Shuangshuang Jiang, Shuting Zhang, Kyoin Koo, Jean Chan, Kentaro Sakaniwa, Umeharu Ohto, Albert Candia, Toshiyuki Shimizu, and Hang Yin. Small-Molecule TLR8 Antagonists via Structure-Based Rational Design. *Cell Chemical Biology*, 25(10):1286–1291.e3, October 2018.

[168] Song Jiang, Xinyan Li, Nicholas J. Hess, Yue Guan, and Richard I. Tapping. TLR10 Is a Negative Regulator of Both MyD88-Dependent and -Independent TLR Signaling. *The Journal of Immunology*, 196(9):3834–3841, May 2016.

[169] Dörthe Masemann, Stephan Ludwig, and Yvonne Boergeling. Advances in Transgenic Mouse Models to Study Infections by Human Pathogenic Viruses. *International Journal of Molecular Sciences*, 21(23):9289, December 2020.

[170] Seii Ohka, Hiroko Igarashi, Noriyo Nagata, Mai Sakai, Satoshi Koike, Tomonori Nochi, Hiroshi Kiyono, and Akio Nomoto. Establishment of a poliovirus oral infection system in human poliovirus receptor-expressing transgenic mice that are deficient in alpha/beta interferon receptor. *Journal of Virology*, 81(15):7902–7912, August 2007.

[171] Miki Ida-Hosonuma, Takuya Iwasaki, Tomoki Yoshikawa, Noriyo Nagata, Yuko Sato, Tetsutaro Sata, Mitsutoshi Yoneyama, Takashi Fujita, Choji Taya, Hiromichi Yonekawa, and Satoshi Koike. The Alpha/Beta Interferon Response Controls Tissue Tropism and Pathogenicity of Poliovirus. *Journal of Virology*, 79(7):4460–4469, April 2005.

[172] Marko Zivcec, Christina F. Spiropoulou, and Jessica R. Spengler. The use of mice lacking type I or both type I and type II interferon responses in research on hemorrhagic fever viruses. Part 2: Vaccine efficacy studies. *Antiviral research*, 174:104702, February 2020.

[173] Laura Roßmann, Katrin Bagola, Tharshana Stephen, Anna-Lisa Gerards, Bianca Walber, Anja Ullrich, Stefan Schülke, Christel Kamp, Ingo Spreitzer, Milena Hasan, Brigitte David-Watine, Spencer L. Shorte, Max Bastian, and Ger van Zandbergen. Distinct single-component adjuvants steer human DC-mediated T-cell polarization via

Toll-like receptor signaling toward a potent antiviral immune response. *Proceedings of the National Academy of Sciences*, 118(39):e2103651118, September 2021.

[174] Katherine Chew, Branden Lee, Simon D. van Haren, Etsuro Nanishi, Timothy O'Meara, Jennifer B. Splaine, Maria DeLeon, Dheeraj Soni, Hyuk-Soo Seo, Sirano Dhe-Paganon, Al Ozonoff, Jennifer A. Smith, Ofer Levy, and David J. Dowling. Adjuvant Discovery via a High Throughput Screen using Human Primary Mononuclear Cells. *bioRxiv: The Preprint Server for Biology*, page 2022.06.17.496630, July 2022.

[175] Yi Fan, Joseph G. Naglich, Jennifer D. Koenitzer, Humberto Ribeiro, Jonathan Lippy, Jordan Blum, Xin Li, Christina Milburn, Bryan Barnhart, Litao Zhang, and Mark P. Fereshteh. Miniaturized High-Throughput Multiparameter Flow Cytometry Assays Measuring In Vitro Human Dendritic Cell Maturation and T-Cell Activation in Mixed Lymphocyte Reactions. *SLAS DISCOVERY: Advancing the Science of Drug Discovery*, 23(7):742–750, August 2018. Publisher: SAGE Publications Inc STM.

[176] Jihoon Kim, Bon-Kyoung Koo, and Juergen A. Knoblich. Human organoids: model systems for human biology and medicine. *Nature Reviews Molecular Cell Biology*, 21(10):571–584, October 2020. Number: 10 Publisher: Nature Publishing Group.

[177] Christopher DC Allen, Takaharu Okada, and Jason G Cyster. Germinal Center Organization and Cellular Dynamics. *Immunity*, 27(2):190–202, August 2007.

[178] Christina Lisk, Rachel Yuen, Jeff Kuniholm, Danielle Antos, Michael L. Reiser, and Lee M. Wetzler. Toll-Like Receptor Ligand Based Adjuvant, PorB, Increases Antigen Deposition on Germinal Center Follicular Dendritic Cells While Enhancing the Follicular Dendritic Cells Network. *Frontiers in Immunology*, 11, 2020.

[179] Kyung-Ho Roh, Hannah W. Song, Pallab Pradhan, Kevin Bai, Caitlin D. Bohannon, Gordon Dale, Jardin Leleux, Joshy Jacob, and Krishnendu Roy. A synthetic stroma-free germinal center niche for efficient generation of humoral immunity ex vivo. *Biomaterials*, 164:106–120, May 2018.

[180] Lisa E. Wagar, Ameen Salahudeen, Christian M. Constantz, Ben S. Wendel, Michael M. Lyons, Vamsee Mallajosyula, Lauren P. Jatt, Julia Z. Adamska, Lisa K. Blum, Neha Gupta, Katherine J. L. Jackson, Fan Yang, Katharina Röltgen, Krishna M. Roskin, Kelly M. Blaine, Kara D. Meister, Iram N. Ahmad, Mario Cortese, Emery G. Dora, Sean N. Tucker, Anne I. Sperling, Aarti Jain, D. Huw Davies, Philip L. Felgner, Gregory B. Hammer, Peter S. Kim, William H. Robinson, Scott D. Boyd, Calvin J. Kuo, and Mark M. Davis. Modeling human adaptive immune responses with tonsil organoids. *Nature Medicine*, 27(1):125–135, January 2021.

[181] Alberto Purwada, Manish K. Jaiswal, Haelee Ahn, Takuya Nojima, Daisuke Kitamura, Akhilesh K. Gaharwar, Leandro Cerchietti, and Ankur Singh. Ex vivo engineered immune organoids for controlled germinal center reactions. *Biomaterials*, 63:24–34, September 2015.

[182] B. A. Moser, R. C. Steinhardt, Y. Escalante-Buendia, D. A. Boltz, K. M. Barker, B. J. Cassaidy, M. G. Rosenberger, S. Yoo, B. G. McGonnigal, and A. P. Esser-Kahn. Increased vaccine tolerability and protection via NF-B modulation. *Science Advances*, 6(37):eaaz8700, September 2020. Publisher: American Association for the Advancement of Science Section: Research Article.

[183] Brittany A. Moser, Yoseline Escalante-Buendia, Rachel C. Steinhardt, Matthew G. Rosenberger, Britteny J. Cassaidy, Nihesh Naorem, Alfred C. Chon, Minh H. Nguyen, Ngoctran T. Tran, and Aaron P. Esser-Kahn. Small Molecule NF-B Inhibitors as Immune Potentiators for Enhancement of Vaccine Adjuvants. *Frontiers in Immunology*, 11, 2020. Publisher: Frontiers.

[184] Y. Z. Lin, S. Y. Yao, R. A. Veach, T. R. Torgerson, and J. Hawiger. Inhibition of nuclear translocation of transcription factor NF-kappa B by a synthetic peptide containing a cell membrane-permeable motif and nuclear localization sequence. *The Journal of Biological Chemistry*, 270(24):14255–14258, June 1995.

[185] Jozef Zienkiewicz, Amy Armitage, and Jacek Hawiger. Targeting nuclear import shuttles, importins/karyopherins alpha by a peptide mimicking the NFB1/p50 nuclear localization sequence. *Journal of the American Heart Association*, 2(5):e000386, September 2013.

[186] WHO Coronavirus (COVID-19) Dashboard.

[187] Timothy B. Baker, Daniel M. Bolt, Stevens S. Smith, Thomas M. Piasecki, Karen L. Conner, Steven L. Bernstein, Todd Hayes-Birchler, Wendy E. Theobald, and Michael C. Fiore. The Relationship of COVID-19 Vaccination with Mortality Among 86,732 Hospitalized Patients: Subpopulations, Patient Factors, and Changes over Time. *Journal of General Internal Medicine*, 38(5):1248–1255, April 2023.

[188] Sophia T. Tan, Ada T. Kwan, Isabel Rodríguez-Barraquer, Benjamin J. Singer, Hailey J. Park, Joseph A. Lewnard, David Sears, and Nathan C. Lo. Infectiousness of SARS-CoV-2 breakthrough infections and reinfections during the Omicron wave. *Nature Medicine*, 29(2):358–365, February 2023. Number: 2 Publisher: Nature Publishing Group.

[189] Hannah E. Davis, Lisa McCorkell, Julia Moore Vogel, and Eric J. Topol. Long COVID: major findings, mechanisms and recommendations. *Nature Reviews Microbiology*, 21(3):133–146, March 2023. Number: 3 Publisher: Nature Publishing Group.

[190] Ziyad Al-Aly, Benjamin Bowe, and Yan Xie. Long COVID after breakthrough SARS-CoV-2 infection. *Nature Medicine*, 28(7):1461–1467, July 2022. Number: 7 Publisher: Nature Publishing Group.

[191] Daniel Ayoubkhani, Matthew L. Bosworth, Sasha King, Koen B. Pouwels, Myer Glickman, Vahé Nafilyan, Francesco Zaccardi, Kamlesh Khunti, Nisreen A. Alwan, and

A. Sarah Walker. Risk of Long COVID in People Infected With Severe Acute Respiratory Syndrome Coronavirus 2 After 2 Doses of a Coronavirus Disease 2019 Vaccine: Community-Based, Matched Cohort Study. *Open Forum Infectious Diseases*, 9(9):ofac464, September 2022.

[192] Alessio Facciolà, Giuseppa Visalli, Antonio Laganà, and Angela Di Pietro. An Overview of Vaccine Adjuvants: Current Evidence and Future Perspectives. *Vaccines*, 10(5):819, May 2022.

[193] Jeremiah Y. Kim, Matthew G. Rosenberger, Nakisha S. Rutledge, and Aaron P. Esser-Kahn. Next-Generation Adjuvants: Applying Engineering Methods to Create and Evaluate Novel Immunological Responses. *Pharmaceutics*, 15(6):1687, June 2023. Number: 6 Publisher: Multidisciplinary Digital Publishing Institute.

[194] COVID-19 vaccine tracker and landscape.

[195] James A. Triccas, Joeri Kint, and Florian M. Wurm. Affordable SARS-CoV-2 protein vaccines for the pandemic endgame. *npj Vaccines*, 7(1):1–2, August 2022. Number: 1 Publisher: Nature Publishing Group.

[196] Volker Vetter, Gülhan Denizer, Leonard R. Friedland, Jyothsna Krishnan, and Marla Shapiro. Understanding modern-day vaccines: what you need to know. *Annals of Medicine*, 50(2):110–120, February 2018. Publisher: Taylor & Francis _eprint: https://doi.org/10.1080/07853890.2017.1407035.

[197] John D. Campbell. Development of the CpG Adjuvant 1018: A Case Study. In Christopher B. Fox, editor, *Vaccine Adjuvants: Methods and Protocols*, Methods in Molecular Biology, pages 15–27. Springer, New York, NY, 2017.

[198] Julio Torales, Osmar Cuenca-Torres, Laurentino Barrios, Luis Armoa-Garcia, Gladys Estigarribia, Gabriela Sanabria, Meei-Yun Lin, Josue Antonio Estrada, Lila Estephan, Hao-Yuan Cheng, Charles Chen, Robert Janssen, and Chia-En Lien. An evaluation of the safety and immunogenicity of MVC-COV1901: Results of an interim analysis of a phase III, parallel group, randomized, double-blind, active-controlled immunobridging study in Paraguay. *Vaccine*, 41(1):109–118, January 2023.

[199] Lulu Bravo, Igor Smolenov, Htay Htay Han, Ping Li, Romana Hosain, Frank Rockhold, Sue Ann Costa Clemens, Camilo Roa, Charissa Borja-Tabora, Antoinette Quinsaat, Pio Lopez, Eduardo López-Medina, Leonardo Brochado, Eder A. Hernández, Humberto Reynales, Tatiana Medina, Hector Velasquez, Leonardo Bautista Toloza, Edith Johana Rodriguez, Dora Ines Molina de Salazar, Camilo A. Rodríguez, Eduardo Sprinz, José Cerbino-Neto, Kleber Giovanni Luz, Alexandre Vargas Schwarzbold, Maria Sanali Paiva, Josefina Carlos, May Emmeline B. Montellano, Mari Rose A. de Los Reyes, Charles Y. Yu, Edison R. Alberto, Mario M. Panaligan, Milagros Salvani-Bautista, Erik Buntinx, Maya Hites, Jean-Benoit Martinot, Qasim E. Bhorat, Aysha Badat, Carmen Baccarini, Branda Hu, Jaco Jurgens, Jan Engelbrecht,

Donna Ambrosino, Peter Richmond, George Siber, Joshua Liang, and Ralf Clemens. Efficacy of the adjuvanted subunit protein COVID-19 vaccine, SCB-2019: a phase 2 and 3 multicentre, double-blind, randomised, placebo-controlled trial. *The Lancet*, 399(10323):461–472, January 2022. Publisher: Elsevier.

[200] Rajeka Lazarus, Benedicte Querton, Irena Corbic Ramljak, Shailesh Dewasthaly, Juan Carlos Jaramillo, Katrin Dubischar, Michael Krammer, Petronela Weisova, Romana Hochreiter, Susanne Eder-Lingelbach, Christian Taucher, Adam Finn, Claire Bethune, Marta Boffito, Marcin Bula, Fiona M. Burns, Rebecca Clark, Dileep Dasyam, Simon Drysdale, Saul Faust, Effrossyni Gkrania-Klotsas, Christopher Green, Hana Hassanin, Paul Heath, Amardeep Heer, Toby Helliwell, Anil Hormis, Philip Kalra, Rajeka Lazarus, Ed Moran, John Ndikum, Iain Page, David Price, Nick Probert, Mahadev Ramjee, Tommy Rampling, Harpal S. Randeva, Stephen Ryder, John Steer, Emma Thompson, and David Torku. Immunogenicity and safety of an inactivated whole-virus COVID-19 vaccine (VLA2001) compared with the adenoviral vector vaccine ChAdOx1-S in adults in the UK (COV-COMPARE): interim analysis of a randomised, controlled, phase 3, immunobridging trial. *The Lancet Infectious Diseases*, 22(12):1716–1727, December 2022. Publisher: Elsevier.

[201] Subhash Thuluva, Vikram Paradkar, SubbaReddy Gunneri, Vijay Yerroju, Rammohan Reddy Mogulla, Pothakamuri Venkata Suneetha, Kishore Turaga, Mahesh Kyasani, Senthil Kumar Manoharan, Srikanth Adabala, Aditya Sri Javvadi, Guruprasad Medigeshi, Janmejay Singh, Heena Shaman, Akshay Binayke, Aymaan Zaheer, Amit Awasthi, Manish Narang, Pradeep Nanjappa, Niranjana Mahantshetti, Bishan Swarup Garg, and Anil Kumar Pandey. Safety, tolerability and immunogenicity of Biological E's CORBEVAX™ vaccine in children and adolescents: A prospective, randomised, double-blind, placebo controlled, phase-2/3 study. *Vaccine*, 40(49):7130–7140, November 2022.

[202] Tsun-Yung Kuo, Meei-Yun Lin, Robert L. Coffman, John D. Campbell, Paula Traquina, Yi-Jiun Lin, Luke Tzu-Chi Liu, Jinyi Cheng, Yu-Chi Wu, Chung-Chin Wu, Wei-Hsuan Tang, Chung-Guei Huang, Kuo-Chien Tsao, and Charles Chen. Development of CpG-adjuvanted stable prefusion SARS-CoV-2 spike antigen as a subunit vaccine against COVID-19. *Scientific Reports*, 10(1):20085, November 2020. Number: 1 Publisher: Nature Publishing Group.

[203] Chia-En Lien, Yi-Jiun Lin, Charles Chen, Wei-Cheng Lian, Tsun-Yung Kuo, John D. Campbell, Paula Traquina, Meei-Yun Lin, Luke Tzu-Chi Liu, Ya-Shan Chuang, Hui-Ying Ko, Chun-Che Liao, Yen-Hui Chen, Jia-Tsrong Jan, Hsiu-Hua Ma, Cheng-Pu Sun, Yin-Shiou Lin, Ping-Yi Wu, Yu-Chiuan Wang, Mi-Hua Tao, and Yi-Ling Lin. CpG-adjuvanted stable prefusion SARS-CoV-2 spike protein protected hamsters from SARS-CoV-2 challenge. *Scientific Reports*, 11(1):8761, April 2021. Number: 1 Publisher: Nature Publishing Group.

[204] Purnima Bhat, Graham Leggatt, Nigel Waterhouse, and Ian H. Frazer. Interferon-derived from cytotoxic lymphocytes directly enhances their motility and cytotoxicity.

Cell Death & Disease, 8(6):e2836–e2836, June 2017. Number: 6 Publisher: Nature Publishing Group.

[205] Xiaolei Wang, Terrence Tsz-Tai Yuen, Ying Dou, Jingchu Hu, Renhao Li, Zheng Zeng, Xuansheng Lin, Huarui Gong, Celia Hoi-Ching Chan, Chaemin Yoon, Huiping Shuai, Deborah Tip-Yin Ho, Ivan Fan-Ngai Hung, Bao-Zhong Zhang, Hin Chu, and Jian-Dong Huang. Vaccine-induced protection against SARS-CoV-2 requires IFN--driven cellular immune response. *Nature Communications*, 14(1):3440, June 2023. Number: 1 Publisher: Nature Publishing Group.

[206] David S. Khoury, Deborah Cromer, Arnold Reynaldi, Timothy E. Schlub, Adam K. Wheatley, Jennifer A. Juno, Kanta Subbarao, Stephen J. Kent, James A. Triccas, and Miles P. Davenport. Neutralizing antibody levels are highly predictive of immune protection from symptomatic SARS-CoV-2 infection. *Nature Medicine*, 27(7):1205–1211, July 2021. Number: 7 Publisher: Nature Publishing Group.

[207] César Muñoz-Fontela, William E. Dowling, Simon G. P. Funnell, Pierre-S. Gsell, A. Ximena Riveros-Balta, Randy A. Albrecht, Hanne Andersen, Ralph S. Baric, Miles W. Carroll, Marco Cavaleri, Chuan Qin, Ian Crozier, Kai Dallmeier, Leon de Waal, Emmie de Wit, Leen Delang, Erik Dohm, W. Paul Duprex, Darryl Falzarano, Courtney L. Finch, Matthew B. Frieman, Barney S. Graham, Lisa E. Gralinski, Kate Guilfoyle, Bart L. Haagmans, Geraldine A. Hamilton, Amy L. Hartman, Sander Herfst, Suzanne J. F. Kaptein, William B. Klimstra, Ivana Knezevic, Philip R. Krause, Jens H. Kuhn, Roger Le Grand, Mark G. Lewis, Wen-Chun Liu, Pauline Maisonnasse, Anita K. McElroy, Vincent Munster, Nadia Oreshkova, Angela L. Rasmussen, Joana Rocha-Pereira, Barry Rockx, Estefanía Rodríguez, Thomas F. Rogers, Francisco J. Salguero, Michael Schotsaert, Koert J. Stittelaar, Hendrik Jan Thibaut, Chien-Te Tseng, Júlia Vergara-Alert, Martin Beer, Trevor Brasel, Jasper F. W. Chan, Adolfo García-Sastre, Johan Neyts, Stanley Perlman, Douglas S. Reed, Juergen A. Richt, Chad J. Roy, Joaquim Segalés, Seshadri S. Vasan, Ana María Henao-Restrepo, and Dan H. Barouch. Animal models for COVID-19. *Nature*, 586(7830):509–515, October 2020. Number: 7830 Publisher: Nature Publishing Group.

[208] Sin Fun Sia, Li-Meng Yan, Alex W. H. Chin, Kevin Fung, Ka-Tim Choy, Alvina Y. L. Wong, Prathanporn Kaewpreedee, Ranawaka A. P. M. Perera, Leo L. M. Poon, John M. Nicholls, Malik Peiris, and Hui-Ling Yen. Pathogenesis and transmission of SARS-CoV-2 in golden hamsters. *Nature*, 583(7818):834–838, July 2020. Number: 7818 Publisher: Nature Publishing Group.

[209] Masaki Imai, Kiyoko Iwatsuki-Horimoto, Masato Hatta, Samantha Loeber, Peter J. Halfmann, Noriko Nakajima, Tokiko Watanabe, Michiko Ujie, Kenta Takahashi, Mutsumi Ito, Shinya Yamada, Shufang Fan, Shiho Chiba, Makoto Kuroda, Lizheng Guan, Kosuke Takada, Tammy Armbrust, Aaron Balogh, Yuri Furusawa, Moe Okuda, Hiroshi Ueki, Atsuhiro Yasuhara, Yuko Sakai-Tagawa, Tiago J. S. Lopes, Maki Kiso, Seiya Yamayoshi, Noriko Kinoshita, Norio Ohmagari, Shin-ichiro Hattori, Makoto Takeda,

Hiroaki Mitsuya, Florian Krammer, Tadaki Suzuki, and Yoshihiro Kawaoka. Syrian hamsters as a small animal model for SARS-CoV-2 infection and countermeasure development. *Proceedings of the National Academy of Sciences*, 117(28):16587–16595, July 2020. Publisher: Proceedings of the National Academy of Sciences.

[210] Masoomeh Sofian, Behzad Khansarinejad, Ehsanollah Ghaznavi-Rad, Farzaneh Shokoohi, Hossein Mazaherpour, Farzane Farmani, Mona Sadat Larijani, Leila Pakpour, and Amitis Ramezani. SARS-CoV-2 Viral Shedding and Associated Factors among COVID-19 Inpatients and Outpatients. *Interdisciplinary Perspectives on Infectious Diseases*, 2022:1411106, June 2022.

[211] Jiwon Jung, Ji Yeun Kim, Heedo Park, Sunghee Park, Joon Seo Lim, So Yun Lim, Seongman Bae, Young-Ju Lim, Eun Ok Kim, Jineui Kim, Man-Seong Park, and Sung-Han Kim. Transmission and Infectious SARS-CoV-2 Shedding Kinetics in Vaccinated and Unvaccinated Individuals. *JAMA Network Open*, 5(5):e2213606, May 2022.

[212] Luca Carsana, Aurelio Sonzogni, Ahmed Nasr, Roberta Simona Rossi, Alessandro Pellegrinelli, Pietro Zerbi, Roberto Rech, Riccardo Colombo, Spinello Antinori, Mario Corbellino, Massimo Galli, Emanuele Catena, Antonella Tosoni, Andrea Gianatti, and Manuela Nebuloni. Pulmonary post-mortem findings in a series of COVID-19 cases from northern Italy: a two-centre descriptive study. *The Lancet Infectious Diseases*, 20(10):1135–1140, October 2020. Publisher: Elsevier.

[213] Claudio Doglioni, Claudia Ravaglia, Marco Chilosi, Giulio Rossi, Alessandra Dubini, Federica Pedica, Sara Piciucchi, Antonio Vizzuso, Franco Stella, Stefano Maitan, Vanni Agnoletti, Silvia Puglisi, Giovanni Poletti, Vittorio Sambri, Giovanni Pizzolo, Vincenzo Bronte, Athol U. Wells, and Venerino Poletti. Covid-19 Interstitial Pneumonia: Histological and Immunohistochemical Features on Cryobiopsies. *Respiration*, pages 1–11, March 2021.

[214] Christiaan J. M. Vrints, Konstantin A. Krychtiuk, Emeline M. Van Craenenbroeck, Vincent F. Segers, Susanna Price, and Hein Heidbuchel. Endothelialitis plays a central role in the pathophysiology of severe COVID-19 and its cardiovascular complications. *Acta Cardiologica*, pages 1–16.

[215] Yvonne Perrie, Afzal R. Mohammed, Daniel J. Kirby, Sarah E. McNeil, and Vincent W. Bramwell. Vaccine adjuvant systems: enhancing the efficacy of sub-unit protein antigens. *International Journal of Pharmaceutics*, 364(2):272–280, December 2008.

[216] Derek T. O'Hagan and Ennio De Gregorio. The path to a successful vaccine adjuvant–'the long and winding road'. *Drug Discovery Today*, 14(11-12):541–551, June 2009.

[217] Ali M Harandi, Gwyn Davies, and Ole F Olesen. Vaccine adjuvants: scientific challenges and strategic initiatives. *Expert Review of Vaccines*, 8(3):293–298, March 2009. Publisher: Taylor & Francis _eprint: https://doi.org/10.1586/14760584.8.3.293.

[218] David H. Munn and Vincenzo Bronte. Immune suppressive mechanisms in the tumor microenvironment. *Current opinion in immunology*, 39:1–6, April 2016.

[219] Ekaterini Platanitis and Thomas Decker. Regulatory Networks Involving STATs, IRFs, and NFB in Inflammation. *Frontiers in Immunology*, 9, 2018.

[220] Colleen Olive. Pattern recognition receptors: sentinels in innate immunity and targets of new vaccine adjuvants. *Expert Review of Vaccines*, 11(2):237–256, February 2012. Publisher: Taylor & Francis _eprint: https://doi.org/10.1586/erv.11.189.

[221] Taro Kawai and Shizuo Akira. The role of pattern-recognition receptors in innate immunity: update on Toll-like receptors. *Nature Immunology*, 11(5):373–384, May 2010. Number: 5 Publisher: Nature Publishing Group.

[222] Bastian Hoesel and Johannes A. Schmid. The complexity of NF-B signaling in inflammation and cancer. *Molecular Cancer*, 12(1):86, August 2013.

[223] Alex C. D. Salyer, Giuseppe Caruso, Karishma K. Khetani, Lauren M. Fox, Subbalakshmi S. Malladi, and Sunil A. David. Identification of Adjuvantic Activity of Amphotericin B in a Novel, Multiplexed, Poly-TLR/NLR High-Throughput Screen. *PLOS ONE*, 11(2):e0149848, February 2016. Publisher: Public Library of Science.

[224] Yue Guan, Katherine Omueti-Ayoade, Sarita K. Mutha, Paul J. Hergenrother, and Richard I. Tapping. Identification of Novel Synthetic Toll-like Receptor 2 Agonists by High Throughput Screening *. *Journal of Biological Chemistry*, 285(31):23755–23762, July 2010. Publisher: Elsevier.

[225] Luis Martínez-Gil, Juan Ayllon, Mila Brum Ortigoza, Adolfo García-Sastre, Megan L. Shaw, and Peter Palese. Identification of Small Molecules with Type I Interferon Inducing Properties by High-Throughput Screening. *PLOS ONE*, 7(11):e49049, November 2012. Publisher: Public Library of Science.

[226] Yasuo Tanaka and Zhijian J. Chen. STING specifies IRF3 phosphorylation by TBK1 in the cytosolic DNA signaling pathway. *Science Signaling*, 5(214):ra20, March 2012.

[227] Nasiha S. Ahmed, Jovylyn Gatchalian, Josephine Ho, Mannix J. Burns, Nasun Hah, Zong Wei, Michael Downes, Ronald M. Evans, and Diana C. Hargreaves. BRD9 regulates interferon-stimulated genes during macrophage activation via cooperation with BET protein BRD4. *Proceedings of the National Academy of Sciences of the United States of America*, 119(1):e2110812119, January 2022.

[228] Clinton B Maddox, Lynn Rasmussen, and E. Lucile White. Adapting Cell-Based Assays to the High Throughput Screening Platform: Problems Encountered and Lessons Learned. *JALA (Charlottesville, Va.)*, 13(3):168–173, June 2008.

[229] W. Frank An and Nicola Tolliday. Cell-Based Assays for High-Throughput Screening. *Molecular Biotechnology*, 45(2):180–186, June 2010.

[230] Dara L. Burdette, Kathryn M. Monroe, Katia Sotelo-Troha, Jeff S. Iwig, Barbara Eckert, Mamoru Hyodo, Yoshihiro Hayakawa, and Russell E. Vance. STING is a direct innate immune sensor of cyclic di-GMP. *Nature*, 478(7370):515–518, October 2011. Number: 7370 Publisher: Nature Publishing Group.

[231] Jake Lever, Martin Krzywinski, and Naomi Altman. Principal component analysis. *Nature Methods*, 14(7):641–642, July 2017. Number: 7 Publisher: Nature Publishing Group.

[232] Geeta Ramesh, Andrew G. MacLean, and Mario T. Philipp. Cytokines and chemokines at the crossroads of neuroinflammation, neurodegeneration, and neuropathic pain. *Mediators of Inflammation*, 2013:480739, 2013.

[233] Whitney L. Simon, Hannah M. Salk, Inna G. Ovsyannikova, Richard B. Kennedy, and Gregory A. Poland. Cytokine production associated with smallpox vaccine responses. *Immunotherapy*, 6(10):1097–1112, 2014.

[234] Martina Bielefeld-Sevigny. AlphaLISA Immunoassay Platform— The "No-Wash" High-Throughput Alternative to ELISA. *ASSAY and Drug Development Technologies*, 7(1):90–92, February 2009.

[235] Xiaohu Tang, Kathleen I. Seyb, Mickey Huang, Eli R. Schuman, Ping Shi, Haining Zhu, and Marcie A. Glicksman. A high-throughput screening method for small-molecule inhibitors of the aberrant mutant SOD1 and dynein complex interaction. *Journal of Biomolecular Screening*, 17(3):314–326, March 2012.

[236] Lakshmi Prabhu, Lan Chen, Han Wei, Özlem Demir, Ahmad Safa, Lifan Zeng, Rommie E. Amaro, Bert H. O'Neil, Zhon-Yin Zhang, and Tao Lu. Development of an AlphaLISA high throughput technique to screen for small molecule inhibitors targeting protein arginine methyltransferases. *Molecular bioSystems*, 13(12):2509–2520, November 2017.

[237] Wasaporn Chanput, Jurriaan J. Mes, and Harry J. Wichers. THP-1 cell line: An in vitro cell model for immune modulation approach. *International Immunopharmacology*, 23(1):37–45, November 2014.

[238] Charles A. Dinarello. Cytokines as Endogenous Pyrogens. *The Journal of Infectious Diseases*, 179(Supplement_2):S294–S304, March 1999.

[239] Ke Ren and Richard Torres. Role of interleukin-1 during pain and inflammation. *Brain research reviews*, 60(1):57–64, April 2009.

[240] T Fujita, L F Reis, N Watanabe, Y Kimura, T Taniguchi, and J Vilcek. Induction of the transcription factor IRF-1 and interferon-beta mRNAs by cytokines and activators of second-messenger pathways. *Proceedings of the National Academy of Sciences of the United States of America*, 86(24):9936–9940, December 1989.

[241] X. Ma, J. M. Chow, G. Gri, G. Carra, F. Gerosa, S. F. Wolf, R. Dzialo, and G. Trinchieri. The interleukin 12 p40 gene promoter is primed by interferon gamma in monocytic cells. *The Journal of Experimental Medicine*, 183(1):147–157, January 1996.

[242] D. D. Taub, A. R. Lloyd, K. Conlon, J. M. Wang, J. R. Ortaldo, A. Harada, K. Matsushima, D. J. Kelvin, and J. J. Oppenheim. Recombinant human interferon-inducible protein 10 is a chemoattractant for human monocytes and T lymphocytes and promotes T cell adhesion to endothelial cells. *The Journal of Experimental Medicine*, 177(6):1809–1814, June 1993.

[243] Sardar Sindhu, Shihab Kochumon, Steve Shenouda, Ajit Wilson, Fahd Al-Mulla, and Rasheed Ahmad. The Cooperative Induction of CCL4 in Human Monocytic Cells by TNF- and Palmitate Requires MyD88 and Involves MAPK/NF-B Signaling Pathways. *International Journal of Molecular Sciences*, 20(18):4658, September 2019.

[244] Cristina Bergamaschi, Evangelos Terpos, Margherita Rosati, Matthew Angel, Jenifer Bear, Dimitris Stellas, Sevasti Karaliota, Filia Apostolakou, Tina Bagratuni, Dimitris Patseas, Sentiljana Gumeni, Ioannis P. Trougakos, Meletios A. Dimopoulos, Barbara K. Felber, and George N. Pavlakis. Systemic IL-15, IFN-, and IP-10/CXCL10 signature associated with effective immune response to SARS-CoV-2 in BNT162b2 mRNA vaccine recipients. *Cell Reports*, 36(6):109504, August 2021.

[245] Nathalie Malo, James A. Hanley, Sonia Cerquozzi, Jerry Pelletier, and Robert Nadon. Statistical practice in high-throughput screening data analysis. *Nature Biotechnology*, 24(2):167–175, February 2006. Number: 2 Publisher: Nature Publishing Group.

[246] Chatchakorn Eurtivong and Jóhannes Reynisson. The Development of a Weighted Index to Optimise Compound Libraries for High Throughput Screening. *Molecular Informatics*, 38(3):1800068, 2019. _eprint: https://onlinelibrary.wiley.com/doi/pdf/10.1002/minf.201800068.

[247] Steven F. Josephs, Thomas E. Ichim, Stephen M. Prince, Santosh Kesari, Francesco M. Marincola, Anton Rolando Escobedo, and Amir Jafri. Unleashing endogenous TNF-alpha as a cancer immunotherapeutic. *Journal of Translational Medicine*, 16(1):242, August 2018.

[248] Teena Mohan, Wandi Zhu, Ye Wang, and Bao-Zhong Wang. Applications of chemokines as adjuvants for vaccine immunotherapy. *Immunobiology*, 223(6-7):477–485, 2018.

[249] Megan A. Forrester, Heather J. Wassall, Lindsay S. Hall, Huan Cao, Heather M. Wilson, Robert N. Barker, and Mark A. Vickers. Similarities and differences in surface receptor expression by THP-1 monocytes and differentiated macrophages polarized using seven different conditioning regimens. *Cellular Immunology*, 332:58–76, October 2018.

[250] Peter O. Krutzik, Matthew R. Clutter, Angelica Trejo, and Garry P. Nolan. Fluorescent Cell Barcoding for Multiplex Flow Cytometry. *Current protocols in cytometry / editorial board, J. Paul Robinson, managing editor ... [et al.]*, CHAPTER:Unit–6.31, January 2011.

[251] David J. Dowling. Recent Advances in the Discovery and Delivery of TLR7/8 Agonists as Vaccine Adjuvants. *ImmunoHorizons*, 2(6):185–197, July 2018.

[252] Baofeng Cui, Xinsheng Liu, Yuzhen Fang, Peng Zhou, Yongguang Zhang, and Yonglu Wang. Flagellin as a vaccine adjuvant. *Expert Review of Vaccines*, 17(4):335–349, April 2018.

[253] Christian Bode, Gan Zhao, Folkert Steinhagen, Takeshi Kinjo, and Dennis M Klinman. CpG DNA as a vaccine adjuvant. *Expert review of vaccines*, 10(4):499–511, April 2011.

[254] Ben F. Brian and Tanya S. Freedman. The Src-family Kinase Lyn in Immunoreceptor Signaling. *Endocrinology*, 162(10):bqab152, October 2021.

[255] S. Dallari, M. Macal, M. E. Loureiro, Y. Jo, L. Swanson, C. Hesser, P. Ghosh, and E. I. Zuniga. Src family kinases Fyn and Lyn are constitutively activated and mediate plasmacytoid dendritic cell responses. *Nature Communications*, 8:14830, April 2017.

[256] Ken Yamada, Hyi-Man Park, Dean F. Rigel, Keith DiPetrillo, Erin J. Whalen, Anthony Anisowicz, Michael Beil, James Berstler, Cara Emily Brocklehurst, Debra A. Burdick, Shari L. Caplan, Michael P. Capparelli, Guanjing Chen, Wei Chen, Bethany Dale, Lin Deng, Fumin Fu, Norio Hamamatsu, Kouki Harasaki, Tracey Herr, Peter Hoffmann, Qi-Ying Hu, Waan-Jeng Huang, Neeraja Idamakanti, Hidetomo Imase, Yuki Iwaki, Monish Jain, Jey Jeyaseelan, Mitsunori Kato, Virendar K. Kaushik, Darcy Kohls, Vidya Kunjathoor, Daniel LaSala, Jongchan Lee, Jing Liu, Yang Luo, Fupeng Ma, Ruowei Mo, Sarah Mowbray, Muneto Mogi, Flavio Ossola, Pramod Pandey, Sejal J. Patel, Swetha Raghavan, Bahaa Salem, Yuka H. Shanado, Gary M. Trakshel, Gordon Turner, Hiromichi Wakai, Chunhua Wang, Stephen Weldon, Jennifer B. Wielicki, Xiaoling Xie, Lingfei Xu, Yukiko I. Yagi, Kayo Yasoshima, Jianning Yin, David Yowe, Ji-Hu Zhang, Gang Zheng, and Lauren Monovich. Small-molecule WNK inhibition regulates cardiovascular and renal function. *Nature Chemical Biology*, 12(11):896–898, November 2016.

[257] Sachith Gallolu Kankanamalage, Aroon S. Karra, and Melanie H. Cobb. WNK pathways in cancer signaling networks. *Cell Communication and Signaling : CCS*, 16:72, November 2018.

[258] Yifeng Tang, Jeremiah Y. Kim, Carman K. M. Ip, Azadeh Bahmani, Qing Chen, Matthew G. Rosenberger, Aaron P. Esser-Kahn, and Andrew L. Ferguson. Data-driven discovery of innate immunomodulators via machine learning-guided high throughput screening. *Chemical Science*, 14(44):12747–12766, November 2023. Publisher: The Royal Society of Chemistry.

[259] Erik Van Dis, Kimberly M. Sogi, Chris S. Rae, Kelsey E. Sivick, Natalie H. Surh, Meredith L. Leong, David B. Kanne, Ken Metchette, Justin J. Leong, Jacob R. Bruml, Vivian Chen, Kartoosh Heydari, Nathalie Cadieux, Tom Evans, Sarah M. McWhirter, Thomas W. Dubensky, Daniel A. Portnoy, and Sarah A. Stanley. STING-Activating Adjuvants Elicit a Th17 Immune Response and Protect against Mycobacterium tuberculosis Infection. *Cell Reports*, 23(5):1435–1447, May 2018.

[260] Etsuro Nanishi, Asimenia Angelidou, Chloe Rotman, David J Dowling, Ofer Levy, and Al Ozonoff. Precision Vaccine Adjuvants for Older Adults: A Scoping Review. *Clinical Infectious Diseases: An Official Publication of the Infectious Diseases Society of America*, 75(Suppl 1):S72–S80, April 2022.

[261] Annalisa Ciabattini, Christine Nardini, Francesco Santoro, Paolo Garagnani, Claudio Franceschi, and Donata Medaglini. Vaccination in the elderly: The challenge of immune changes with aging. *Seminars in Immunology*, 40:83–94, December 2018.

[262] Luigi Ferrucci and Elisa Fabbri. Inflammageing: chronic inflammation in ageing, cardiovascular disease, and frailty. *Nature reviews. Cardiology*, 15(9):505–522, September 2018.

[263] Jeremiah Y. Kim, Matthew G. Rosenberger, Siquan Chen, Carman KM IP, Azadeh Bahmani, Qing Chen, Jinjing Shen, Yifeng Tang, Andrew Wang, Emma Kenna, Minjun Son, Savaş Tay, Andrew L. Ferguson, and Aaron P. Esser-Kahn. Discovery of New States of Immunomodulation for Vaccine Adjuvants via High Throughput Screening: Expanding Innate Responses to PRRs. *ACS Central Science*, February 2023. Publisher: American Chemical Society.

[264] John Paget, Peter Spreeuwenberg, Vivek Charu, Robert J. Taylor, A. Danielle Iuliano, Joseph Bresee, Lone Simonsen, Cecile Viboud, and Global Seasonal Influenza-associated Mortality Collaborator Network and GLaMOR Collaborating Teams*. Global mortality associated with seasonal influenza epidemics: New burden estimates and predictors from the GLaMOR Project. *Journal of Global Health*, 9(2):020421, December 2019.

[265] Saloni Dattani, Fiona Spooner, and Max Roser. How many people die from the flu? *Our World in Data*, November 2023.

[266] Lone Simonsen, Peter Spreeuwenberg, Roger Lustig, Robert J. Taylor, Douglas M. Fleming, Madelon Kroneman, Maria D. Van Kerkhove, Anthony W. Mounts, and W. John Paget. Global Mortality Estimates for the 2009 Influenza Pandemic from the GLaMOR Project: A Modeling Study. *PLoS Medicine*, 10(11):e1001558, November 2013.

[267] FastStats, November 2023.

[268] Andrea Callegaro, Wivine Burny, Caroline Hervé, Joon Hyung Kim, Myron J Levin, Toufik Zahaf, Anthony L Cunningham, and Arnaud M Didierlaurent. Association

Between Immunogenicity and Reactogenicity: A Post Hoc Analysis of 2 Phase 3 Studies With the Adjuvanted Recombinant Zoster Vaccine. *The Journal of Infectious Diseases*, 226(11):1943–1948, October 2021.

[269] Caroline Hervé, Béatrice Laupèze, Giuseppe Del Giudice, Arnaud M. Didierlaurent, and Fernanda Tavares Da Silva. The how's and what's of vaccine reactogenicity. *npj Vaccines*, 4(1):1–11, September 2019. Number: 1 Publisher: Nature Publishing Group.

[270] Lukas Kaufmann, Mohammedyaseen Syedbasha, Dominik Vogt, Yvonne Hollenstein, Julia Hartmann, Janina E. Linnik, and Adrian Egli. An Optimized Hemagglutination Inhibition (HI) Assay to Quantify Influenza-specific Antibody Titers. *Journal of Visualized Experiments : JoVE*, (130):55833, December 2017.

[271] Nicole M. Bouvier and Anice C. Lowen. Animal Models for Influenza Virus Pathogenesis and Transmission. *Viruses*, 2(8):1530–1563, 2010.

[272] Simone Nüssing, Sneha Sant, Marios Koutsakos, Kanta Subbarao, Thi H. O. Nguyen, and Katherine Kedzierska. Innate and adaptive T cells in influenza disease. *Frontiers of Medicine*, 12(1):34–47, February 2018.

[273] Shannon M. Miller, Bethany Crouse, Linda Hicks, Hardik Amin, Shelby Cole, Helene G. Bazin, David J. Burkhart, Marco Pravetoni, and Jay T. Evans. A lipidated TLR7/8 adjuvant enhances the efficacy of a vaccine against fentanyl in mice. *npj Vaccines*, 8(1):1–14, July 2023. Number: 1 Publisher: Nature Publishing Group.

[274] Fabio P. S. Santos, Hagop Kantarjian, Jorge Cortes, and Alfonso Quintas-Cardama. Bafetinib, a dual Bcr-Abl/Lyn tyrosine kinase inhibitor for the potential treatment of leukemia. *Current Opinion in Investigational Drugs (London, England: 2000)*, 11(12):1450–1465, December 2010.

[275] Neal K. Williams, Isabelle S. Lucet, S. Peter Klinken, Evan Ingley, and Jamie Rossjohn. Crystal structures of the Lyn protein tyrosine kinase domain in its Apo- and inhibitor-bound state. *The Journal of Biological Chemistry*, 284(1):284–291, January 2009.

[276] Tomoko Niwa, Tetsuo Asaki, and Shinya Kimura. NS-187 (INNO-406), a Bcr-Abl/Lyn Dual Tyrosine Kinase Inhibitor. *Analytical Chemistry Insights*, 2:93–106, November 2007.

[277] Yan Xu. Optimized conditions for the CDC Influenza SARS-CoV-2 (Flu SC2) Multiplex Assay using Luna® One-Step RT-qPCR Reagents.